Aus dem Medizinischen Zentrum für Orthopädie und Unfallchirurgie

Geschäftsführender Direktor: Univ.-Prof. Dr. med. Steffen Ruchholtz

Medizinische Direktorin: Univ.-Prof. Dr. med. Susanne Fuchs-Winkelmann

des Fachbereichs Medizin der Philipps-Universität Marburg

Characterization of clinical *S. aureus* isolates from implant-associated infections with regard to adhesion to and invasion into osteoblasts

Inaugural-Dissertation

zur

Erlangung des Doktorgrades der gesamten Humanmedizin

dem Fachbereich Medizin

der Philipps-Universität Marburg

vorgelegt von Lei Song

aus Hubei, China

Marburg, 2022

Angenommen vom Fachbereich Medizin der Philipps-Universität Marburg am: 12.09.2022

Gedruckt mit Genehmigung des Fachbereichs Medizin

Dekanin: Frau Prof. Dr. D. Hilfiker-Kleiner

Referent: Herr PD Dr. J. Paletta

1. Korreferent: Herr Prof. Dr. S. Vogt

Dedication

This dissertation is sincerely dedicated to my respectful parents-in-law and beloved wife, without whose endless support this paper was not possible. To my deceased parents I dedicate this paper in token of affection and gratitude, hoping they are happy and healthy in another parallel world.

Table of Contents

LIST OF ABBREVIATIONS

A	Adenosin
ADP	Adenosine diphosphate
ATP	Adenosine triphosphate
BafA1	Bafilomycin A1
BEM	Bone extracellular matrix
BSA	Bovine serum albumin
C	Cytosine
CCCP	Carbonyl cyanide m-chlorophenylhydrazone
cDNA	Complementary deoxyribonucleic acid
CFU	Colony forming units
CHO	Chinese hamster ovary
Cn	Collagen
Cna	Collagen adhesin
CO_2	Carbon dioxide
Ct	Cycle threshold
DMEM	Dulbecco's Modified Eagle Medium
DMSO	Dimethyl sulfoxide
DNA	Deoxyribonucleic acid
eDNA	Extracellular DNA
EDTA	Ethylenediaminetetraacetic acid
EPSs	Extracellular polymeric substances
et al.	Et alii (and others)
ETHBR	Ethidium bromide
Exo I	Exonuclease I
FCS	Fatal calf serum
Fn	Fibronectin
FnBPs	Fibronectin- binding proteins
g	Gram
G	Guanine
g	Gram
Glu	Glutamate
GSSP	Giant *Staphylococcal* Surface Protein
h	Hour(s)

H_2O	Water
HCl	Hydrochloric acid
Hla	α-Hemolysin
HUVECs	Primary human umbilical vein endothelial cells
kb	Kilobases
L	Liter
LAMP-1	lysosome-associated membrane protein-1
LB	Lysogeny broth
m	Meter
M	Molar
Mal	Malate
min	Minute(s)
mRNA	Messenger ribonucleic acid
MRSA	Methicillin-sensitive *S. aureus*
MSCRAMMs	Microbial surface component recognizing adhesive matrix molecules
MSSA	Methicillin-resistant *S. aureus*
MTT	3-(4,5-dimethylthiazol-2-yl)-2,5-diphenyltetrazolium bromide
n	Nano (10^{-9})
NaCl	Sodium chloride
OD	Optical density
p	Pico (10^{-12})
Pat	Patient
PBS	Phosphate buffered saline
PCI	Phenol/chloroform/Isoamyl alcohol
PCR	Polymerase chain reaction
pH	Negative decadal logarithm of molar concentration of hydrogen ions
PIA	Polysaccharide intercellular adhesin
PNAG	Poly-N-acetylglucosamine
PSA	Polysaccharide adhesin
PSMs	Phenol soluble modulins
p-value	Probability value
RNA	Ribonucleic acid
rpm	Rounds per minute
rRNA	Ribosomal RNA

rSAP	Shrimp Alkaline Phosphatase
RT-PCR/qPCR	Reverse transcription-polymerase chain reaction
S. aureus	*Staphylococcus aureus*
S. epidermidis	*Staphylococcus epidermidis*
SCVs	Small colony variants
SD	Standard deviation
SDS	Sodium dodechyl sulfate
sec	seconds
T	Thymine
Taq	Thermus aquaticus polymerase
TBS	Tris-buffered saline
TE	Tris-EDTA buffer
Tris	Tris-(hydroxyethyl) aminomethane
UV	Ultraviolet
WGA	Wheat germ agglutinin
µ	Micro (10^{-6})
%	Percent
°C	Degrees Celsius

LIST OF FIGURES

LIST OF TABLES

1 INTRODUCTION

Through the course of the aging population and higher demands of activities for elderly people, the number of endoprostheses implantations is constantly increasing. Every year, approximately 1,000,000 total hip replacements and 250,000 knee replacements are performed worldwide (Schierholz and Beuth, 2001). Within the United States, more than one million total joint arthroplastys have been performed annually (Etkin and Springer, 2017). Applying the most conservative estimates to current trend of population aging, the number is expected to increase to nearly 4 million by 2030 (Kurtz et al., 2007). In addition to these artificial join replacements, various internal fixation devices like plates, intramedullary nails, external fixation screws or pins are implanted. Even if the clinical results are good, the average durability of the prostheses is usually 15 or more years (Rand et al., 2003), however, the most frequent cause for failure of implants is aseptic loosening, with the highest occurrence rate of 76% in all risk factors (Apostu et al., 2018).

1.1 Implant-associated infection

Although aseptic loosening of prosthetic components is the most common cause of failure, infection can be one of the most frequent and devastating complication of surgically inserted prosthetic implants (El-Sayed and Nouvong, 2019; Arciola et al., 2018). Periprosthetic infections are particularly problematic as long as the prosthetic remains in the body (Dale et al., 2012; Jamsen et al., 2009; Phillips and Ker, 2006). These infections can deteriorate into significant morbidity associated with delayed healing and nonunion of the fracture, requiring multiple antimicrobial therapy, debridement, replacement, and revision, and possibly resulting in permanent functional loss or even amputation (Metsemakers et al., 2018). Nevertheless, implant-associated infections are hard to treat because of the antimicrobial resistance, tolerance and/or persistence, often causing chronic and/or relapsing disease (Schierholz and Beuth, 2001; Brady et al., 2011). Furthermore, identifying the infectious agent and its antimicrobial sensitivity can also be arduous for the diagnosis of orthopaedic implant infections, extending the desired time to microbial identification and recommended targeted treatment (Noone et al., 2021).

1.2 *Staphylococcus aureus*

The most common pathogens involved in implant-associated infections belong to the Staphylococcaceae family. Alongside *Staphylococcus epidermidis* (*S. epidermidis*) and some other *Staphylococcus species, Staphylococcus aureus* (*S. aureus*) is the most prevalent pathogen responsible

for orthopaedic infection (Webb et al., 2007; Lew and Waldvogel, 2004; Seghrouchni et al., 2012; Zimmerli et al., 2004; Arciola et al., 2005a). *S. aureus* is a gram positive, chemoorganotrophic, facultative anaerobic coccus with 0.6 µm in diameter. All strains are coagulase positive and most are haemolytic. It is a harmless saprobiont and commensal that belongs to the microbiome of the skin and mucous membranes in humans. About 20% of all human population is persistently colonized with these bacteria, but it can also be pathogenic (Singh, 2017). The first *S. aureus* infection was reported by Alexander Ogston in 1881 (Ogston, 1881). The bacteria generally colonize on skin scratch and cause soft tissue injury. But when gaining access to blood stream, the bacteria can reach other organs and can lead to serious clinical conditions including endocarditis, bones, and joints infections bacteraemia, sepsis and death (Thomer et al., 2016).

A range of extracellular and cell-associated factors issue the virulence of *S. aureus*. The first set of factors is bacteria adhesin, which belongs to the microbial surface component recognizing adhesive matrix molecules (MSCRAMMs) family (Foster et al., 2014b) and plays a crucial role in enhancing the ability of *S. aureus* to adhere and colonize of host tissue, implanted biomaterial, or both (Shi and Zhang, 2012; Löffler et al., 2014). The accurate repertoire of these proteins on the surface differs among strains: *S. aureus* can express up to 24 different MSCRAMMs, whereas coagulase-negative *staphylococci* such as *S. epidermidis* and *Staphylococcus lugdunensis* express much less (McCarthy and Lindsay, 2010; Heilbronner et al., 2011; Bowden et al., 2005). Several of these adhesins are covalently attached to peptidoglycan on the surface of *S. aureus* itself, each specifically interacting with one host protein component, such as fibrinogen, fibronectin, collagen, vitronectin, elastin, laminin, thrombospondin, bone sialoprotein or von Willebrand factor (Speziale et al., 2014; Heilmann, 2011; Lew and Waldvogel, 2004; Campoccia et al., 2009b; Zong et al., 2005). The second set of factors can help *S. aureus to* evade host defenses (some toxins, protein A, capsular polysaccharides) (Becker et al., 2014; Paharik and Horswill, 2016). The third set factors can facilitate the invasion by specifically attacking host cells (exotoxins) or degrading components of bone extracellular matrix (BEM, various hydrolases), and host cells will be damaged from within by bacterial cytotoxins sequentially (Foster et al., 2014a). Many of the above factors have been cloned, sequenced, and physically located on the chromosome map of *S. aureus* (Harris et al., 2013; Kuroda et al., 2001; Baba et al., 2002). The development of implant infection is related to complex interactions between the pathogen, the biomaterial and the host immune response to both (Arciola et al., 2018), resulting in the formation of biofilm, or the invasion and survival in osteoblasts.

1.3 Biofilm formation

In general, implant infection associated bacteria are not sparsely distributed, but rather form biofilm in which bacterial aggregates tightly adhere to the surface of prosthesis (Gristina and Costerton, 1985). Biofilm is another element responsible for the persistence of implant infections and a source of bacterial spread to other parts of the body (Fisher et al., 2017). Biofilm develops in three steps: Initial surface adhesion, micro-colony formation and biofilm maturation with bacterial detachment. Bacterial aggregation is promoted by the interaction between adhesins and cell wall proteins, for example, fibronectin- binding proteins (FnBPs) binding to fibronectin (Fn) molecules and then Fn connecting to the osteoblasts through the α5β1 integrin, which is also the main pathway for *S. aureus* entering into osteoblasts (Ahmed et al., 2001; Fowler et al., 2000). In addition, collagen adhesin (Cna) binding to collagen (Cn) primarily through the "collagen hug" mechanism plays an important role in the process of *S. aureus* infection in bone tissue, because Cn is the main component in extracellular matrix of bone cells (Kang et al., 2013).

Extracellular polymeric substances (EPSs), such as polysaccharide intercellular adhesin (PIA), polysaccharide adhesin (PSA), poly-N-acetylglucosamine (PNAG) or *S. aureus* exopolysaccharide (Limoli et al., 2015), are produced as a part of the biofilm maturation process, which involves the gradual formation of the biofilm matrix and the formation of larger bacterial aggregates known as towers (Moormeier and Bayles, 2017). The mechanisms involved in biofilm formation in *S. aureus* and *S. epidermidis* include the expression of the PIA and the release of extracellular DNA (eDNA) derived from bacterial autolysis and dead host cells (Flemming et al., 2016; Arciola et al., 2015). Biofilm dispersal can lead to bacterial dissemination, causing systematic infections (Gristina, 1987; Boles and Horswill, 2008). Phenol soluble modulins (PSMs) play a significant role in the dispersal phase, especially in implant-associated biofilm infections (Le et al., 2014). Bacteria in biofilms can be 500-5,000 times more resistant to antibiotics than planktonic bacteria (Oliveira et al., 2018). Several mechanisms contribute to biofilm resistance to antimicrobials, including low antimicrobial agent penetration due to biofilm matrix barrier function (Stewart, 2002). In addition, *S. aureus* can persist in a semi-dormant state with limited metabolism known as small colony variants (SCVs), which renders them less sensitive to antibiotic therapy (Sendi and Proctor, 2009; Guo et al., 2022).

1.4 Intracellular survival

Besides the formation of biofilm, invasion of non-professional phagocytes essentially contributes to the infection development (Alexander and Hudson, 2001). A broad spectrum of cells like endothelial

cells (HUVECs) (primary human umbilical vein endothelial cells) and EA. hy923 (endothelial cell line), epithelial cells (A549 (lung epithelial cell line) and HaCaT (human keratinocyte cell line), osteoblasts (primary human osteoblasts and CRL-11372 (osteoblast cell line) and connective tissue cells CCD-32-SK (fibroblast cell line) are affected by this phenomenon (Strobel et al., 2016). The concomitant bone formation and resorption achieve perpetual physiological homeostasis, performed by osteoblasts and osteoclasts (Dallas and Bonewald, 2010; Edwards and Mundy, 2011). The main function of osteoblasts is to synthesize bone matrix and modulate the activity of osteoclasts (Gay et al., 2000). In pathological conditions, such as cancer, autoimmune diseases, and infections, the osteoblast activity can be altered (Josse et al., 2015).

Process of *S. aureus* infecting osteoblasts can be simply summarized in three stages: (1) *S. aureus* initiates the invasion process by adhering to host cell membranes via the expression of adhesins; (2) Corresponding factors mediate *S. aureus* internalization into osteoblasts; (3) Infected osteoblasts are induced to apoptosis/programmed cell death and self-destroyed. Notably, live and dead *S. aureus* are equally effective for invasion, manifesting that the live bacteria are not mandatory in the invasion process; however, live osteoblasts are required, which implies that the internalization process is more an active eukaryotic mechanism than an active prokaryotic mechanism (Hudson et al., 1995). After adhering to cells, *S. aureus* can enter osteoblasts via internalization (Siebers et al., 2005; Shuaib et al., 2019). Here, *S. aureus* is able to gain entrance into osteoblasts through a fibronectin bridge between the integrin and the bacterial adhesin (Khalil et al., 2007). The ability of fibronectin to link with α5β1 integrin is considered as the most common pathway for the internalization of *S. aureus* in osteoblasts. Moreover, Cna and Bbp (bone sialoprotein binding protein) practically prefer the FnBP-mediated internalization whereas other MSCRAMMs of *S. aureus* favor the integrin-mediated internalization (Testoni et al., 2011; Hirschhausen et al., 2010; Zapotoczna et al., 2013). Other BEM components, such as collagen and bone sialoprotein, also bind to multiple integrins, suggesting the possibility of yet-unidentified "MSCRAMM/BEM component/integrin" bridge systems to initiate *S. aureus* internalization by osteoblasts (Grzesik and Robey, 1994). Independent of extracellular events, the involvement of cytoskeletal elements, particularly actin microfilaments, has been demonstrated during *S. aureus* internalization (Ellington et al., 1999).

The further fate of both the bacteria and the host cell depends on the genotype of *S. aureus* (Krut et al., 2003; Yang et al., 2018). Studies have shown that internalized *S. aureus* can survive within osteoblasts both *in vitro* (Webb et al., 2007; Wright and Nair, 2010; Ellington et al., 2006)and *in vivo* (Reilly et al., 2000; Gordon et al., 2020). The ability of internalized *S. aureus* to survive in osteoblasts and the unique role of osteoblasts harboring *S. aureus* protect *S. aureus* not only from host immunity but also from the antibiotics, which have a weak penetration in eukaryotic cells (Valour et al., 2015;

Krauss et al., 2019; Tuchscherr et al., 2016; Selan et al., 2017), thus increasing the difficulties of eradicating the pathogen. Therefore, targeting intracellular *S. aureus* is one of the key points to lower the recurrence of orthopaedic infection (Dusane et al., 2018). In addition to hiding in osteoblasts, *S. aureus* has also been observed to enter live cortical bone canaliculi (de Mesy Bentley et al., 2017). The ability to hide in bone tissue contributes to the resistance of orthopaedic implant infections to host defenses and antibiotic treatment.

Antibiotic resistance is a crucial issue for orthopaedic implant-associated infections (Campoccia et al., 2006). *S. aureus* strains related to these infections have high rates of antibiotic resistance, and notably, there is an alarming increase of antibiotic resistance in other species, such as *S. epidermidis* (Li and Webster, 2018). Moreover, the number of MSSA (methicillin-resistant *S. aureus*) infections was around 2.5-fold more when compared with the number of MRSA (methicillin-sensitive *S. aureus*) infections (Guo et al., 2017). Several studies have revealed that up to 40% of *S. epidermidis* and 32% of *S. aureus* strains isolated from implant-associated infections were resistant to gentamicin (Campoccia et al., 2009a; Campoccia et al., 2008). Therefore, prevention of implant-associated infections is a crucial but formidable task and it starts with the mastering of the interactions of multiple risk factors and spans the preoperative, intraoperative, and postoperative periods.

1.5 Objectives

Aim of this study is the characterization of clinical isolates related to an implant-associated infection of *S. aureus* with respect to its intracellular survival. Therefore, an infection model has been initially established in order to investigate invasion and persistence of *S. aureus*. Secondly, different *S. aureus* strains isolated from patients were characterized and analysed with respect to adhesion and invasion. Thirdly, the interaction of different *S. aureus* isolates with osteoblasts has been focused.

2 MATERIALS AND METHODS

2.1 Bacterial strains

Staphylococcus aureus Rosenbachii (ATCC® 29213™) was used as a known lab strain. Bacteria isolated from patients with an implant-associated infection were collected after signing of the informed consent. In total, we chose 12 valid isolates from samples of 50 patients, which were named as Patient (Pat) 2, Pat 4, Pat 6, Pat 9, Pat 28, Pat 29, Pat 32, Pat 36, Pat 37, Pat 42, Pat 45, and Pat 47. The ethics committee of the Philipps-University Marburg granted full ethical approval for the project (Az: 116/17).

2.2 Characterization of the staphylococci isolates

Isolates suspected to be *Staphylococcus* according to their shape, growth appearance, agility as well as enzymatic properties were further characterized. Gram-positive non-motile spherical isolates with bacteria cells arranged individually, in pairs or in irregular clusters, catalase-positive and oxidase negative were subjected to API® Staph. Test and 16S rRNA analysis.

Clear zone forming. Isolated bacteria were cultured overnight at 37 °C on Columbia blood agar plates, then the clear zone forming conditions of our isolates were identified by observation.

Growth curve. Isolated bacteria were cultured overnight at 37 °C (Incubator UE 500, Schwabach, Germany) on Columbia blood agar plates (Roth, Karlsruhe, Germany), separately. Then, colonies were individually cultured in LB-medium under shaking condition. OD_{600} (Eppendorf BioPhotometer plus, Hamburg, Germany; Cuvettes 10*4*45 mm, SARSTEDT, Nümbrecht, Germany) was tested at different time points (0, 1, 2, 3, 4, 5, 6, 7, 8, 9 h).

Collagenase test. Collagenase Test Kit (VWR Chemicals, Darmstadt, Germany) was used to differentiate *Staphylococcus aureus* from coagulase-negative Staphylococci. Freeze-dried product was rehydrated with 10 mL of sterile water previously heated at 37 °C and dispensed into tubes, 0.3 mL each. After that, each tube was inoculated directly with a loop from an isolate colony, incubating at 37 °C without shaking. Coagulations were analysed after 30 min, 1 h, 4 h and 6 h (up to 24 h). Presence of *S. aureus* (and other *Staphylococci* coagulase positive) was evident because of a solidification of the medium.

Oxidase test. Oxidase Reagent kit (BioMérieux, Marcy l'Etoile, France) was used to detect the production of the enzyme cytochrome oxidase by bacteria. This enzyme is characteristic of the genus

Neisseria and most species of Pseudomonas. A positive test was indicated by the development of a violet to purple colour within 10-30 sec.

API® Staph. Test. API® Staph. Test kit (BioMérieux, Marcy l'Etoile, France) was used to identify the staphylococcus genera of the isolates. Young cultures (18-24 h old) of our isolates were used to prepare homogeneous bacterial suspensions, then they were used to inoculate API Staph medium immediately. Afterwards, microtubes on the strip were filled with the medium above according to the manufacturer instructions and incubated at 37 °C for 18-24 h. The last step was to add different reagents to the microtubes and identify them by colour change according to the reading table of the handbook.

16S rRNA sequencing. DNA was isolated as described below. 16S rRNA gene was amplified by polymerase chain reaction (PCR) using specific primers (27 Forward 5´-AGA GTT TGA TCM TGG CTC AG-3'; 1492 Reverse 5´-GGT TAC CTT GTT ACG ACT T-3') (Ibrahim, 2016). Purity of the PCR products were tested by electrophoresis through 1% agarose gels (Carl Roth GmbH, Karlsruhe, Germany) with ethidium bromide (ETHBR). Afterwards, 5 µL of the PCR products were further purified with 1 µL of Exonuclease I (Exo I) and 2 µL of Shrimp Alkaline Phosphatase (rSAP) (New England Biolabs, Ipswich, Massachusetts, USA) for each DNA product, keeping them in the PCR device (Eppendorf AG, Hamburg, Germany) at 37 °C for 15 min and 80 °C for 15 min. DNA products were quantified and a total volume of 15 µL was collected for commercial analysis (Microsynth SEQLAB, Göttingen Germany), which was made up of 3 µL 27 forward primer and PCR product and nuclease-free water according to the calculating formula in the instruction of the commercial company. After getting results from the company, sequences of the isolates were aligned to known sequences of *S. aureus* by searching on BLAST: Basic Local Alignment Search Tool (nih.gov).

Assignment of isolates based on sequence homologies. Based on the sequence analysis, Maximum Likelihood method with molecular clock (version 3.6a2.1) was used to make a family tree of our bacteria isolates.

2.3 Culture of bacteria

Bacteria were cultured overnight at 37 °C on Columbia blood agar plates (Merck KGaA, Darmstadt, Germany). For most of the experiments, the colonies were cultured in LB-medium (Luria/Miller) (Carl Roth GmbH, Karlsruhe, Germany). For the different conditions analysis, LB-medium supplemented with 0.5% glucose and/or 3% NaCl solution were then used (Beenken et al., 2003).

2.4 Different media assay

Selected isolates (Pat 9, Pat 36, and *S. aureus*) were cultured overnight at 37 °C in four different media: LB-medium, LB-medium supplemented with 0.5% glucose solution, LB-medium supplemented with 3% NaCl solution, LB-medium supplemented with 0.5% glucose and 3% NaCl solutions. These cultures were then used to adhere both SaOS2 and MG63. Simultaneously, qPCRs were used to test the gene expression of primers mentioned above. In addition, different media were also used for biofilm formation analysis on metal plates and OD_{600} was measured after crystal violet staining.

2.5 Biofilm formation assay

Gentamicin concentration test. The effect of sub-inhibitory concentrations of gentamicin on survival under biofilm conditions was examined for all isolates in two different media: LB-medium and LB-medium supplemented with 0.5% glucose and 3% NaCl. Previous reports have indicated that the optimized biofilm conditions: LB-medium supplemented with 0.5% glucose and 3% NaCl can be effective to induce biofilm (Beenken et al., 2003; Götz, 2002). The concentration gradient of gentamicin in the 96-well plate (Carl Roth GmbH, Karlsruhe, Germany) was 120, 60, 30, 15, 7.5, 3.75, 1.88, 0.94, 0.47, 0.24, 0.12, 0 µg/mL. After incubating for 18 and 24 h at 37 °C, growth was measured by OD_{570} measurements using an Emax precision microplate reader (Molecular Devices, Sunnyvale, California, USA) equipped with the appropriate software (SoftMax Pro 6.4, Molecular Devices) (Naparstek et al., 2014).

Crystal violet staining. Biofilm formation was examined for all isolates in two different media: LB-medium and LB-medium supplemented with 0.5% glucose and 3% NaCl. The *S. aureus* isolates were cultured in the 96-well plates. After one day, OD_{570} was measured before staining. Then biofilm formed in each well was measured using crystal violet (Sigma, St Louis, MO, USA) staining, washing with PBS, eluting with 100% ethanol and quantifying by OD_{570}. Biofilm assays were repeated three times in three independent experiments.

The formation of biofilms on different surfaces (8 cm^2), such as metal and plastic plates, were examined and quantified for *S. arueus* ATCC 29213. After coating the plates with 20% human plasma in a carbonate buffer (pH 8.4) for 24 h at 4°C with mild shaking, the plates were washed with PBS and dried at room temperature. In order to inoculate the plates with bacteria, plates were immersed into the bacteria solution in PBS over a period of 5 min. Bacteria that did not attach during this time were washed away with sterile PBS. Then, the plates were placed in 50 mL reaction tubes with filter lid and incubated in different media over a period of 3, 5, 10 days at 37 °C and slightly shaking. Growing biofilm

were characterized with respect to cell density (plate count), metabolic activity (MTT), amount of biofilm (crystal violet staining) and Poly-β-1, 6-*N*-acetyl-D-glucosamine (PNAG) with wheat germ agglutinin (WGA) staining. Following elution of the crystal violet staining, 100 µL sample with 900 µL 100% ethanol were transferred into a cuvette for spectroscopy and the OD_{600} was measured.

2.6 Bacterial DNA isolation and PCR

The chromosomal DNA used as an amplification template was extracted from the bacterial cultures using innuPREP Bacteria DNA kit (Analytik, Berlin, Germany), according to the manufacturer's instruction.

An alternative method was also adopted. Bacteria pellet (in a 2 mL tube) was suspended in 200 µL of TE Buffer (40 mM EDTA-0.75 mM sucrose-50 mM Tris-HCl, pH 8.3). 10 µL lysostaphin (PROSPECT®, Ness-Ziona, Israel) was added and the suspension was incubated at 37 °C with shaking for 30 min. After that, 200 µL of lysis solution (STRATEC, Berlin, Germany) and 25 µL of proteinase K (Omega Bio-tek, Norcross, Georgia) were added. The mixture was incubated at 50°C with shaking for 15 min. Then, the conventional solution-based DNA extraction method with phenol/chloroform/Isoamyl alcohol (PCI; Roth, Karlsruhe, Germany) was used. Sample was added with 1 mL PCI and mixed thoroughly for 5 min. The mixture was centrifuged for 10 min at 4000 rpm. Supernatant was transferred into a new 2 mL tube and added with 1 mL of 100% ethanol. DNA pellet was obtained by centrifuging for 30 min at 16000 rpm and then washed by 70% ethanol and centrifuged again. The pellet was dried for 10 min and lastly, eluted in 200 µL of TE buffer.

PCR was performed according to the published literatures with minor modifications (Tristan et al., 2003; Serray et al., 2016). All primers were purchased at Microsynth SeqLab (Goettingen, Germany). The PCR reaction volume was in 20 µL, containing primers listed in Table 1 (0.8 µL each), 1 µL of the extracted DNA, 0.1 µL of MyTaq DNA polymerase (BIOLINE), 4 µL of 5* MyTaq Red Reaction Buffer (BIOLINE) and 14.1 µL of Nuclease-free water (BIOLINE). The cycling conditions included an initial denaturation (1 min at 94°C) followed by 40 cycles of amplification: denaturation for 30 sec at 94°C, annealing for 30 sec at 50-55°C, and extension for 30 sec at 72°C. After amplification, 5 µL of amplicon was used and the 1kb DNA ladder (New England Biolabs, Ipswich, Massachusetts, USA) was used as a DNA size marker. The electrophoresis was performed through 1% agarose gels with ETHBR at 70 V for 90 min. After electrophoresis, gels were visualized under UV light and photographed.

Table 1. Primers used in this study.

Gene	Primer	Nucleotide sequence	Literature
16S*	16S-Forward (F)	5'-ACT CCT ACG GGA GGC AGC AGT-3'	(DeLong, 1992)
	16S-Reverse (R)	5'-TAT TAC CGC GGC TGC TGG C-3'	
bbp	bbp-F	5'-AAC TAC ATC TAG TAC TCA ACA ACA G-3'	(Tristan et al., 2003)
	bbp-R	5'-ATG TGC TTG AAT AAC ACC ATC ATC T-3'	
cna	cna-F	5'-GTC AAG CAG TTA TTA ACA CCA GAC-3'	(Tristan et al., 2003)
	cna-R	5'-AAT CAG TAA TTG CAC TTT GTC CAC TG-3'	
eno	eno-F	5'-ACG TGC AGC AGC TGA CT-3'	(Tristan et al., 2003)
	eno-R	5'-CAA CAG CAT YCT TCA GTA CCT TC-3'	
ebp	ebp-F	5'-CAT CCA GAA CCA ATC GAA GAC-3'	(Tristan et al., 2003)
	ebp-R	5'-CTT AAC AGT TAC ATC ATC ATG TTT ATC TTT G-3'	
fnbA	fnbA-F	5'-CAT AAA TTG GGA GCA GCA TCA-3'	(Vancraeynest et al., 2004)
	fnbA-R	5'-ATC AGC AGC TGA ATT CCC ATT-3'	
fnbB	fnbB-F	5'-GTA ACA GCT AAT GGT CGA ATT GAT ACT-3'	(Tristan et al., 2003)
	fnbB-R	5'-CAA GTT CGA TAG GAG TAC TAT GTT C-3'	
fib	fib-F	5'-CTA CAA CTA CAA TTG CCG TCA ACA G-3'	(Tristan et al., 2003)
	fib-R	5'-GCT CTT GTA AGA CCA TTT TCT TCA C-3'	
clfA	clfA-F	5'-ATT GGC GTG GCT TCA GTG CT-3'	(Tristan et al., 2003)
	clfA-R	5'-CGT TTC TTC CGT AGT TGC ATT TG-3'	
clfB	clfB-F	5'-ACA TCA GTA ATA GTA GGG GGC AAC-3'	(Tristan et al., 2003)
	clfB-R	5'-TTC GCA CTG TTT GTG TTT GCA C-3'	
ebpS	ebpS-F	5'-AGA ATG CTT TTG CAA TGG AT-3'	(Vancraeynest et al., 2004)
	ebpS-R	5'-AAT ATC GCT AAT GCA CCG AT-3'	
psmA	psmA-F	5'-TAT CAT CGC TGG CAT CAT TA-3	(Xu et al., 2017)
	psmA-R	5'-AGA CCT CCT TTG TTT GTT ATG-3'	
psmB	psmB-F	5'-CAA AGG TGA GGG AGA GAT T-3'	(Xu et al., 2017)
	psmB-R	5'-TTA GCA ACG ATG TCT ACG A-3'	
arcB	arcB-F	5'-CAA GTA TTT CAG GGA CGC-3'	(Griswold et al., 2004)
	arcB-R	5'-CAT CTG TCA AGC CAT TCC-3'	
eap	eap-F	5'-TAC TAA CGA AGC ATC TGC C-3'	(Hussain et al., 2008)
	eap-R	5'-TTA AAT CGA TAT CAC TAA TAC CTC-3'	
sdrD	sdrD-F	5'-CAA TAA CAA GGA AAG GCA TG-3'	(Belikova et al., 2020)
	sdrD-R	5'-ACC GAA TAA CAA TAA TGA ACC-3'	
fmtB	fmtB-F	5'-AAT GAA GAT GCG AAT CAT GTT G-3'	(Sung et al., 2008)
	fmtB-R	5'-CAT CCA TTT TTG TTT GCG TAG A-3'	
ebh	ebh-F	5'-TGC GAA GAA GCG TGA AGC AGA AAC-3	(Walker et al., 2013)
	ebh-R	5'-TTG TTG CAC TGC TTG CTC TAA GGC-3'	

**housekeeping gene; The nucleotide sequences of bbp (encoding bone sialoprotein binding protein), cna (collagen binding protein), eno (laminin binding protein), fnbA and fnbB (fibronectin binding proteins A and B), fib (fibrinogen binding protein), clfA and clfB (clumping factors A and B), ebpS (elastin binding protein); psmA and psmB (Phenol-soluble modulins A and B); arcB (ornithine carbamoyltransferase); eap (extracellular adherence protein); sdrD (SD-repeat containing protein D); fmtB (methicillin resistance determinant FmtB protein); ebh (extracellular matrix-binding protein).*

2.7 Bacterial RNA isolation and real-time reverse transcription-polymerase chain reaction (RT-PCR/qPCR)

For RNA extraction from bacteria, the peqGOLD Total RNA Kit (PeqLab) was used following the manufacturer's instructions and quantified spectrometrically.

For RT-PCR, cDNA was synthesized from extracted RNA using an iScript cDNA synthesis kit (Biorad, HercuLes CA, USA) according to recommendations of the manufacturer. The components volume was 20 µL, containing 5 µL of RNA template, 4 µL of 5* iScript reaction mix, 1 µL of iScript reverse transcriptase and 10 µL of Nuclease-free water. Then, the complete reaction mixtures were incubated in the PCR device (5 min at 25 °C, 30 min at 42 °C and 5 min at 85 °C) to obtain the cDNA products.

Real time amplification was conducted using specific primers (Table 1) and was carried out on Realplex^2 Mastercycler (Eppendorf AG, Hamburg, Germany) using the SsoAdvanced Universal SYBR® Green Supermix (Bio-Rad Laboratories, Hercules CA, USA). The 20 µL of reaction mixtures (1 µL of cDNA template, 2 µL of 10x forward and reverse primers, 7 µL of Nuclease-free water and 10 µL of SYBR® Green Supermix) were incubated for 30 sec at 95 °C followed by 40 cycles of 15 sec at 95 °C, 35 sec at 55 °C, and 15 sec at 95 °C, then kept at 65 °C for 10 sec and at last, temperature was increased from 65 °C to 95 °C in 30 min (1°C/min). Gene expression rates were calculated using delta-delta Ct method from corresponding threshold cycles after melting-curve analysis.

2.8 Culture of osteoblasts

The human musculoskeletal osteoblast-like cell lines MG63 (ATCC® CRL-1427™) and SaOS2 (ATCC® HTB85™) were grown in Dulbecco's Modified Eagle Medium (DMEM) (Gibco, Karlsruhe, Germany) with 10% Fetal Calf Serum (FCS; Biochrom, Berlin, Germany) and 1% penicillin/ streptomycin (10,000 U/mL) (PAA Laboratories, Pasching, Austria) at 37 °C in a 5% CO_2 humidified atmosphere (Heracell™ 150i CO_2 Incubator, Waltham, USA) in 75 cm^2 flasks (SARSTEDT, Nümbrecht, Germany). Sub-confluent cells were trypsinized with 1 mL trypsin-EDTA and washed with phosphate buffered saline (PBS) (Michel et al., 2016).

Cell growth was controlled using phase-contrast light microscopy. With respect to osteoblasts, the SaOS2 and MG63 cell lines are a standard *in vitro* model for the study of bacterial infection mechanisms, especially during *S. aureus* internalization (Valour et al., 2015; Ahmed et al., 2001; Nair et al., 2003; Khalil et al., 2007; Testoni et al., 2011; Jauregui et al., 2013; Pérez-Tanoira et al., 2017; Gunn et al., 2021). According to the guideline of the US-Office for Human Research Protection, *in vitro* research using already derived and established cell lines do not need an IRB review.

2.9 Infection model establishment with *S. aureus* (ATCC® 29213™)

S. aureus was cultured in LB-Medium and harvested in the stationary and logarithmic phase by centrifugation. Pellet was washed twice with PBS. The pellet was resuspended in DMEM with 10% FCS and the bacterial concentration was calibrated and adjusted by optical density at 600 nm (OD_{600} 0.3-0.5). Osteoblasts were cultured in DMEM with 10% FCS and 1% penicillin/ streptomycin (10,000 U/mL) until they reached sub-confluency. The osteoblasts were detached with 0.05% Trypsin (Gibco Thermo Fisher Scientific GmbH-Dreieich, Germany), then seeded (0.3 x 10^6 cells/well) and let them grow overnight to reach a confluent layer (1.2 x 10^6 cells/well) in 6-well plates (SARSTEDT, Nümbrecht, Germany). Then, the culture medium was removed and replaced with *S. aureus* suspension. Both stationary and logarithmic phase *S. aureus* were used to infect the SaOS2 and MG63 osteoblasts with different incubation time points (30 sec, 1 min, 2 min, 5 min, 10 min and 30 min) at 37 °C in a 5% CO_2 humidified atmosphere. The supernatant fluids were discarded and the cells were washed 5 times (4 mL/time) with 1x PBS, in order to remove unattached bacteria, and then lysed with 0.2 % Triton X-100 for 20 min. Then cells were thoroughly mixed to achieve complete lysis. The lysates were diluted 10 times (1:10, 1:100, 1:1000, 1:10000) in 1x PBS and plated onto LB-agar plates. After 24 h of incubation at 37 °C, the number of bacterial colonies were counted and the total colony forming units (CFU) were determined.

2.10 Adhesion assay

Based on the infection model described above, adhesion of all *S. aureus* isolates was tested. The time for bacteria adhering to osteoblasts was set as 30 min for a completely adhesion. For both the adhesion and invasion assays, results were expressed as the mean ± standard deviation (SD) of the adherent or internalized bacteria with respect to inoculated bacteria, derived from independent experiments performed in triplicate.

2.11 Invasion assay

For *in vitro* invasion, DMEM supplemented with 10% FCS and 30 µg/mL gentamicin was used to kill only the remaining extracellular bacteria without affecting the intracellular bacteria (Drevets et al., 1994). Cells were then incubated over a period of 1 day, 2 days and 3 days before lysis. During the incubation, culture medium with gentamicin was refreshed once a day in order to inhibit the proliferation of the residual extracellular bacteria.

2.12 MTT assay

The MTT assay was used for assessing cell metabolic activity of MG63 and SAOS2 osteoblast cell lines with and without infection. The MTT tetrazolium ring is cleaved only by active mitochondria, yielding purple formazan crystals. The amount directly correlates with the viable cell count. An increase in the number of viable cells results in an increase of the amount of MTT formazan salt and an increase of absorbance. After a period of 1 day, 2 days and 3 days, the culture medium was removed and 1 mL (5 mg/mL in PBS) MTT reagent (Thiazolyl Blue Tetrazolium Bromide (Sigma-Aldrich, St. Louis MO, USA) was administered to the cells. Then, the osteoblasts were incubated at 37 °C for at least 4 h. After incubation, 1 mL Dimethyl sulfoxide (DMSO; Uvasol®, Darmstadt, Germany) was added to the osteoblasts well. The resulting purple solution was diluted with DMSO and spectrophotometrically measured with OD_{550}.

2.13 Quantitative protein identification

Two different osteoblast cell lines with or without infection with *S. aureus* were cultured and obtained as described above.

For quantitative protein identification, mass spectrometry (in cooperation with Dr. Uwe Linne, Department of mass spectrometry and element analysis, Philipps-University Marburg) was used. Cells were dissolved in lysis buffer consisting of 8 M Urea and 0.1 M Ammoniumbicarbonate (Sigma, Saint Quentin Fallavier, France). After Vortexing for 10 sec, samples were ultra-sonicated for 3 x 10 sec with vial Tweeter (Ultrasonicator, Hielscher Ultrasonics GmbH, Teltow Germany). Samples were stored on ice between steps. Then lysed samples were rotated 5 min at 25°C at 1,400 rpm and centrifuged at 10,000 rpm for 10 sec (Centrifuge 5417 R, Eppendorf, Hamburg, Germany).

Bradford assay was used to measure protein concentration from the supernatant with bovine serum albumin (BSA) dissolved in lysis buffer as reference curve. For standard protein digests use 100 µg protein was used.

Samples were reduced, carbamidomethylated and digested by the addition of Sequencing Grade Modified Trypsin (Serva) and incubated at 37 °C overnight. Peptides were desalted and concentrated using Chromabond C18WP spin columns (Macherey-Nagel, Part No. 730522). Finally, Peptides were dissolved in 25 µL of water with 5% acetonitrile and 0.1% formic acid. The mass spectrometric analysis of the samples was performed using an Orbitrap Velos Pro mass spectrometer (ThermoScientific). An Ultimate nano RSLC-HPLC system (Dionex), equipped with a custom end-fritted 50 cm x 75 µm C18 RP

column filled with 2.4 µm beads (Dr. Maisch) was connected online to the mass spectrometer through a Proxeon nanospray source. 1-15 µL (depending on peptide concentration and sample complexity) of the tryptic digest were injected onto a 300 µm ID x 1 cm C18 PepMap pre-concentration column (Thermo Scientific). Automated trapping and desalting of the sample was performed at a flow rate of 6 µL/min using water/0.05% formic acid as solvent. Separation of the tryptic peptides was achieved with the following gradient of water/0.05% formic acid (solvent A) and 80% acetonitrile/0.045% formic acid (solvent B) at a flow rate of 300 nL/min: holding 4% B for 5 min, followed by a linear gradient to 45% B within 30 min and linear increase to 95% solvent B in additional 5 min. The column was connected to a stainless steel nanoemitter (Proxeon, Denmark) and the eluent was sprayed directly towards the heated capillary of the mass spectrometer using a potential of 2300 V. A survey scan with a resolution of 60000 within the Orbitrap mass analyzer was combined with at least three data-dependent MS/MS scans with dynamic exclusion for 30 sec either using CID with the linear ion-trap or using HCD combined with Orbitrap detection at a resolution of 7500. Data analysis was performed using Proteome Discoverer 2.2 (ThermoScientific) with SEQUEST search engine or MaxQuant with Andromeda search engine. Uniprot databases were used.

2.14 Autophagy induction assay

SaOS2 and MG63 cell lines were cultured to confluence in 6-well plates. DMEM without FCS was administered for 24 h to induce autophagy. Selected isolates (Pat 9, Pat 36, Pat 42, Pat45 and *S. aureus*) were used to infect SaOS2 and MG63 cell lines. DMEM supplemented with 30 µg/mL gentamicin was used to kill the remaining extracellular bacteria. Cells were lysed after 1 day, 2 days and 3 days. Plate count was performed at a dilution of 1:10, 1:100, and 1:1000 in order to determine the amount of the intracellular bacteria.

2.15 Autophagy inhibition assay

SaOS2 and MG63 cell lines were cultured to confluence in 6-well plates. DMEM implemented with FCS and 500 pM Bafilomycin A1 (BafA1; InvivoGen, Toulouse, France) was administered for 24 h to inhibit autophagy. After washing the cells with PBS, isolates (Pat 9, Pat 36, Pat 42, Pat45 and *S. aureus*) were used to infect both cell lines. After 1 day, 2 days and 3 days, cells were lysed and plate count was performed at a dilution of 1:10, 1:100, and 1:1000 in order to determine the amount of the intracellular bacteria.

2.16 Western blot analysis

SaOS2 and MG63 cell lines were cultured to confluence in 175 cm^2 flask (SARSTEDT, Nümbrecht, Germany). Medium without FCS was administered to induce autophagy as well as medium implemented with FCS was used as normal physiologic condition to analyse the interaction with bacteria. After 24 h, isolates (Pat 9, Pat 36, Pat 42, Pat45 and *S. aureus*) were selected to infect SaOS2 and MG63 cell lines. Both cell lines cultured in two different media without infection were also used as control. After 2 days, cells were harvested and the whole cell lysates were prepared with Jie's buffer (10 mM NaCl, 0.5% Nonidet P40, 20 mM Tris-HCl pH 7.4, 5 mM $MgCl_2$, 1 mM PMSF, complete protease inhibitor, and phosphatase inhibitor [Roche, Basel, Switzerland]). All proteins were quantified using Pierce™ BCA Protein Assay Kit (Thermo Fisher Scientific, Rockford, Illinois, USA). The proteins (30 µg of each sample) were separated through NuPAGE®10% BIS-Tris Gel (NP0315BOX; Life Technologies, Carlsbad, CA, USA) according to the quick reference of NuPAGE® BIS-Tris Mini Gels and transferred to nitrocellulose blotting membranes (10600006; GE Healthcare Life Science, Chicago, IL, USA) by semidry-blotting with Trans-Blot®Turbo™ Transfer System (Bio-Rad Laboratories, Hercules CA, USA). Novex® Sharp Pre-Stained Protein Standard (Invitrogen™, Carlsbad, CA, USA) was loaded as standard marker protein. The membranes were further sliced according to the required molecular weight of the proteins of interest, blocked in 4% BSA (Sigma-Aldrich, St Louis, MO, USA) in TBS-Tween 20 (0.5%; Th. Geyer GmbH & Co. KG., Renningen, Germany), and incubated with primary antibodies against Beclin1 (ab92389; Abcam, Cambridge, UK), LC3B (ab51520; Abcam, Cambridge, UK), SQSTM1/p62 (ab96706; Abcam, Cambridge, UK), β-actin (A5441; Sigma-Aldrich, St Louis, MO, USA). Bound primary antibodies were detected by secondary Polyclonal Goat Anti-Mouse Immunoglobulins (Dako Denmark A/S, Glostrup, Denmark) and Polyclonal Goat Anti-Rabbit Immunoglobulins (Dako Denmark A/S, Glostrup, Denmark) antibodies and SuperSignal West Pico Chemiluminescent Substrate (Thermo Fisher Scientific, Waltham, MA, USA). The immunodetection was quantified with the Fusion image capture (Vilber Lourmat Deutschland GmbH, Eberhardzell, Germany) and Bio-1D analysis system (Vilber Lourmat Deutschland GmbH).

2.17 Respiration assay

Respiration assay was done in collaboration with Prof. Dr. Sebastian Vogt in the Laboratory of Heart, Thoracic and Vascular Surgery, Philipps-University Marburg), and based on the aerobic respiration model of its previous study (Ramzan et al., 2010). Interactions of cellular components, such as metabolic compartmentation, channeling, and functional coupling mechanisms, are momentous for regulation of the energy transfer between mitochondrial respiration and ATP synthesis (Weiss et al.,

2006; Saks et al., 2009). Therefore, we used respiration assay to analyse the metabolic rate of our osteoblasts after infection with different isolates.

SaOS2 and MG63 cell lines were cultured to confluence in 175 cm^2 flask. Isolates (Pat 9, Pat 36, Pat 42, Pat45 and *S. aureus*) were selected to infect SaOS2 and MG63 cell lines. Both osteoblast cell lines without infection were also used as control. After 2 days, cells were harvested and the number of each individual sample was counted. Respiration of both infected and non-infected osteoblasts was measured polarographically at 25 °C using an Oxygraph System (Hansatech, Norfolk, U.K.) in 0.5 mL of "KCl-medium" (130 mM KCl, 3 mM Hepes, 0.5 mM EDTA, 2 mM KH2PO4, pH 7.4, 0.5% fatty acid-free BSA). Further additions, 5 µL 5 mM glutamate (Glu) + 1 µL 1 mM malate (Mal), 5 µL 0.5 M adenosine diphosphate (ADP), 0.5 µL 4 mM carbonyl cyanide m-chlorophenylhydrazone (CCCP), 10 µL 0.5 M adenosine triphosphate (ATP) were added in order at a proper time point. The rates of oxygen consumption (nmol O_2 min^{-1} mL^{-1}) were calculated after each step of adding additional ingredient and presented graphically in the end.

2.18 Statistical analysis

Statistical analysis was carried out with IBM SPSS Statistics 27. Data were representative of at least three independent experiments and tested for normal distribution using a Kolmogorov-Smirnov-Test test and results were compared using Student's t-test, Mann-Whitney-U Test, Kruskal-Wallis, followed by ANOVA, respectively. A p-value of ≤ 0.05 was considered statistically significant.

3 RESULTS

3.1 Characterization of *Staphylococci* associated with an implant-associated infection

The first step in this study was to classify the clinical isolates. Several methods, such as clear zone formation, growth curve analysis, collagenase test, oxidase reagent test, API® Staph. test, and 16S rRNA sequencing, were used to accomplish the classification of *S. aureus*.

3.1.1 Clear zone formation

Clear zone formation of our isolates was observed from the bottom of the blood agar plates. As shown in the figure below (Figure 1), some isolates could form a clear zone around the colonies after cultivation, while the others could not. Zone formation around the colony denoted the haemolysin secreted by the bacteria. According to the different behaviours, our isolates were grouped in Table 2.

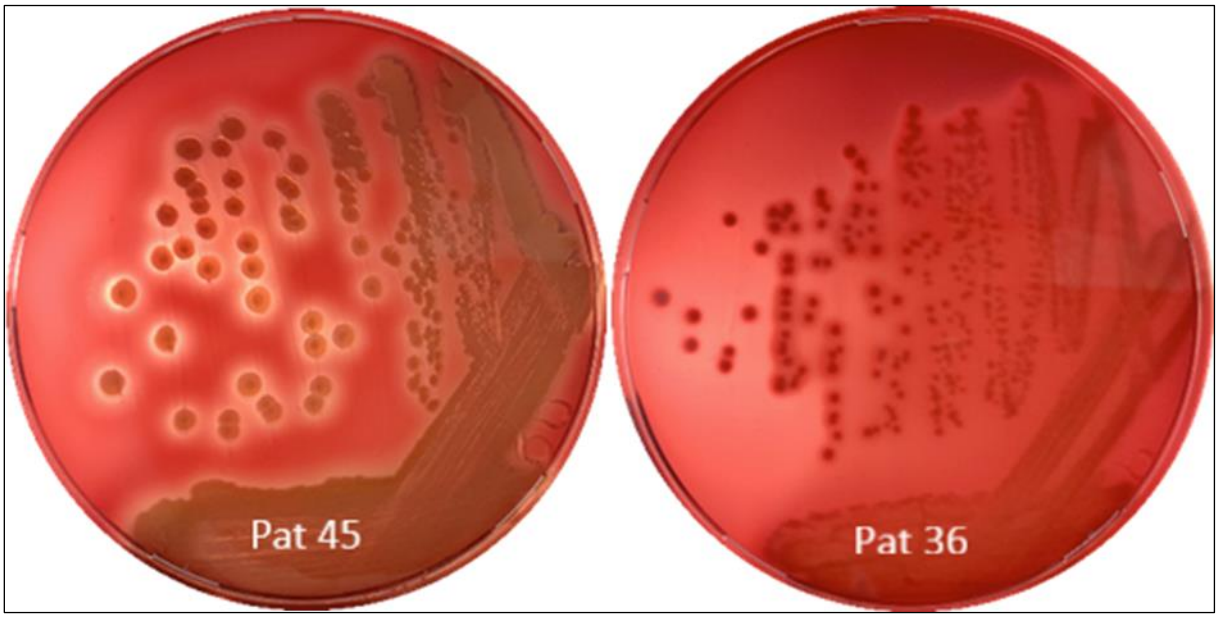

Figure 1. Clear zone formation results of isolates Pat 45 (clear zone) and Pat 36 (non-clear zone) on blood agar plates. Isolated bacteria were cultured overnight at 37 °C on Columbia blood agar plates, then the clear zone forming conditions of isolates were identified by observation.

Table 2. Clear zone formation results of the isolated bacteria.

Performance	Isolate No.
Clear zone formation	Pat 2, 4, 6, 9, 28, 42, 45
Non-clear zone formation	Pat 29, 32, 36, 37, 47

3.1.2 Growth curve

Isolated bacteria were cultured and quantified with OD_{600} at different time points as described in the Material and Methods section. Results shown in Figure 2 indicated that Pat 2, 4, 6, 9, 28, 36, 42, 45 and *S. arueus* ATCC 29213 were likely to proliferate faster than Pat 29, 32, 37, 47. Pat 42, 45, 36 and *S. arueus* ATCC 29213 were the fastest growing isolates.

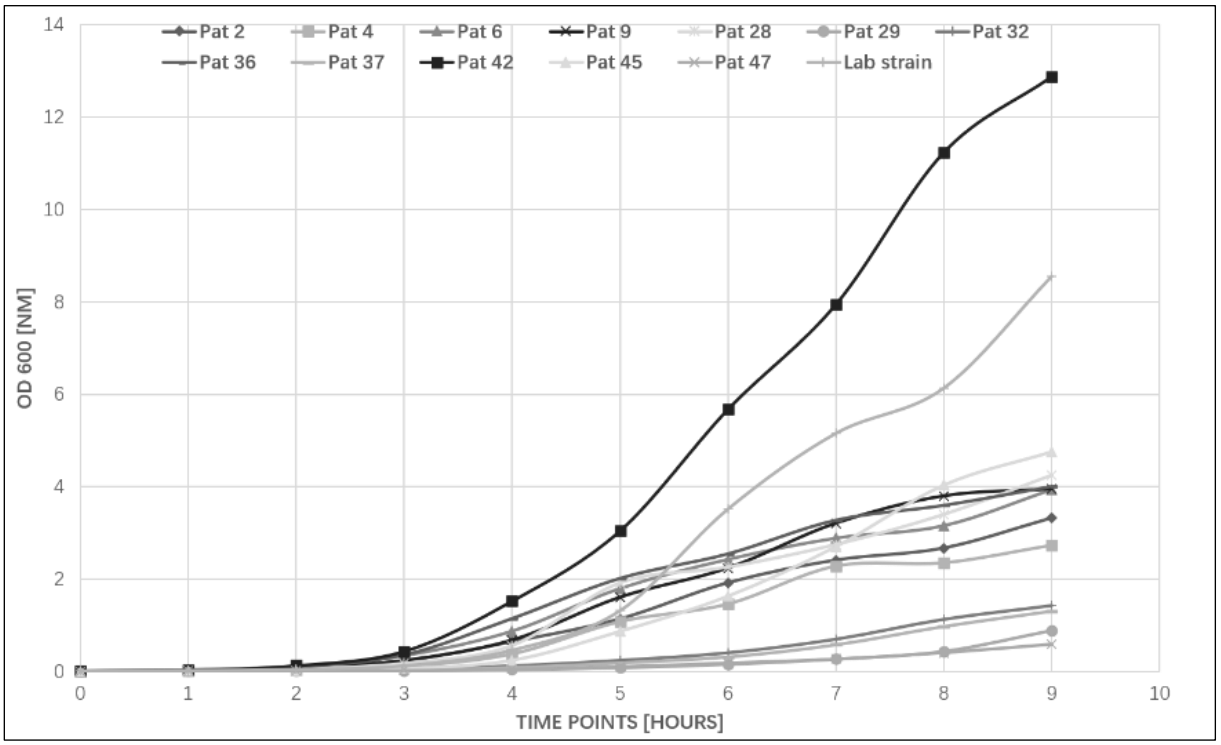

Figure 2. Growth curve of all isolated bacteria. Bacteria were cultured at 37 °C in a 5% CO_2 humidified atmosphere. OD_{600} was measured at every time point.

3.1.3 Collagenase test

Coagulase test was emplyed to confirm whether the isolates are coagulase-positive or coagulase-negative. Test medium became solid when it comes to *S. aureus* (and other Staphylococci coagulase-positive). We divided the isolates into two groups as below in Table 3.

Table 3. Collagenase test of the isolated bacteria.

Performance	Isolate No.
Coagulase-positive (+)	Pat 2, 4, 6, 9, 28, 36, 42, 45
Coagulase-negative (-)	Pat 29, 32, 37, 47

3.1.4 Oxidase reagent

The isolated bacteria were tested with the kit mentioned above and all results were nagative, indicating that none of our isolate were the genus Neisseria and most species of Pseudomonas.

3.1.5 API® Staph. test

With the API® Staph. test kit testing, a colour-changed strip was obtained, taking Pat 42 as an example (Figure 3). According to the reading table in the manufacture's instruction, the pattern of metabolic activity of Pat 42 was highly likely to indicate *S. aureus* after comparing with the standard *S. aureus*. As shown in Table 4, Pat 2, 4, 6, 9, 28, 36, 42, 45 were more likely to be *S. aureus*, while Pat 29, 32, 37, 47 were likely to be *S. epidermidis*.

Figure 3. API® Staph. test result of the isolate Pat 42. API® Staph. Test kit was used to identify the genera *staphylococcus* of the isolates. Identification was obtained by comparing the colour of each microtube with the standard reading table in the manufacture's instruction.

Table 4. Result of the API® Staph. test of all different isolates obtained from patients that underwent surgery for an implant-associated infection.

	GLU	FRU	MNE	MAL	LAC	TRE	MAN	XLT	MEL	NIT	PAL	VP	RAF	XYL	SAC	MDG	NAG	ADH	URE
S. aureus	+	+	+	+	+	+	+	-	-	+	+	+	-	-	+	-	+	+	+
S. epidermidis	+	+	*	+	+	-	-	-	-	+	+	*	-	-	+	-	-	*	+
Pat 2	+	+	+	+	+	+	+	-	-	+	+	+	-	-	+	-	+	+	+
Pat 4	+	+	+	+	+	+	+	-	-	+	+	+	-	-	+	-	-	+	-
Pat 6	+	+	+	+	+	+	+	-	-	+	+	+	-	-	+	-	+	+	+
Pat 9	+	+	+	+	+	+	+	-	-	+	+	-	-	-	+	-	+	+	+
Pat 28	+	+	+	+	+	+	+	-	-	+	+	+	-	-	+	-	+	+	-
Pat 36	+	+	+	+	-	+	-	-	-	+	+	-	-	-	+	-	+	+	+
Pat 42	+	+	+	+	+	-	+	-	-	+	+	+	-	-	+	-	-	+	+
Pat 45	+	+	+	+	+	-	+	-	-	+	+	+	-	-	+	-	-	+	+
Pat 29	+	+	-	+	+	-	-	-	-	+	+	-	-	-	+	-	-	+	+
Pat 32	+	+	+	+	+	-	-	-	-	+	+	+	-	-	+	-	-	+	+
Pat 37	+	+	-	+	+	-	-	-	-	+	+	+	-	-	+	-	-	+	-
Pat 47	+	+	+	+	-	-	-	-	-	+	+	+	-	-	+	-	-	+	+

*GLU: D-Glucose; FRU: D-Fructose; MNE: D-Mannose; MAL: D-Maltose; LAC: D-Lactose; TRE: D-Trehalose; MAN: D-Mannitol; XLT: Xylitol; MEL: D-Melibiose: NIT: Kaliumnitrat: PAL: ß-Naphthol-Phosphat; VP: Voges Proskauer; RAF: D-Raffinose; XYL: D-Xylose; SAC: D-Saccharose; MDG: Methyl-αD Glucopyranoside; NAG: N-acetyl-glucosamine; ADH: Arginine DiHydrolase; URE: UREase; +: Positive; -: Negative; *: Not clear.*

3.1.6 16S rRNA sequencing

To support the results above, 16S rRNA analysis was carried out. And indeed, the comparison of the DNA sequence with the NCBI Database showed the highest level of homology with *S. aureus* or *S. epidermidis* (Table 5).

Table 5. Homologies of staphylococcus isolates based on 16S rRNA sequencing.

Patient No.	Sequence Alignment
Pat 2	*Staphylococcus aureus* gi|1269859156|NR_037007.2; gi|631252758|NR_113956.1; gi|310974964|NR_036828.1; gi|636559546|NR_115606.1
Pat 4	*Staphylococcus aureus* gi|1269859156|NR_037007.2; gi|631252758|NR_113956.1; gi|310974964|NR_036828.1; gi|636559546|NR_115606.1
Pat 6	*Staphylococcus aureus* gi|1269859156|NR_037007.2; gi|631252758|NR_113956.1; gi|310974964|NR_036828.1; gi|636559546|NR_115606.1
Pat 9	*Staphylococcus aureus* gi|1269859156|NR_037007.2; gi|631252758|NR_113956.1; gi|310974964|NR_036828.1; gi|636559546|NR_115606.1
Pat 28	*Staphylococcus aureus* gi|631252758|NR_113956.1; gi|310974964|NR_036828.1; gi|636559546|NR_115606.1
Pat 36	*Staphylococcus aureus* gi|631252758|NR_113956.1; gi|310974964|NR_036828.1; gi|636559546|NR_115606.1
Pat 42	*Staphylococcus aureus* strain PMB 196-1
Pat 45	*Staphylococcus aureus* gi|631252758|NR_113956.1; gi|310974964|NR_036828.1; gi|636559546|NR_115606.1
Pat 29	*Staphylococcus epidermidis* gi|631252759| NR_113957.1; gi|310975040|NR_036904.1
Pat 32	*Staphylococcus epidermidis* gi|631252759| NR_113957.1; gi|310975040|NR_036904.1
Pat 37	*Staphylococcus epidermidis* gi|631252759| NR_113957.1; gi|310975040|NR_036904.1
Pat 47	*Staphylococcus epidermidis* gi|631252759| NR_113957.1; gi|310975040|NR_036904.1

NR: NCBI Reference Sequence

3.1.7 Assignment of isolates based on sequence homologies

Based on the gene data, sequence analysis was conducted by Maximum Likelihood method with molecular clock. The result was shown in Figure 4. After comparing the 16S rRNA sequencing results with NCBI reference sequence, isolates sequences were highly homologous to: NR_113956 (*S. aureus*), NR_037007 (*S. aureus*), NR_118997 (*S. aureus*) and NR_036904 (*S. epidermidis).* Therefore, from the perspective of homology, Pat 2, 4, 6, 9, 28, 36, 42, 45 and *S. arueus* ATCC 29213 belong to the *S. aureus*, while Pat 29, 32, 37, 47 belong to the *S. epidermidis*.

Above all, our isolates were eventually classified as *S. aureus* (Pat 2, 4, 6, 9, 28, 36, 42, 45) and *S. epidermidis* (Pat 29, 32, 37, 47). In the present study, *S. epidermidis* were excluded from the further examinations.

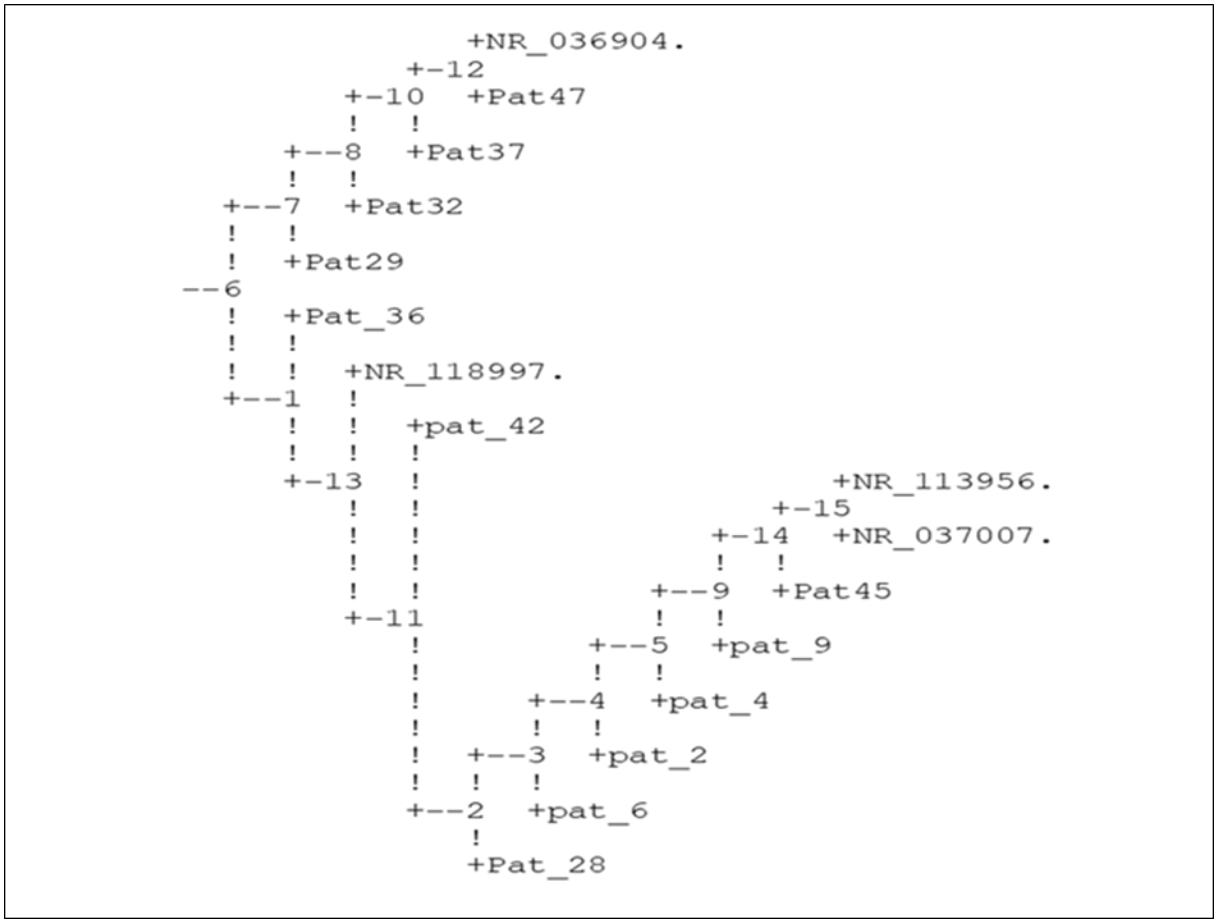

Figure 4. Phylogenetic tree based on maximum likelihood method. Comparing the 16S rRNA sequencing results with NCBI reference sequence, isolates were classified into two different homologies. NR_036904: *Staphylococcus epidermidis* strain Fussel 16S ribosomal RNA, partial sequence; NR_118997: *Staphylococcus aureus* strain ATCC 12600 16S ribosomal RNA, complete sequence; NR_113956: *Staphylococcus aureus* strain NBRC 100910 16S ribosomal RNA gene, partial sequence; NR_037007: *Staphylococcus aureus* strain S33 R 16S ribosomal RNA, complete sequence. Pat 2, 4, 6, 9, 28, 36, 42, 45 were classified as *S. aureus*, while Pat 29, 32, 37, 47 were categorized as *S. epidermidis*.

3.2 Biofilm formation assay

Biofilm was induced according to Previous reports, which have indicated that the optimized biofilm conditions: LB-medium supplemented with 0.5% glucose and 3% NaCl can be effective to induce biofilm (Beenken et al., 2003; Götz, 2002), and this was identified by Michel et al. (Michel et al., 2016).

3.2.1 Gentamicin resistance test

The effect of sub-inhibitory concentrations of gentamicin on biofilm formation was examined for all isolates in two different media: LB-medium and LB-medium supplemented with 0.5% glucose and 3% NaCl. The concentration gradient of gentamicin in the 96-well plate was as described in Figure 5. OD_{570} was measured after incubating for 18 h and 24 h. These data suggest that 30 µg/mL gentamicin is enough to kill extracellular *S. aureus* isolates cultured under growth conditions in LB-medium. Whereas, when optimized biofilm conditions were acquired by adding 0.5% glucose and 3% NaCl, 60 µg/mL gentamicin is insufficient to supress *S. aureus* isolates.

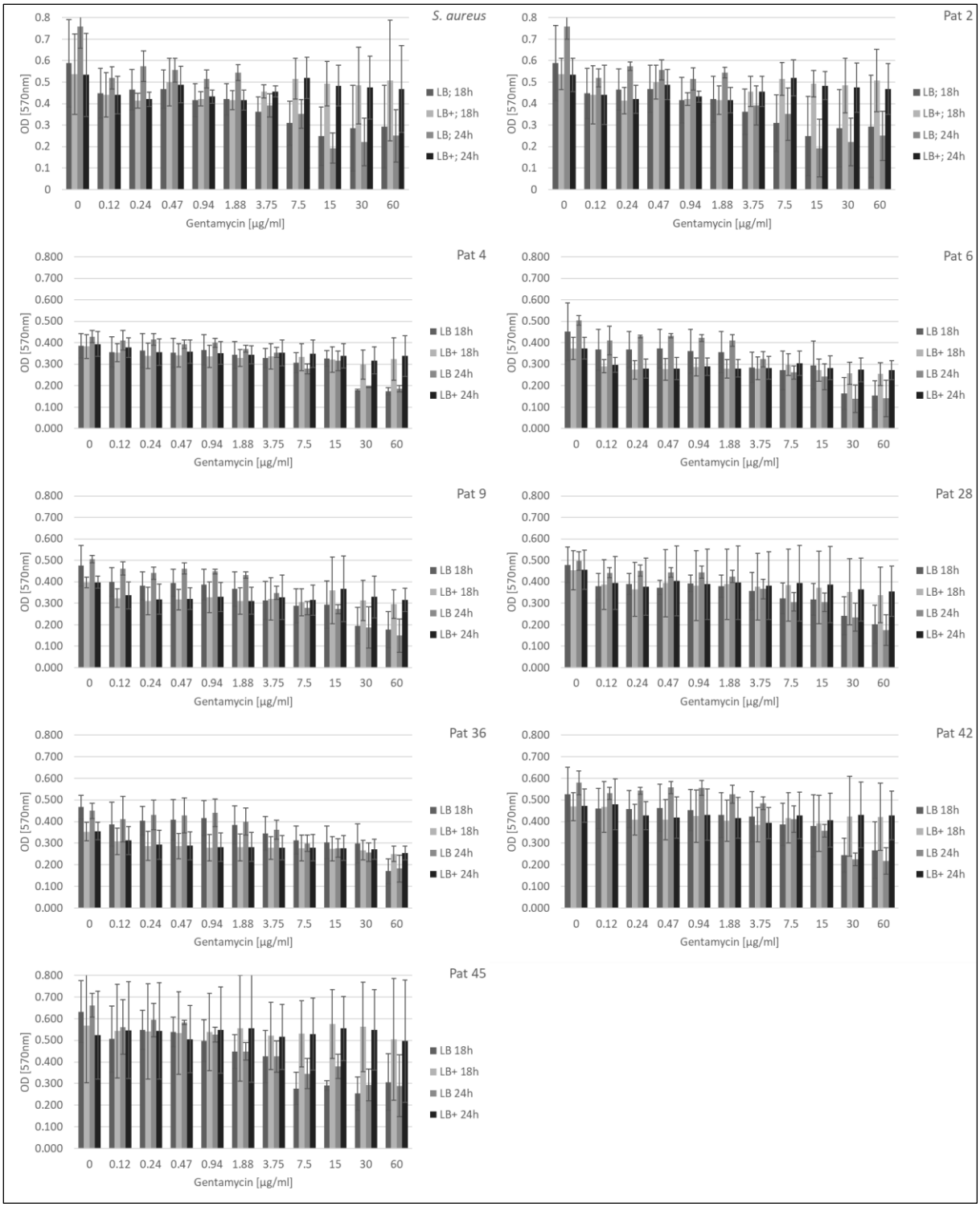

Figure 5. Gentamicin concentration test of *S. aureus* cultured in LB-medium and LB-medium supplemented with 0.5% glucose and 3% NaCl. *S. aureus* isolates cultured with two different media in 96-well plate. The concentrations of gentamicin from 0 to 60 µg/mL were added. OD_{570} was measured after incubating for 18 h and 24 h. *LB: LB-medium; LB+: LB-medium supplemented with 0.5% glucose and 3% NaCl.*

3.2.2 Biofilm formation as determined by crystal violet assay

Through crystal violet staining, biofilm formation was examined for all isolates in two different media: LB-medium and LB-medium supplemented with 0.5% glucose and 3% NaCl. The *S. aureus* isolates were cultured in the 96-well plates. After one day, OD_{570} was measured before staining. Then, biofilm formed in each well was measured using crystal violet staining, washing with PBS, eluting with 100% ethanol and quantifying by OD_{570}. Comparing the two results in Figure 6, it can be seen that LB-medium supplemented with 0.5% glucose and 3% NaCl seems to be able to promote the development of biofilm formation in most but not all isolates. It is noticeable that isolates Pat 2 and 4, which did not start to form a stainable biofilm, showed an inducible resistance to gentamycin under this condition.

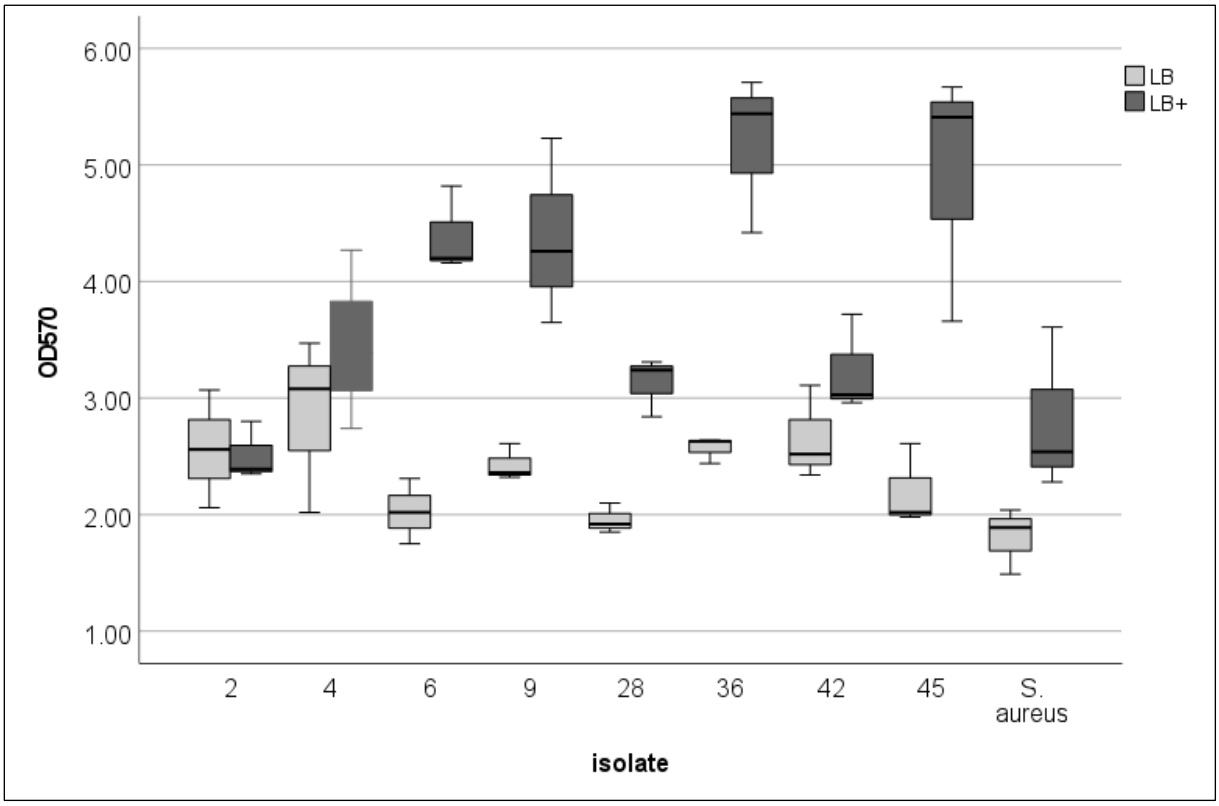

Figure 6. Crystal violet staining for biofilm formation assay. The *S. aureus* isolates were cultured in the 96-well plates with two different media: LB-medium and LB-medium supplemented with 0.5% glucose and 3% NaCl. After one day, OD_{570} was measured before staining. Then, biofilm formed in each well was measured using crystal violet staining, washing with PBS, eluting with 100% ethanol and quantifying by OD_{570}. *LB: LB-medium; LB+: LB-medium supplemented with 0.5% glucose and 3% NaCl.*

3.2.3 Crystal violet staining of biofilm formation on metal plates with LB-medium supplemented with 0.5% glucose and 3% NaCl

The formation of biofilms on metal plates were examined and quantified for all isolated *S. aureus*. After coating the plates with 20% human plasma in a carbonate buffer (pH 8.4) for 24 h at 4°C with mild shaking, the plates were washed with PBS and dried under the bench. In order to inoculate the plates with bacteria, plates were immersed into a bacteria solution in PBS over a period of 5 min. Bacteria that did not attach during this time were washed away in sterile PBS. Then the plates were placed in 50 mL reaction tubes with filter lid and incubated in LB-medium supplemented with 0.5% glucose and 3% NaCl for 24 h at 37 °C and slightly shaking. Growing biofilm were characterized with respect to amount of biofilm (crystal violet staining). Following elution of the crystal violet staining, 100 µL sample with 900 µL 100% ethanol were transferred into a cuvette for spectroscopy and the OD_{600} was measured. The data showed in Figure 7 indicates that *S. aureus*, Pat 36, 42, and 45 act more quickly in biofilm formation when compared with the other isolates.

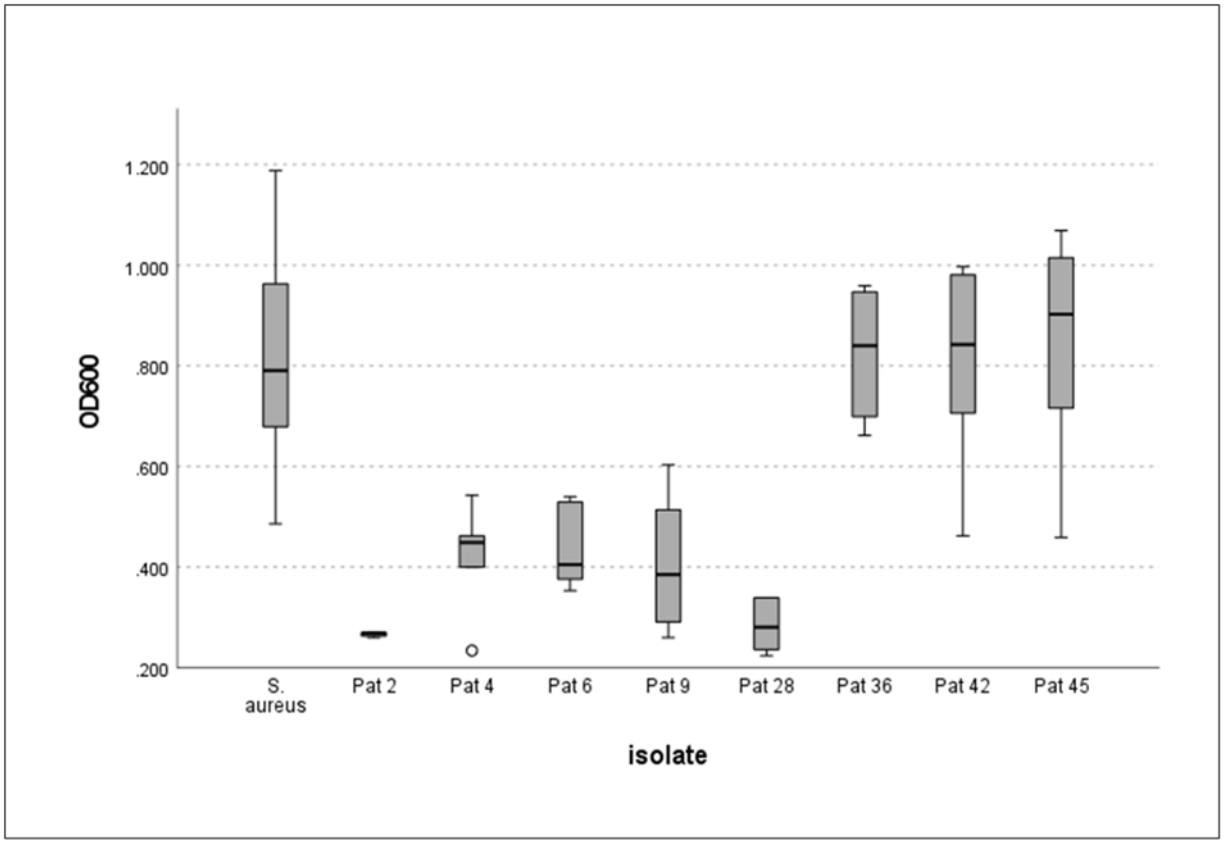

Figure 7. Crystal violet staining of biofilm formation on metal plates with LB-medium supplemented with 0.5% glucose and 3% NaCl. After coating metal plates with 20% human plasma in a carbonate buffer (pH 8.4) for 24 h at 4°C with mild shaking, plates were immersed into a bacteria solution in PBS over a period of 5 min. Then the plates were placed in 50 mL reaction tubes with filter lid and incubated in LB-medium supplemented with 0.5% glucose and 3% NaCl over a period of one day at 37 °C and slightly shaking. Growing biofilm was characterized using crystal violet staining.

3.2.4 Fluorescent microscopy

The formation of biofilms on metal and plastic plates were examined and quantified for *S. arueus* ATCC 29213. After coating the plates with 20% human plasma in a carbonate buffer (pH 8.4) for 24 h at 4°C with mild shaking, the plates were washed with PBS and dried under the bench. In order to inoculate the plates with bacteria, plates were immersed into a bacteria solution in PBS over a period of 5 min. Bacteria that did not attach during this time were washed away in sterile PBS. Then the plates were placed in 50 mL reaction tubes with filter lid and incubated in different media over a period of 3 days at 37 °C and slightly shaking. Growing biofilm was characterized using WGA staining. As is shown in Figure 8, relative staining areas on PE plates are bigger than that on metal plates. For the same kind plate in different media, relative staining areas of plates in optimized biofilm conditions are lagger when compared with that in LB-medium. However, this is only significant with PE plates.

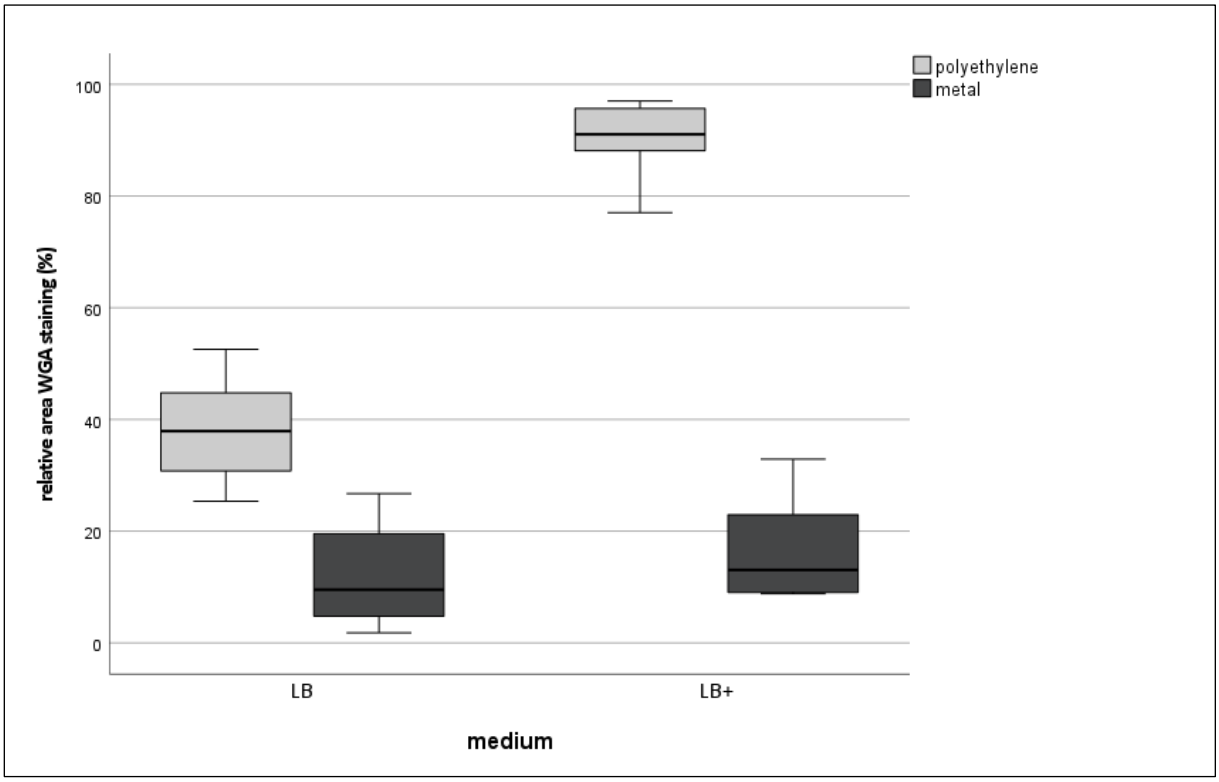

Figure 8. Wheat germ agglutinin (WGA) staining of biofilm formation on metal and plastic plates in different media. After coating the plates with 20% human plasma in a carbonate buffer (pH 8.4) for 24 h at 4°C with mild shaking, plates were immersed into a bacteria solution in PBS over a period of 5 min. Then the plates were placed in 50 mL reaction tubes with filter lid and incubated in different media over a period of 3 days at 37 °C and slightly shaking. Growing biofilm was characterized using WGA staining. *LB: LB-medium; LB+: LB-medium supplemented with 0.5% glucose and 3% NaCl.*

3.3 Establishment of adhesion and invasion assay models

In order to clarify the role of cell invasion and intracellular growth of *S. aureus* in osteoblasts, we first established an infection assay model using the cell lines MG63 and SaOS2 and *S. arueus* ATCC 29213. The assay was designed in such a way that first adhesion and then invasion could be analysed.

3.3.1 Adhesion to osteoblast cell lines

In order to analyse the adhesion of *S. aureus* to osteoblast cell lines, MG63 and SaOS2 cells were seeded into 6-well plates and cultured towards confluence. Then a washed suspension of *S. aureus* - harvested in the stationary growth phase - was added and incubated. Over a period of 30 min, unattached cells were washed away. As shown in Figure 9, adhesion of *S. aureus* increases with time when SaOS2 cell line was used in the assay. Here, the significance was reached after 30 min of incubation.

Furthermore, at every time point tested, there was a difference between the SaOS2 and the MG63, with a significant higher adhesion rate of SaOS2 towards MG63.

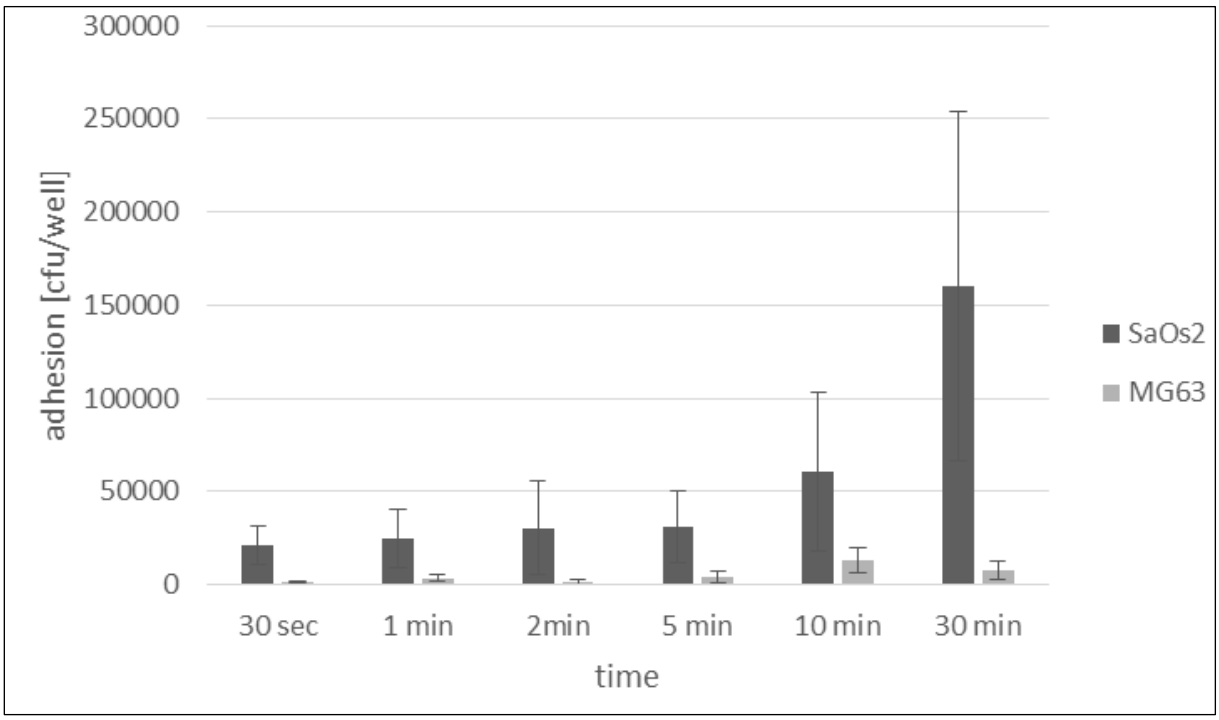

Figure 9. Influence of time on the adhesion of *S. aureus* on osteoblast cell lines. Confluent layers of osteoblast cell lines SaOS2 and MG63 were incubated with *S. aureus* ATCC 29213 over different time. Subsequently, non-adherent cells were washed. Adherent cells were released by means of cell lysis and plated out in order to determine the colony forming.

Based on this result we next analysed whether the growth phase has an influence on the adherence of *S. aureus* on osteoblasts. Therefore, we repeated the previous experiment using *S. aureus* harvested during the logarithmic growth phase. As shown in Figure 10, *S. aureus* from the stationary growth phase showed a stronger adherence towards osteoblasts as compared to cells harvested in the logarithmic growth phase. However, this finding was not statistically significant.

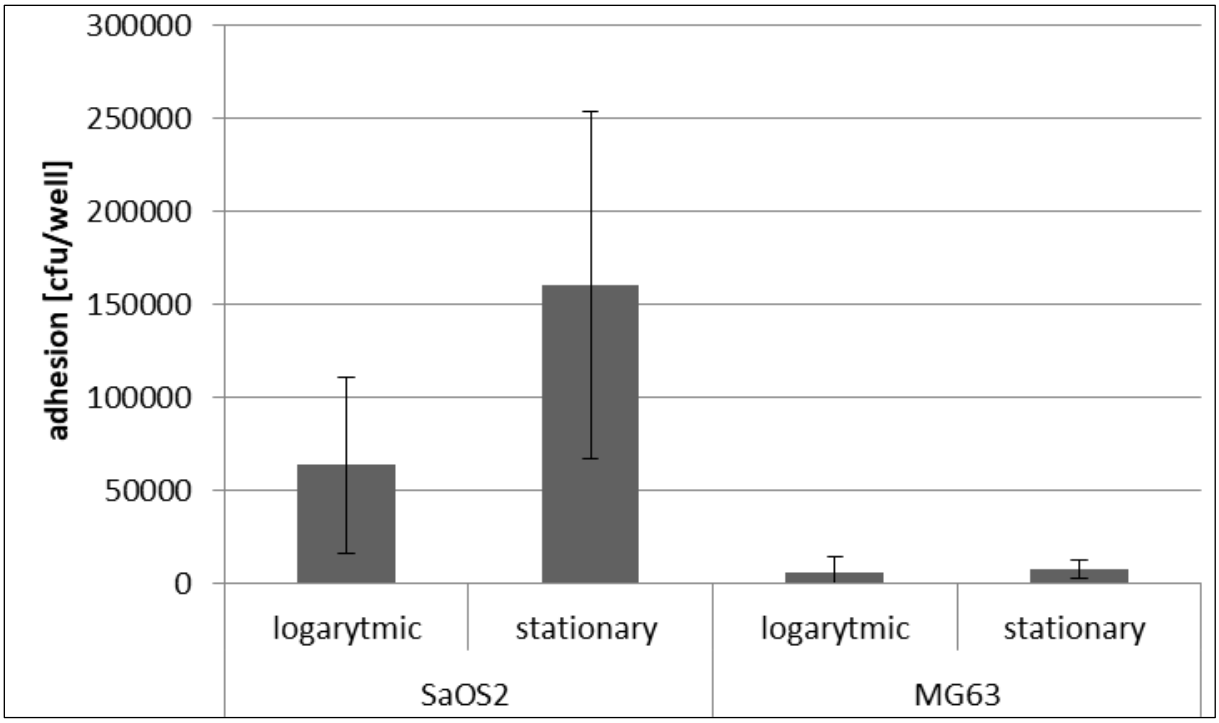

Figure 10. Influence of growth phase on the adhesion of *S. aureus* on osteoblast cell lines. Confluent layers of osteoblast cell lines SaOS2 and MG63 were incubated with *S. aureus* harvested during both the logarithmic (4 h) and the stationary (overnight) growth phase for 30 min. Then, non-adherent cells were washed with PBS. Adherent cells were released by means of cell lysis and plated out in order to determine the colony forming.

3.3.2 Invasion (internalization) of *S. aureus* into osteoblasts

In order to determine the number of *S. aureus* which were able to invade the osteoblast cell lines, gentamycin was added to the assay, 30 min after the bacterial suspension in order to kill the bacteria which were not internalized by the osteoblast cell lines. After 30 min, more bacteria were found in SaOS2 (p=0,007) and MG63 (p= 0,086), when compared to the negative control (blank well without osteoblasts) (Figure 11). Furthermore, it should be noticed that only a small percentage of *S. aureus* was able to invade the osteoblasts as compared to the adhesion assay. This finding was independent of the osteoblast cell line.

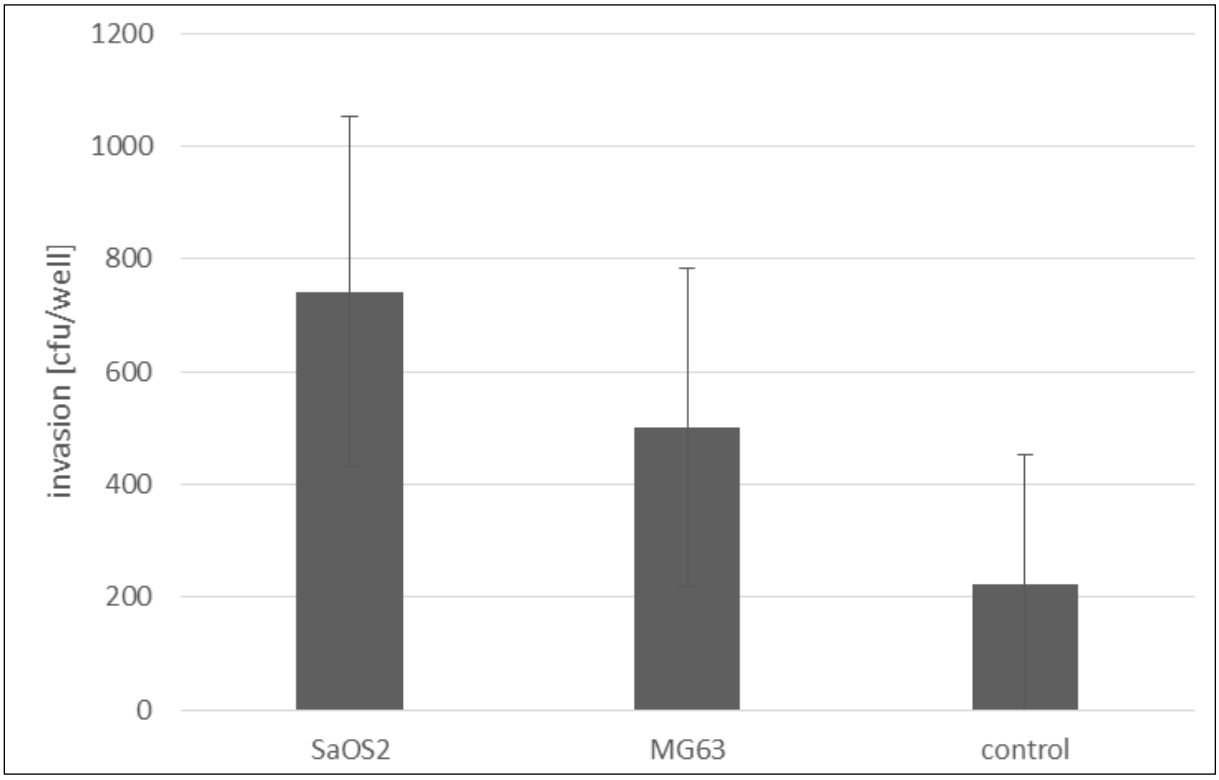

Figure 11. Invasion of *S. aureus* into osteoblast cell line SaSO2 and MG63 as compared to the control. Confluent layers of osteoblast cell lines SaOS2 and MG63 were incubated with *S. aureus* harvested in stationary phase for 30 min. Then, non-adherent cells were washed with PBS. DMEM supplemented with 10% FCS and 30 µg/mL gentamicin was used as culture medium to kill only the remaining extracellular bacteria without affecting the intracellular bacteria. Adherent cells were released by means of cell lysis and plated out in order to determine the colony forming.

3.3.3 Survival of *S. aureus* in osteoblast cells

Based on the infection we next analysed the survival of *S. aureus* in the respective cell lines over a period of three days. As shown in Figure 12, the colony forming units of *S. aureus* decreased within 3 days, when cultured in the cell line SaOS2, while in MG63, *S. aureus* survived over a period of 3 days.

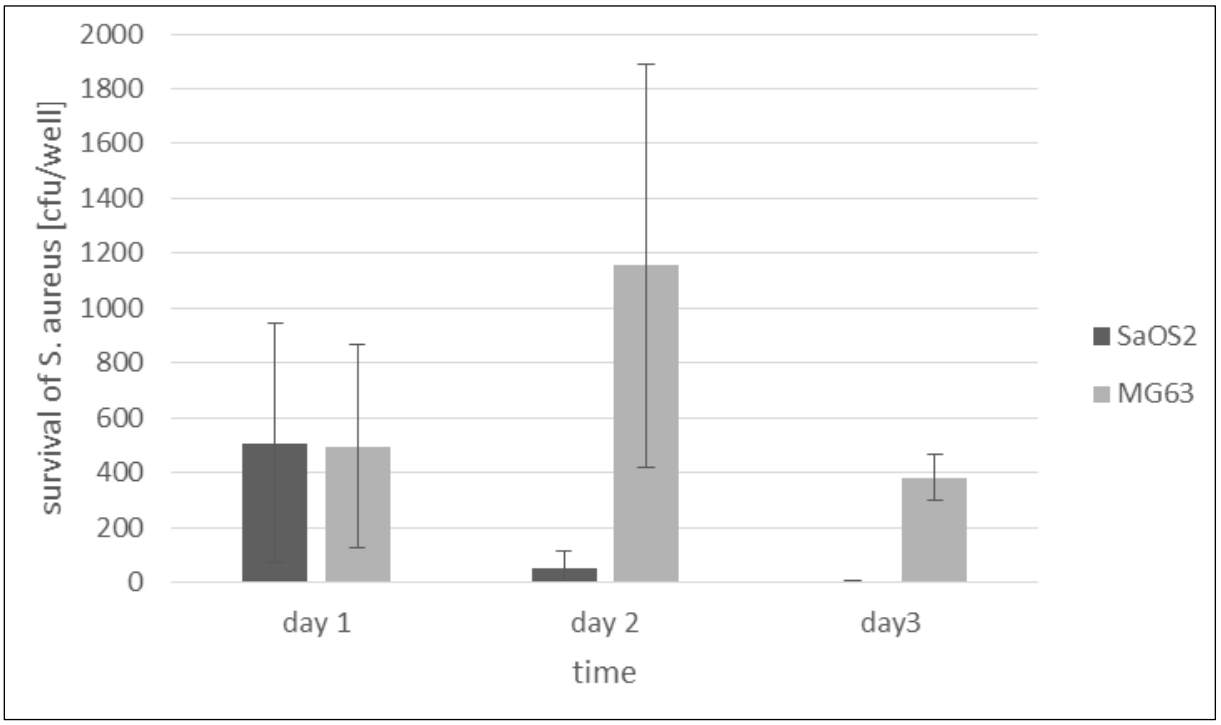

Figure 12. Survival of *S. aureus* in the cell lines SaOS2 and MG63. Confluent layers of osteoblast cell lines SaOS2 and MG63 were incubated with *S. aureus* harvested in stationary phase for 30 min. Then, non-adherent cells were washed with PBS. DMEM supplemented with 10% FCS and 30 µg/mL gentamicin was used as culture medium to kill only the remaining extracellular bacteria without affecting the intracellular bacteria. On each day for 3 days, adherent cells were released by means of cell lysis and plated out in order to determine the colony forming.

3.3.4 Survival of osteoblasts after infection with *S. aureus*

In order to see if the osteoblast were killed by bacteria in the experiment above, we performed MTT assay to get a result of the metabolic activity. Over 3 days, the metabolic activity was found to be equal, independent of the presence of bacteria. Although MG63 had higher metabolic activity, no difference was identified between the infected and control groups (Figure 13).

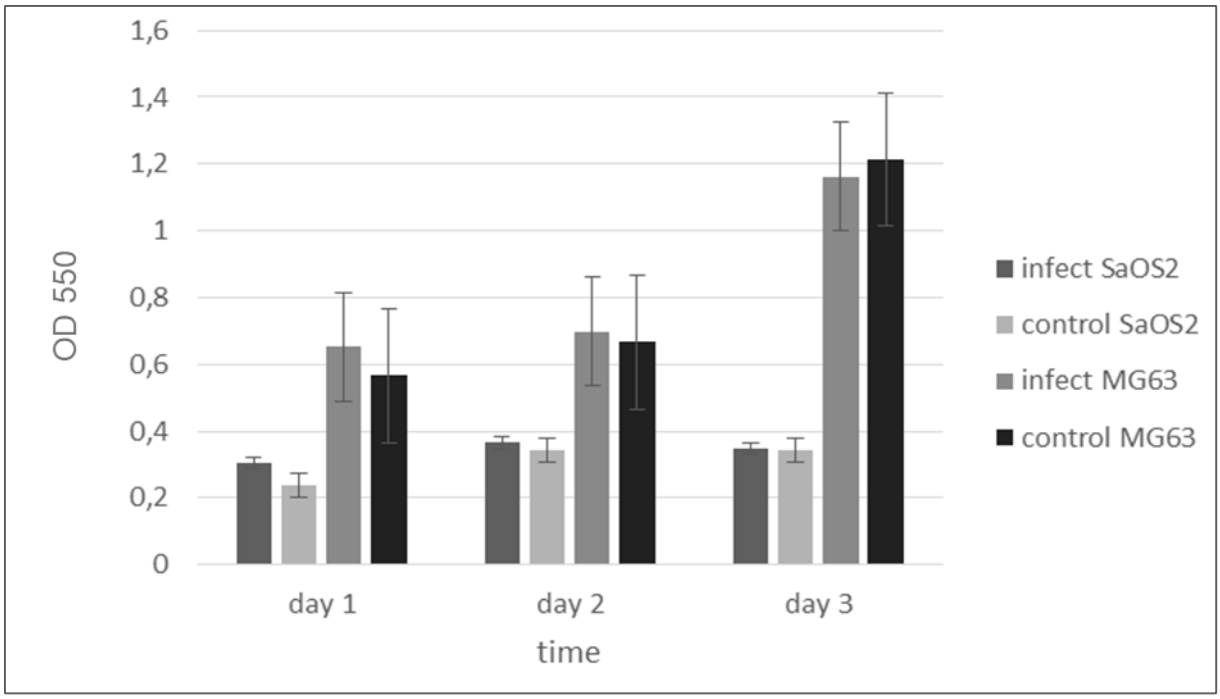

Figure 13. Metabolic activity of the cell lines SaOS2 and MG63 with and without infection with *S. aureus* as determined by MTT assay. Confluent layers of osteoblast cell lines SaOS2 and MG63 were incubated with *S. aureus* harvested in stationary phase for 30 min. Then, non-adherent cells were washed with PBS. DMEM supplemented with 10% FCS and 30 µg/mL gentamicin was used as culture medium to kill only the remaining extracellular bacteria without affecting the intracellular bacteria. Both SaOS2 and MG63 osteoblast cell lines without infection were used as control. After a period of 1 day, 2 days and 3 days, the culture medium was removed and 1 mL (5 mg/mL in PBS) MTT reagent was used. Then, the osteoblasts were incubated at 37 °C for at least 4 h. After incubation, 1 mL DMSO was added to the osteoblasts well. The resulting purple solution was diluted with DMSO and spectrophotometrically measured with OD_{550}.

3.4 Characterization of patient isolates with respect to cell adherence and infection

3.4.1 Adhesion of *S. aureus* isolates on osteoblasts

In order to characterise the ability of the *S. aureus* isolates to adhere to osteoblasts, confluent cell layers of SaOS2 or MG63 were incubated over a period of 30 min with a bacteria suspension, harvested during stationary growth phase. Adhesion to the cell lines was compared to adherence to 6-well plate as control. As shown in Figure 14, isolates Pat 2, 4, 6, 9, 28 and 42 showed comparable adherence to cells or plastic, although the adherence of Pat 42 was approximately 30 times higher as the other. Isolates Pat 36 and Pat 45 showed significant more adherence to cells as compared to the empty bottom of 6-well plates. Among the strains tested, isolate Pat 36 ad *S. aureus* ATCC 29213 differed in the ability to adhere to SaOS2 or MG63.

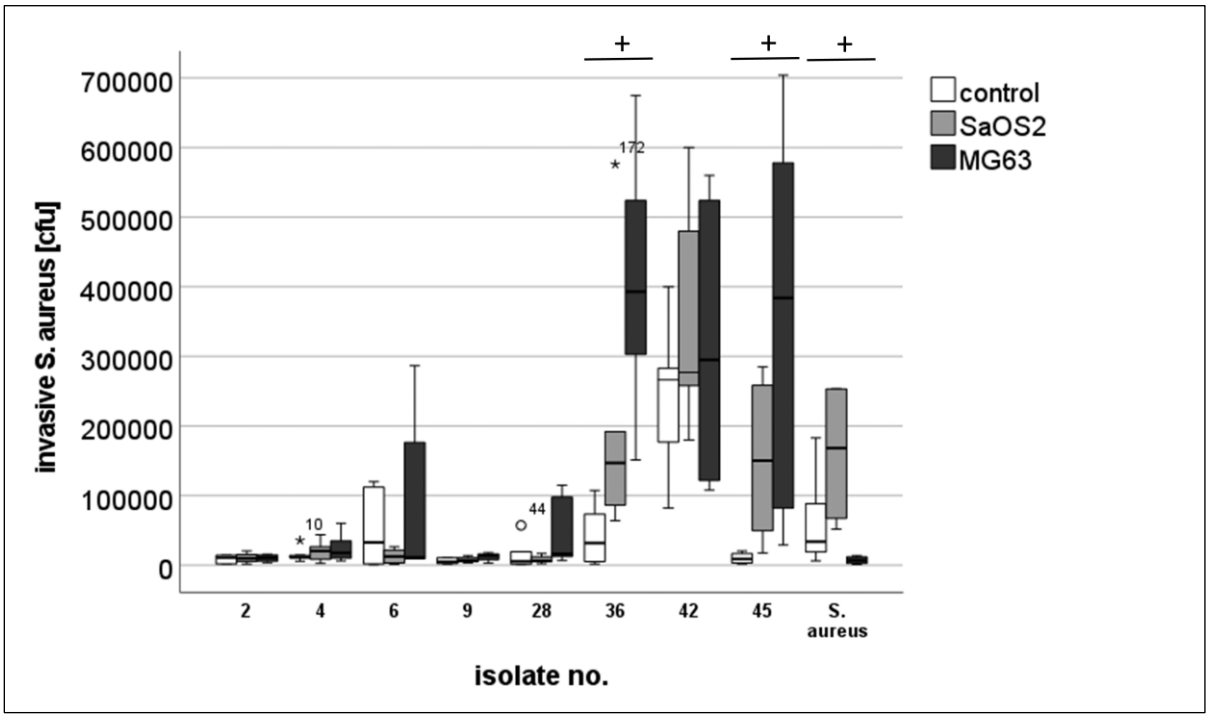

Figure 14. Adhesion of *S. aureus* isolates on osteoblast like cell lines. Cell lines SaOS2 and MG63 were grown to confluence in 6-well plates and then incubated with PBS washed *S. aureus* isolates from stationary growth phase. After 30 min non-adhered bacteria were washed away with PBS. Then osteoblasts were lysed and released bacteria were plated on LB-agar in order to determine colony-forming units.

3.4.2 Role of adhesion proteins in the internalization process of *S. aureus* isolates

Presence of genes for adhesion molecules in isolates and S. aureus. In order to identify the molecule or the genetic background differences that characterize the isolates, we next analysed the occurrence frequency of selected genes involved in the adhesion process. PCR was performed with primers listed in Table 1 and electrophoresis was performed with 1% agarose gels. ETHBR was used as DAN- binding fluorescent dye. After electrophoresis, gels were visualized under UV light and photographed. Taking isolate Pat 9 as an example (Figure 15), the PCR results showed the expression of corresponding genes: bbp (-), cna (+), eno (+), ebp (+), fnbB (-), fnbA (+), fib (-), clfA (+), clfB (+), ebpS (+), psmA (+), psmB (+), eap (+), sdrD (+), fmtB (+) and ebh (+). As is shown in Table 6, the eno, fnbA, clfA, clfB, ebpS, psmA, psmB, eap, sdrD, fmtB and ebh genes were present in 100% of all *S. aureus*.

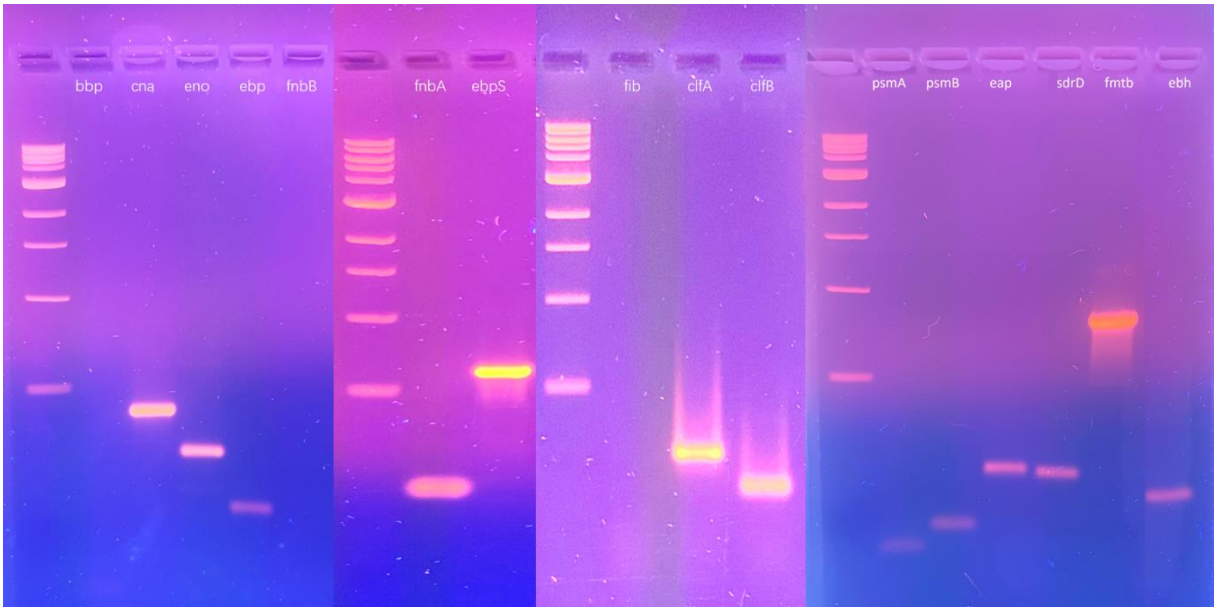

Figure 15. Presentation of genes involved in adhesion with respect to isolate Pat 9. PCR was performed with primers listed in Table 1 and electrophoresis was performed through 1% agarose gels with ETHBR as described above. After electrophoresis, gels were visualized under UV light and photographed.

Table 6. Genes of adhesion proteins present in *S. aureus* isolates.

Pat No. / Primer	Pat 2	Pat 4	Pat 6	Pat 9	Pat 28	Pat 36	Pat 42	Pat 45	*S. aureus*
bbp	+	-	-	-	-	-	-	-	-
cna	-	+	+	+	-	-	-	-	-
eno	+	+	+	+	+	+	+	+	+
ebp	-	-	+	+	+	-	+	+	+
fnbA	+	+	+	+	+	+	+	+	+
fnbB	-	-	-	-	-	+	-	-	-
fib	+	-	-	-	+	+	+	+	+
clfA	+	+	+	+	+	+	+	+	+
clfB	+	+	+	+	+	+	+	+	+
ebpS	+	+	+	+	+	+	+	+	+
psmA	+	+	+	+	+	+	+	+	+
psmB	+	+	+	+	+	+	+	+	+
eap	+	+	+	+	+	+	+	+	+
sdrD	+	+	+	+	+	+	+	+	+
fmtB	+	+	+	+	+	+	+	+	+
ebh	+	+	+	+	+	+	+	+	+

bbp (encoding bone sialoprotein binding protein), cna (collagen binding protein), eno (laminin binding protein), fnbA and fnbB (fibronectin binding proteins A and B), fib (fibrinogen binding protein), clfA and clfB (clumping factors A and B), ebpS (elastin binding protein); psmA and psmB (Phenol-soluble modulins A and B); arcB (ornithine carbamoyltransferase); eap (extracellular adherence protein); sdrD (SD-repeat containing protein D); fmtB (methicillin resistance determinant FmtB protein); ebh (extracellular matrix-binding protein).

Expression of corresponding adhesion proteins in S. aureus isolates. To further clarify if the corresponding genes were translated into proteins in our isolates and *S. aureus*, we next analysed the proteome profile of the *S. aureus* isolates cultured to stationary growth phase, using mass spectrometry. As shown in Table 7, the eno, fnbA, ebpS, psmB, and ebh proteins were expressed in 100% of all isolated *S. aureus*. However, clfA, psmA, sdrD, clfB, fmtB genes partially expressed.

Table 7. Mass spectrometry results of the corresponding adhesion proteins expressed in *S. aureus* isolates.

Pat No. / Protein	Pat 2	Pat 4	Pat 6	Pat 9	Pat 28	Pat 36	Pat 42	Pat 45	*S. aureus*
bbp	-	-	-	-	-	-	-	-	-
cna	-	-	-	+	-	-	-	-	-
eno	+	+	+	+	+	+	+	+	+
ebp	-	-	+	+	+	-	+	+	+
fnbA	+	+	+	+	+	+	+	+	+
fnbB	-	-	-	-	-	+	-	-	-
fib	+	-	-	-	+	+	-	-	-
clfA	+	-	+	+	+	-	+	-	+
clfB	-	-	-	-	+	-	-	-	-
ebpS	+	+	+	+	+	+	+	+	+
psmA	+	+	-	+	+	+	-	+	+
psmB	+	+	+	+	+	+	+	+	+
eap	-	-	-	-	-	-	-	-	-
sdrD	+	-	-	-	+	-	+	+	+
fmtB	-	-	-	-	+	+	-	+	+
ebh	+	+	+	+	+	+	+	+	+

bbp (encoding bone sialoprotein binding protein), cna (collagen binding protein), eno (laminin binding protein), fnbA and fnbB (fibronectin binding proteins A and B), fib (fibrinogen binding protein), clfA and clfB (clumping factors A and B), ebpS (elastin binding protein); psmA and psmB (Phenol-soluble modulins A and B); arcB (ornithine carbamoyltransferase); eap (extracellular adherence protein); sdrD (SD-repeat containing protein D); fmtB (methicillin resistance determinant FmtB protein); ebh (extracellular matrix-binding protein).

3.4.3 Expression of genes for adhesion in *S. aureus* isolates

The qPCR technique was applied to analyse the gene expression. The cDNA was synthesized using an iScript cDNA synthesis kit after RNAs were extracted and quantified spectrometrically. Real time amplification was conducted with specific primers. Gene expression rates were calculated using delta-delta Ct method from corresponding threshold cycles after melting-curve analysis. In Figure 16, the genes eno, fnbA, clfB and ebpS were found to be overexpressed not only in the adhesive *S. aureus*, but also in non-adhesive isolates. However, clfA might be the best candidate gene because it was overexpressed only in the adhesive *S. aureus* (Pat 36, 42, 45 and *S. aureus* ATCC 29213).

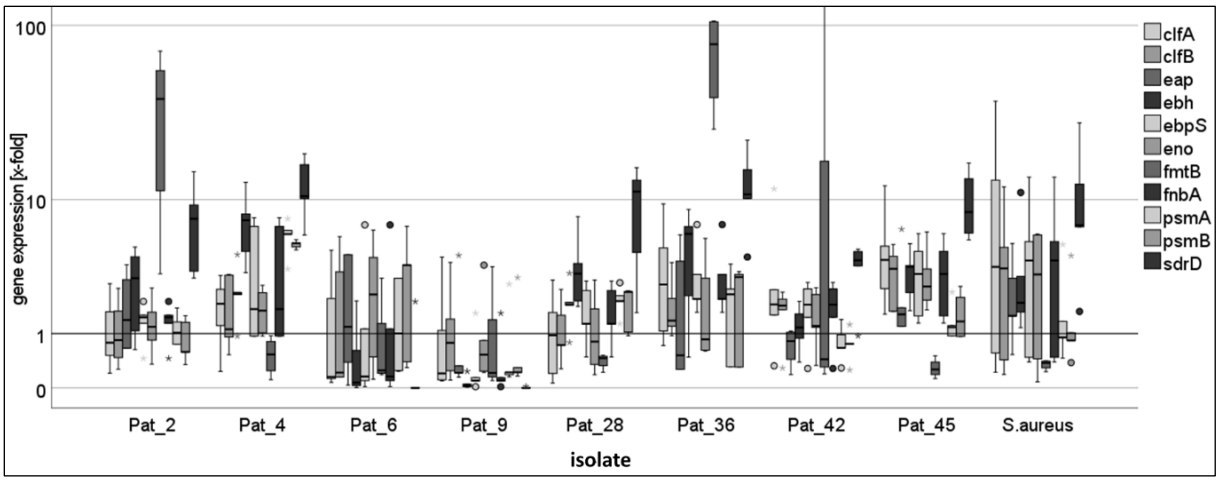

Figure 16. Specific gene expression rates for adhesion in *S. aureus* isolates. Isolate's cDNA was synthesized (5 min at 25 °C, 30 min at 42 °C and 5 min at 85 °C) using an iScript cDNA synthesis kit after RNA was extracted and quantified spectrometrically. Real time amplification was conducted (30 sec at 95 °C followed by 40 cycles of 15 sec at 95 °C, 35 sec at 55 °C, and 15 sec at 95 °C, then kept at 65 °C for 10 sec and at last, temperature was increased from 65 °C to 95 °C in 30 min) with specific primers. Gene expression rates were calculated using delta-delta Ct method from corresponding threshold cycles after melting-curve analysis.

3.4.4 Adhesion of *S. aureus* isolates cultured in biofilm conditions on osteoblasts

In order to study the influence of the growth medium on the ability of *S. aureus* isolates to adhere to osteoblasts, confluent cell layers of SaOS2 or MG63 were incubated for 30 min with selected isolates (Pat 9, Pat 36, and *S. aureus* ATCC 29213) which were previously grown overnight at 37 °C in four different media: LB-medium, LB-medium supplemented with 0.5% glucose solution, LB-medium supplemented with 3% NaCl solution, LB-medium supplemented with 0.5% glucose and 3% NaCl solutions and harvested during stationary growth phase. From here, either the cells were infected or the mRNA was isolated and qPCRs were used to quantify the expression of the genes mentioned in Table 1. As shown in Figure 17, modifications of the medium led to a reduction of cell adhesion. In particular, the combination of glucose and NaCl affected all tested strains. A difference between the infected osteoblast cell lines was observed only in case of *S. aureus* ATCC 29213. There was something provocative when combining the results of cell adhesion and gene expression level. Under the optimized biofilm condition, compared with LB-medium condition, most selected genes were overexpressed while the adhesion was drastically reduced with respect to isolate Pat 9. Similarly, under the condition of LB-medium supplemented with 3% NaCl solution, most selected genes were overexpressed whereas the adhesion was supressed with respect to isolate Pat 9 and Pat 36. Therefore, the cell adhesion and the gene expression under biofilm condition does not closely correlate.

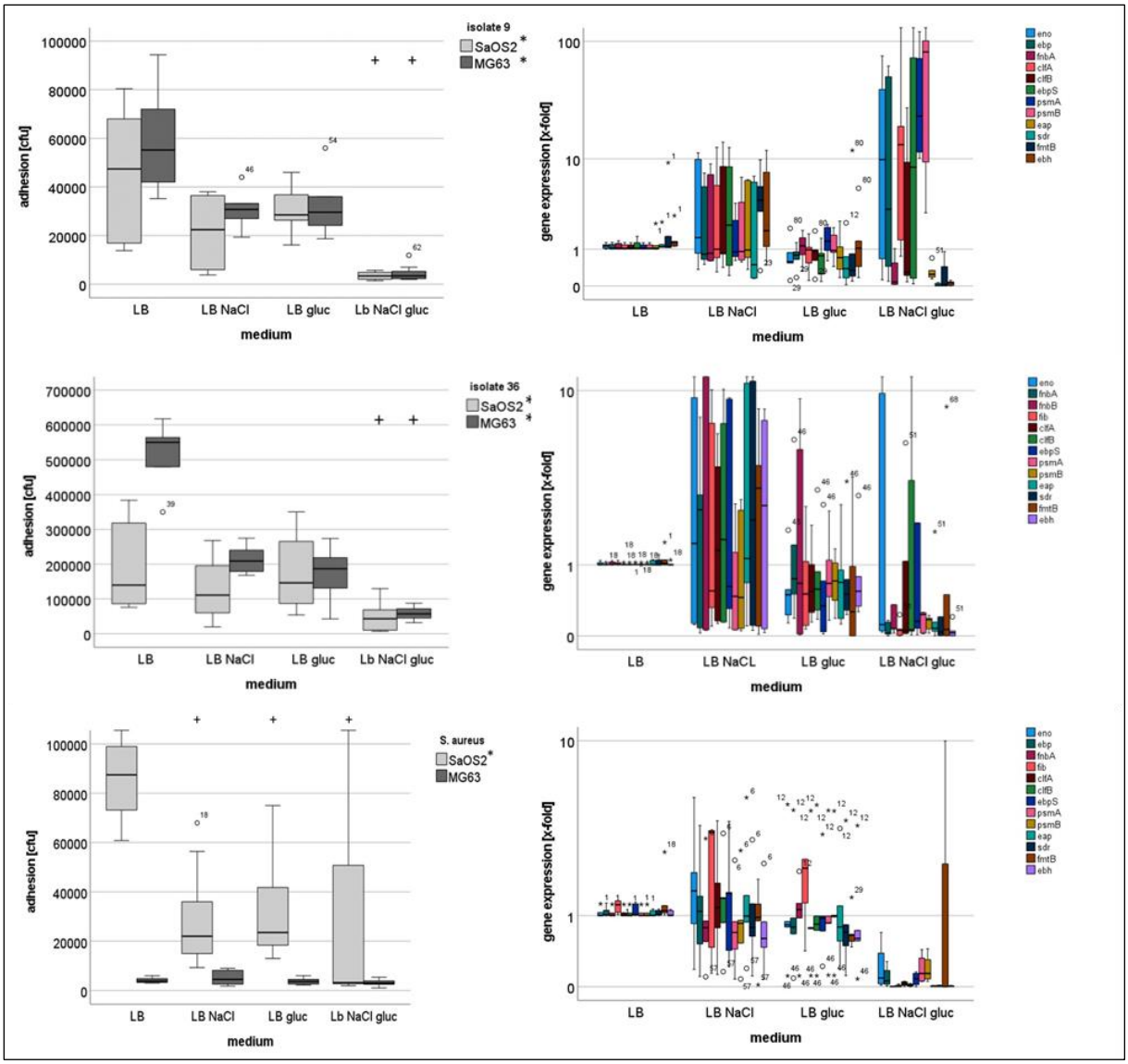

Figure 17. Adhesion and qPCR results of *S. aureus* isolates cultured in different media on osteoblast like cell lines. Cell lines SaOS2 and MG63 were grown to confluence in 6-well plates and then incubated with selected *S. aureus* isolates which were cultured in different media. After 30 min, non-adhered bacteria were washed away with 10x 1 ml PBS. Then osteoblasts were lysed and released bacteria were plated on LB-agar in order to determine colony-forming units (left). Gene expression of selected *S. aureus* isolates (Pat 9, Pat 36, and *S. aureus* ATCC 29213) after cultivation in different media (right). Focusing on the gene expressions level of genes possibly involved in adhesion, a non-uniform expression pattern was found. +: Significant difference when compared to LB-medium; *: Significant difference within one cell line.

3.4.5 Invasion of *S. aureus* isolates in SaOS2 and MG63

For the invasion assay, we also found that three *S. aureus* isolates (Pat 36, 42, 45) were able to invade efficiently the human cells (Figure 18). However, only Pat 42 in MG63 (p=0.023) and Pat 45 in SaOS2 (p=0.009) showed a statistically significant result for both human cells. *S. aureus* ATCC 29213 was only significant in SaOS2 (p=0.012). Pat 36, although the number of bacteria was high in both cell lines,

showed no statistical significance (p=0.376 in SaOS2; p=0.454 in MG63), thus indicating that invasion and adhesion might be independent from each other.

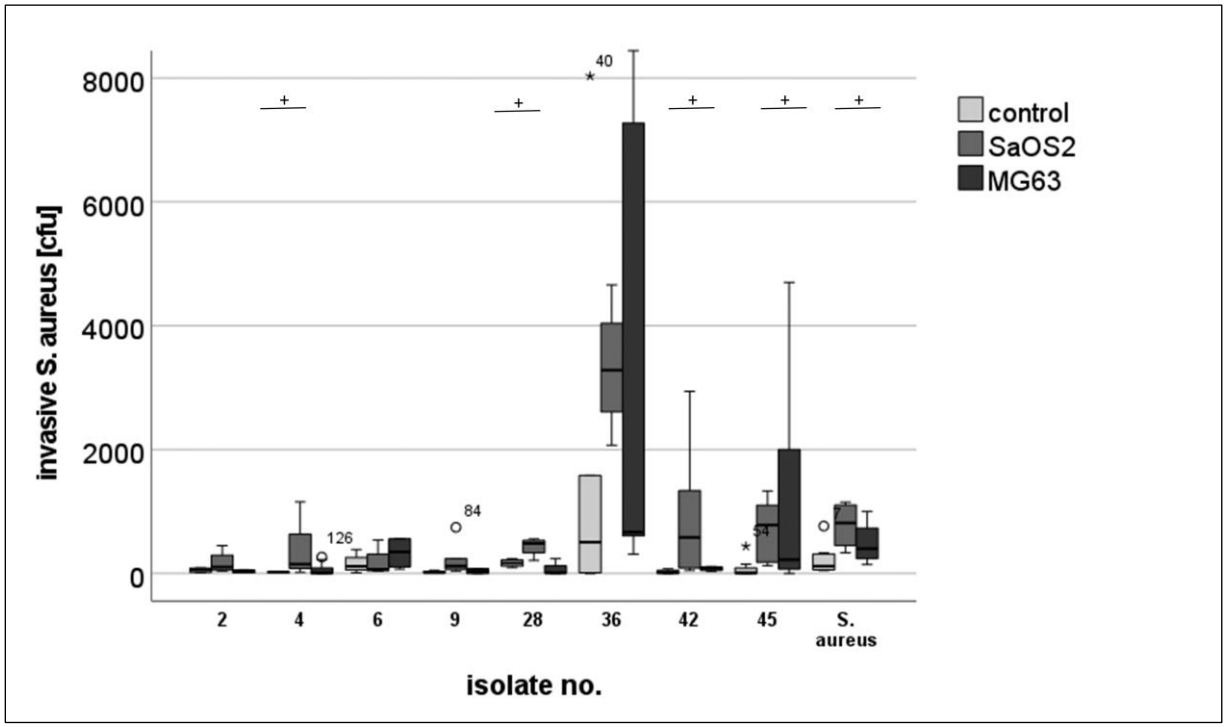

Figure 18. Invasion of all isolates in SaOS2 and MG63. Cell lines SaOS2 and MG63 were grown to confluence in 6-well plates and then incubated with PBS washed *S. aureus* isolates from stationary growth phase. After 30 min, non-adherent cells were washed with PBS. DMEM supplemented with 10% FCS and 30 µg/mL gentamicin was used as culture medium overnight to kill only the remaining extracellular bacteria without affecting the intracellular bacteria. Both SaOS2 and MG63 osteoblast cell lines without infection were also used as control. Then osteoblasts were lysed and released bacteria were plated on LB-agar in order to determine colony-forming units. +: Significant difference when compared to the control.

3.4.6 Survivals of *S. aureus in* osteoblast like cell lines

Focussing on the ability of *S. aureus* to survive in osteoblast like cells, *S. aureus* isolates were incubated together with SaOS2 or MG63 cell lines. In order to kill extracellular bacteria, gentamycin was added after adhesion of *S. aureus* isolates to the cell lines. Incubation was performed for 3 days at 37 °C with 5% CO_2 and 100% humidity. As shown in Figure 19, the survival was different for each osteoblast cell line and *S. aureus* isolate. Here isolates Pat 2, and 45 survived over 3 days in SaOS2 and were eliminated in MG63 cells. On the other hand, isolates Pat 4, 9, and *S. aureus* ATCC 29213 survived in MG63 and not in SaOS2. Both osteoblast cell lines eliminated isolates Pat 6, 42 and 28. Isolate Pat 36 survived in both cell lines and seemed to grow.

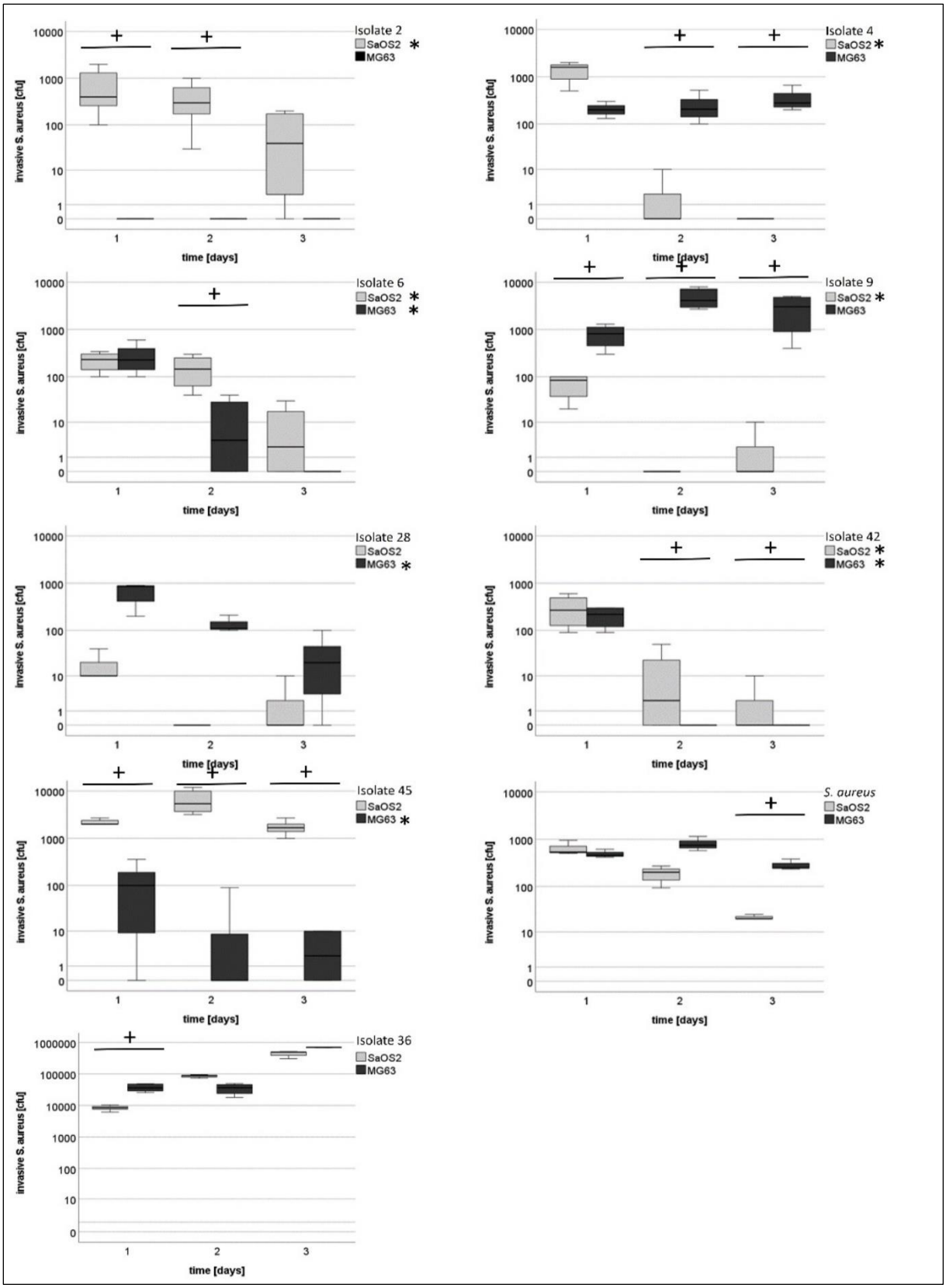

Figure 19. Survival of *S. aureus* isolates within osteoblast like cell lines. After adhesion of the bacteria to SaOS2 or MG63, gentamycin was added to the cells in order to kill extracellular bacteria. After one to three days, osteoblasts were lysed and released bacteria were plated on LB-agar in order to determine colony-forming units. +: Significant difference between SaOS2 and MG63; *: Significant difference during time course.

3.4.7 Survival of osteoblasts after infection

MTT assay was performed to determine the cell viability of osteoblasts after being infected by *S. aureus* isolates. The cell viability of both SaOS2 and MG63 cells was found to be nearly constant and independent of bacterial infection, thus suggesting that osteoblasts can survive after bacterial infection. As shown in Figure 20 below, the cell viability of MG63 cells was lower after being infected by Pat 9 and Pat 28 in comparison with SAOS2 cell line. Focusing on Pat 2, 4, 6, 36, 42, 45 and *S. aureus* ATCC 29213, significant difference between the two cell lines was observed only at some time points, as shown in Figure 20.

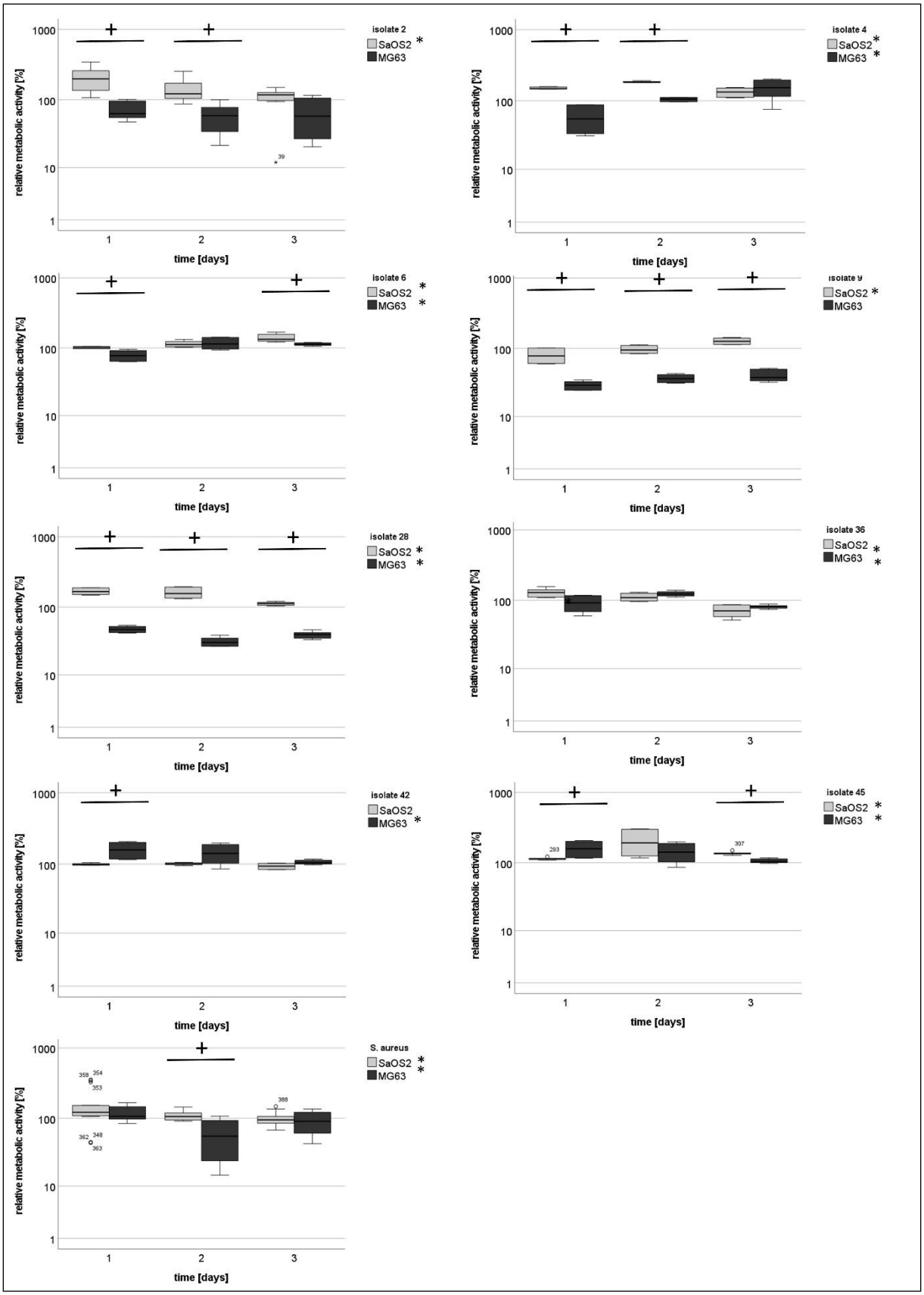

Figure 20. Metabolic activity of the cell lines SaOS2 and MG63 with and without infection with *S. aureus* as determined by MTT assay. Confluent layers of osteoblast cell lines SaOS2 and MG63 were incubated with *S. aureus* isolates harvested in stationary phase for 30 min. Then, non-adherent cells

were washed with PBS. DMEM supplemented with 10% FCS and 30 µg/mL gentamicin was used as culture medium to kill only the remaining extracellular bacteria without affecting the intracellular bacteria. Both SaOS2 and MG63 osteoblast cell lines without infection were also used as control. After a period of 1 day, 2 days and 3 days, the culture medium was removed and 1 mL (5 mg/mL in PBS) MTT reagent was used. Then, the osteoblasts were incubated at 37 °C for at least 4 h. After incubation, 1 mL DMSO was added to the osteoblasts well. The resulting purple solution was diluted with DMSO and spectrophotometrically measured with OD_{550}. +: Significant difference between SaOS2 and MG63; *: Significant difference during time course.

Respiration assay was performed to analyse the metabolic rate of the osteoblasts after being infected by different isolates. Isolates (Pat 9, Pat 36, *S. aureus* ATCC 29213) were selected to infect SaOS2 and MG63 cell lines. Both uninfected osteoblast cell lines were included as control. After 2 days, cells were harvested and the number of each individual sample was counted. The respiration rates of oxygen consumption of both infected and uninfected osteoblasts were measured at a proper time point. Data were collected and showed in Figure 21. In respiration assay, the metabolic activity of both SaOS2 and MG63 cell lines were stimulated after being infected with selected *S. aureus* isolates (Pat 9, 36 and *S. aureus* ATCC 29213).

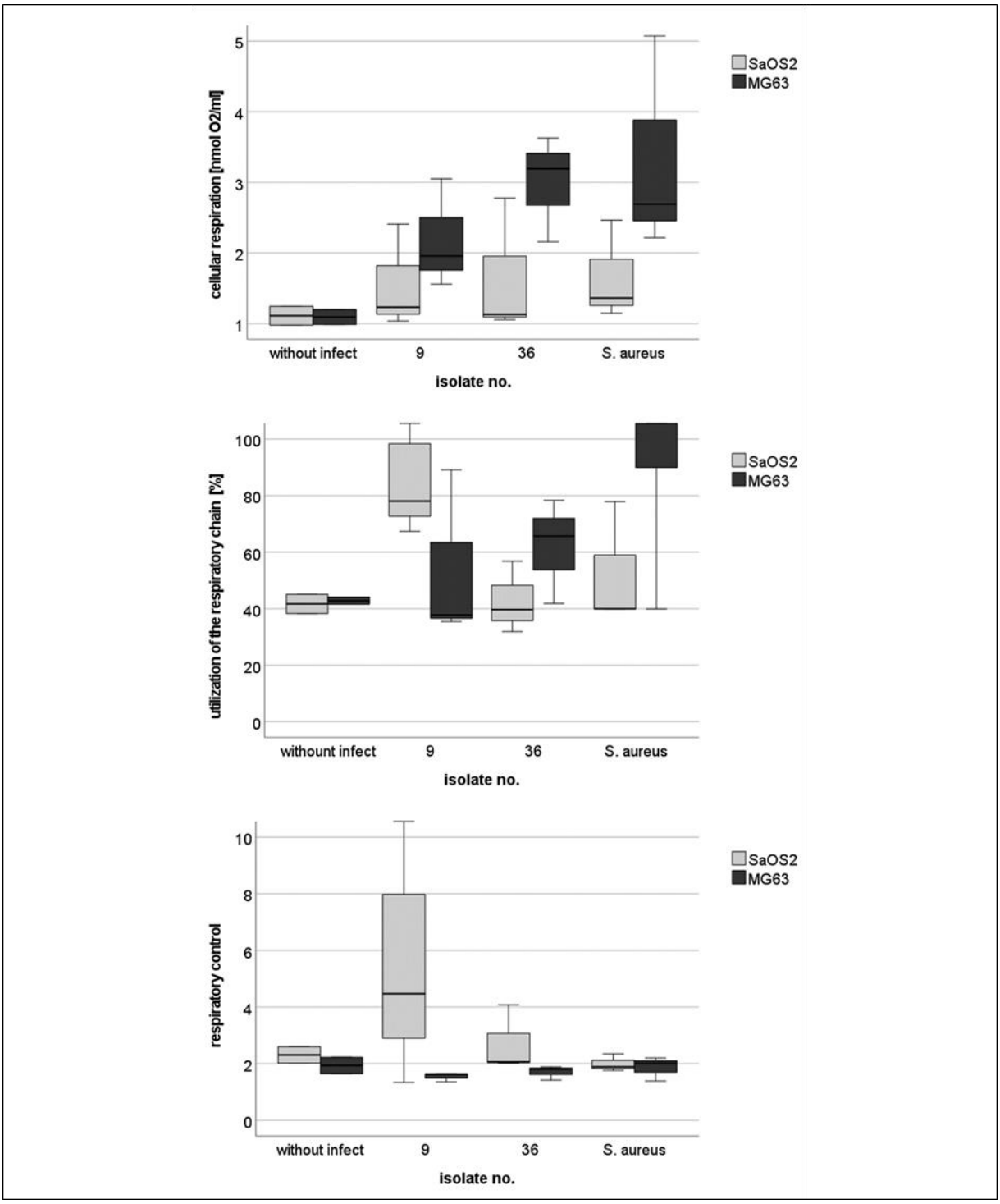

Figure 21. Role of respiration in survival of *S. aureus* isolates in osteoblast like cell lines. SaOS2 and MG63 osteoblast like cell lines were infected with *S. aureus* ATCC 29213 or clinical isolates and gentamycin was added to the cells in order to kill extracellular bacteria. After one day, respiration was determined by oxygen consumption.

3.4.8 Induction of autophagy in selected isolates

In order to clarify whether autophagy plays a role in the internalization process, SaOS2 and MG63 cell lines were pre-cultured for 24 h in DMEM without FCS to induce autophagy. Selected isolates (Pat 9,

Pat 36, Pat 42, Pat 45, and *S. aureus* ATCC 29213) were administered to infect SaOS2 and MG63 cell lines. DMEM without FCS, supplemented with 30 µg/mL gentamicin was used to kill the remaining extracellular bacteria. Infected cells were kept with DMEM without FCS for 3 days. The cells were then lysed and intracellular bacteria were plated out at 1 day, 2 days and at 3 days time point. From the data in Figure 22, it is apparent that only a small number of bacteria (except Pat 9) survived in both osteoblast cell lines after 1 day, and nearly no bacteria persisted after 2 or 3 days. Isolate Pat 9 survived much better after 1 day, but the number of bacteria decreased rapidly on day 2 and day 3.

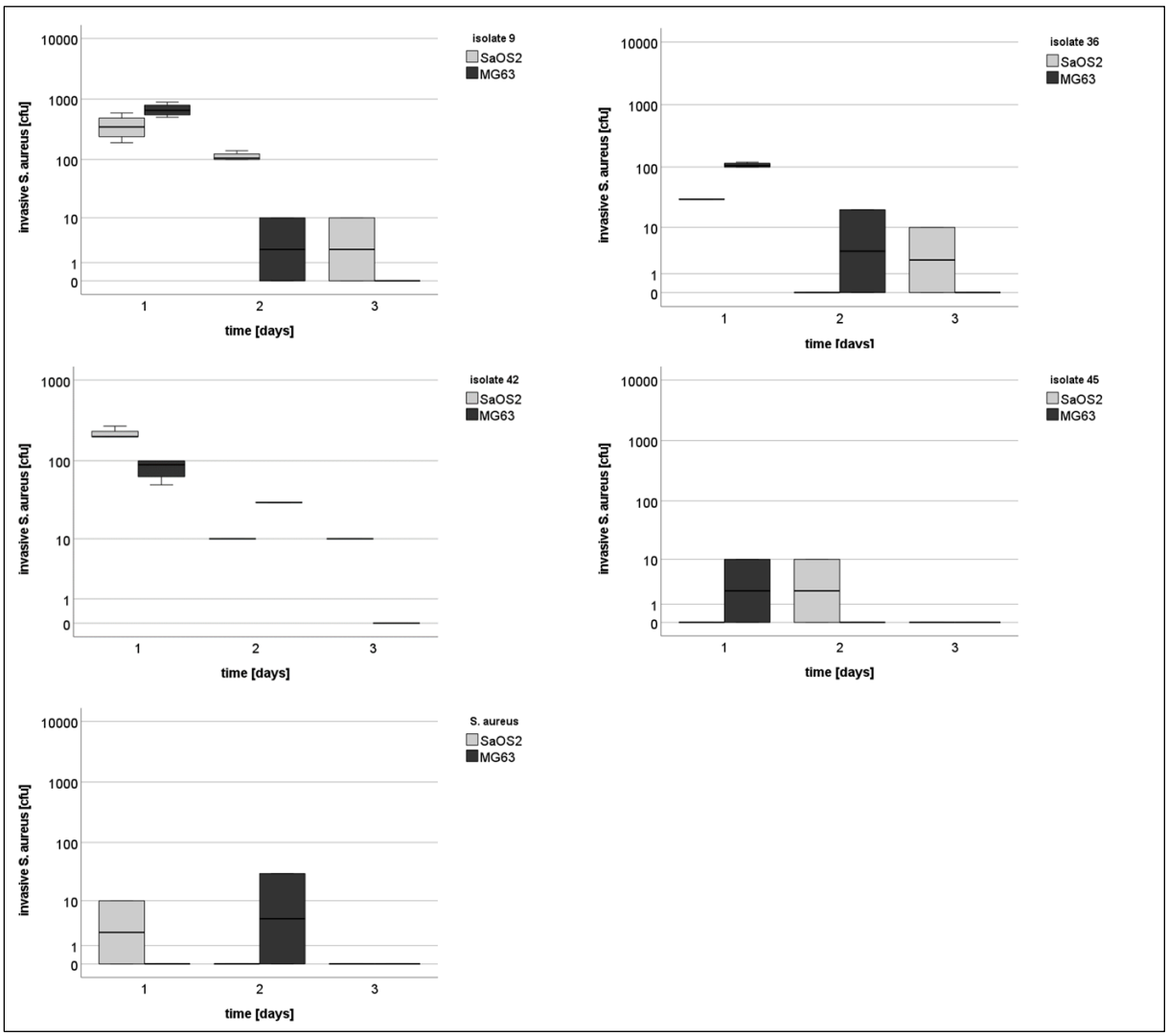

Figure 22. Role of autophagy induction in survival of *S. aureus* isolates in osteoblast like cell lines. SaOS2 and MG63 osteoblast like cell lines were cultured in serum free medium over a period of 24 h in order to induce autophagy. Then the cells were infected with *S. aureus* ATCC 29213 or clinical isolates and gentamycin was added to the cells in order to kill extracellular bacteria. After one to three days, osteoblasts were lysed and released bacteria were plated on LB-agar in order to determine colony-forming units.

3.4.9 Inhibition of autophagy by Bafilomycin A1

SaOS2 and MG63 cell lines were pre-cultured for 24 h with DMEM with 10% FCS and 500 pM BafA1 to inhibit autophagy. After washing the cells with PBS, isolates (Pat 9, Pat 36, Pat 42, Pat 45 and *S. aureus* ATCC 29213) were administered to infect both cell lines. After incubating over a period of 1 day, 2 days and 3 days with DMEM, 10% FCS and BafA1, cells were lysed and the intracellular bacteria were plated out and counted. A large number of bacteria survived in both osteoblast cell lines after 1 day, and then decreased gradually on day 2 and day 3, indicating that the effect of BafA1 is not long lasting. This result highlights that autophagy inhibition sustains bacteria survival in comparison with the results obtained from autophagy active cells, which caused a significant reduction of the number of intracellular bacteria (Figure 23).

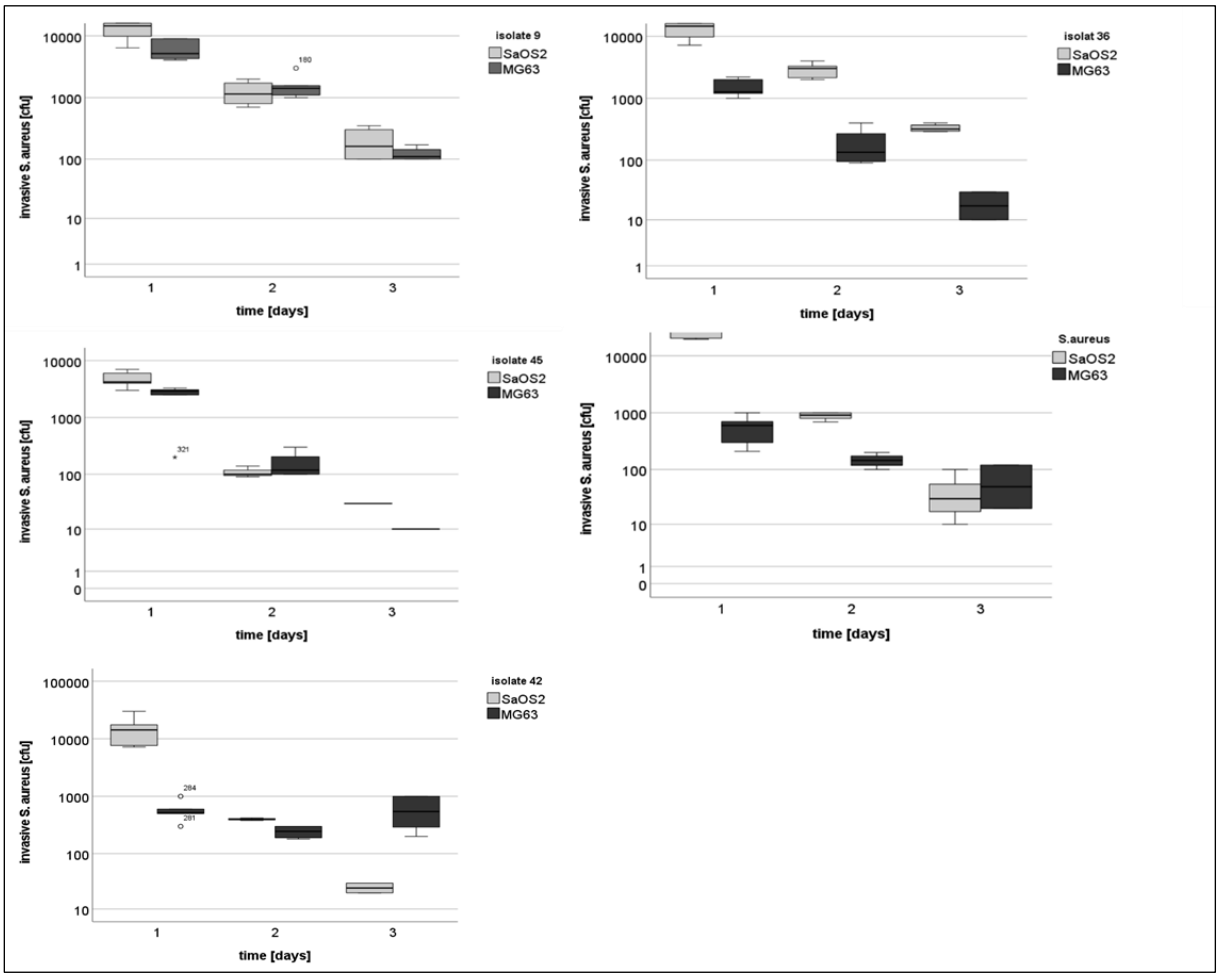

Figure 23. Role of autophagy inhibition in survival of *S. aureus* isolates in osteoblast like cell lines. SaOS2 and MG63 osteoblast like cell lines were cultured in medium containing 500 pM BafA1 over a period of 24 h in order to block the autophagy flux. Then the cells were infected with *S. aureus* ATCC 29213 or clinical isolates and gentamycin was added to the cells in order to kill extracellular bacteria. After one to three days, osteoblasts were lysed and released bacteria were plated on LB-agar in order to determine colony-forming units.

3.4.10 Western blot

SaOS2 and MG63 cell lines were cultured to confluence in 175 cm^2 flask. Medium without FCS was used to induce autophagy and medium with FCS was used as control. After 24 h, isolates (Pat 9, Pat 36, Pat 42, Pat 45 and *S. aureus* ATCC 29213) were selected to infect SaOS2 and MG63 cell lines. Both cell lines cultured in two different media without infection were also used as control. After 2 days, cells were harvested and the whole cell lysates were prepared with Jie's buffer. All proteins were quantified, separated, and transferred to nitrocellulose blotting membranes by semidry-blotting. Primary antibodies against Beclin1, LC3B, p62, β-actin were used and detected. Figure 24-A showed western blot results of control cell lines in two different media without infection. The results of cell lines in two different media with infection were exhibited in Figure 24-B, C, D. In Figure 24-A, the protein level of Beclin1, p62, LC3B-I and LC3B-II was lower in cells kept in the medium without FCS, indicating that autophagy was successfully induced by starvation. Focusing on the infected SaOS2, Beclin1, p62, LC3B-I and LC3B-II were less expressed independent of starvation-induced autophagy, which suggested that the infection itself could be an effective way to induce autophagy. However, in infected MG63, Beclin1 and p62 were over-expressed in starvation-induced autophagy condition. Instead, their protein level was almost not detectable after only bacterial infection (Pat 9, 42,45 and *S. aureus* ATCC 29213), with the exception for Pat 36. LC3B-I and LC3B-II were kept stable.

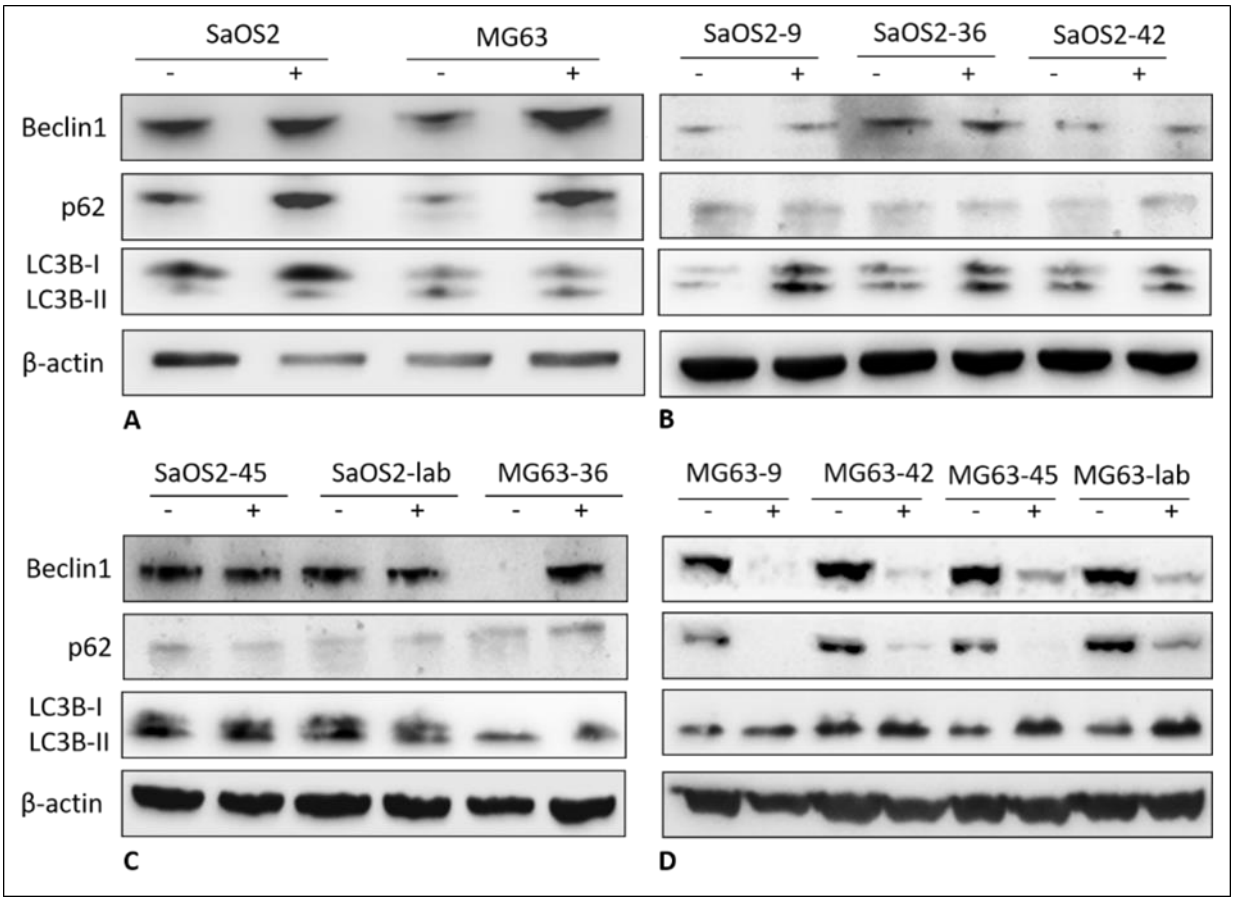

Figure 24. Expression of autophagy marker: Western blot of protein level of Beclin1, LC3B, p62, β-actin. Western blot detected Beclin1, LC3B, p62, β-actin of osteoblast like cell lines SaOS2 and MG63 2 days after infection with *S. aureus* isolates. Cells cultured in serum-free DMEM before infection were marked as "-"; Cells cultured in DMEM with serum before infection were marked as "+".

Focusing on the presence of markers of autophagy (Figure 25), serum withdrawal resulted in a decrease of either Beclin1 or p62 indicating an onset of autophagy. When *S. aureus* isolates (Pat 9, Pat 36, Pat 42, Pat45 and *S. aureus* ATCC 29213) were added to the cells, both cell-lines reacted differently. In SaOS2 the concentration of Beclin1 decreases further independent of the serum status of the medium. This was different in case of MG63 cells. Here the Beclin1 amount after infection decreased only in presence of serum while after serum withdrawal infection with bacteria resulted in an increase of Beclin1 amount. This finding was although seen in case of p62 to some extent.

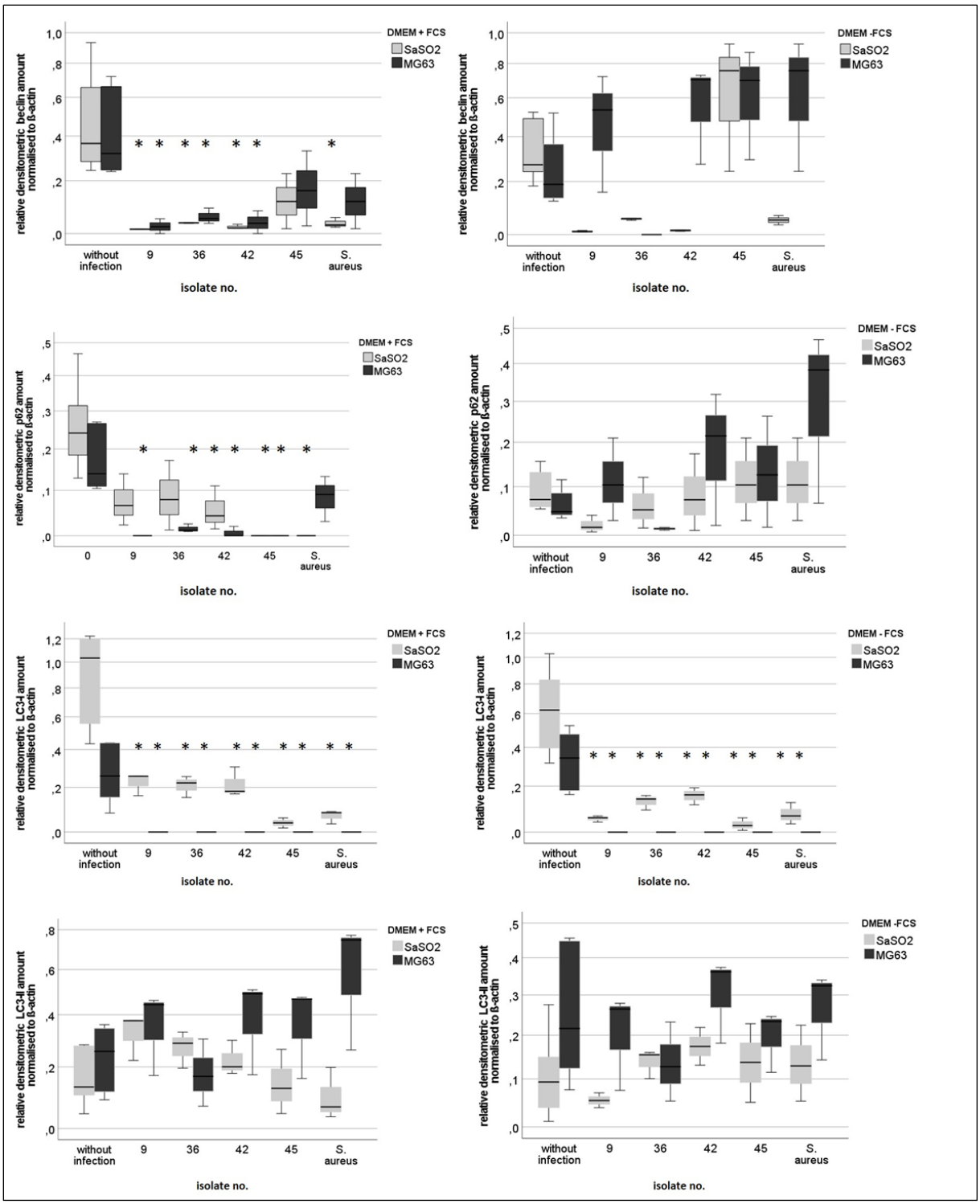

Figure 25. Role of autophagy in survival of *S. aureus* isolates in osteoblast like cell lines. Western-blot detecting Beclin1, p62, LC3-I and LC3-II of osteoblast like cell lines SaOS2 and MG63 one day after infection with *S. aureus* isolates. In some experiments, cells were cultured in serum-free DMEM before infection. Immune detection was quantified as above. Densitometry results were normalized to β-actin content. *: Significant difference between infected and uninfected osteoblasts.

3.4.11 Quantitative protein identification

In order to determine the effect of bacterial invasion into osteoblast, quantitative proteomics of two different osteoblast cell lines with or without bacterial infection were carried out, using mass spectrometry.

As shown in Figure 26, hierarchical clustering shows these peptides' expression variations and patterns between the two control groups, indicating that several proteins were differentially expressed in the SaOS2 as compared to MG63.

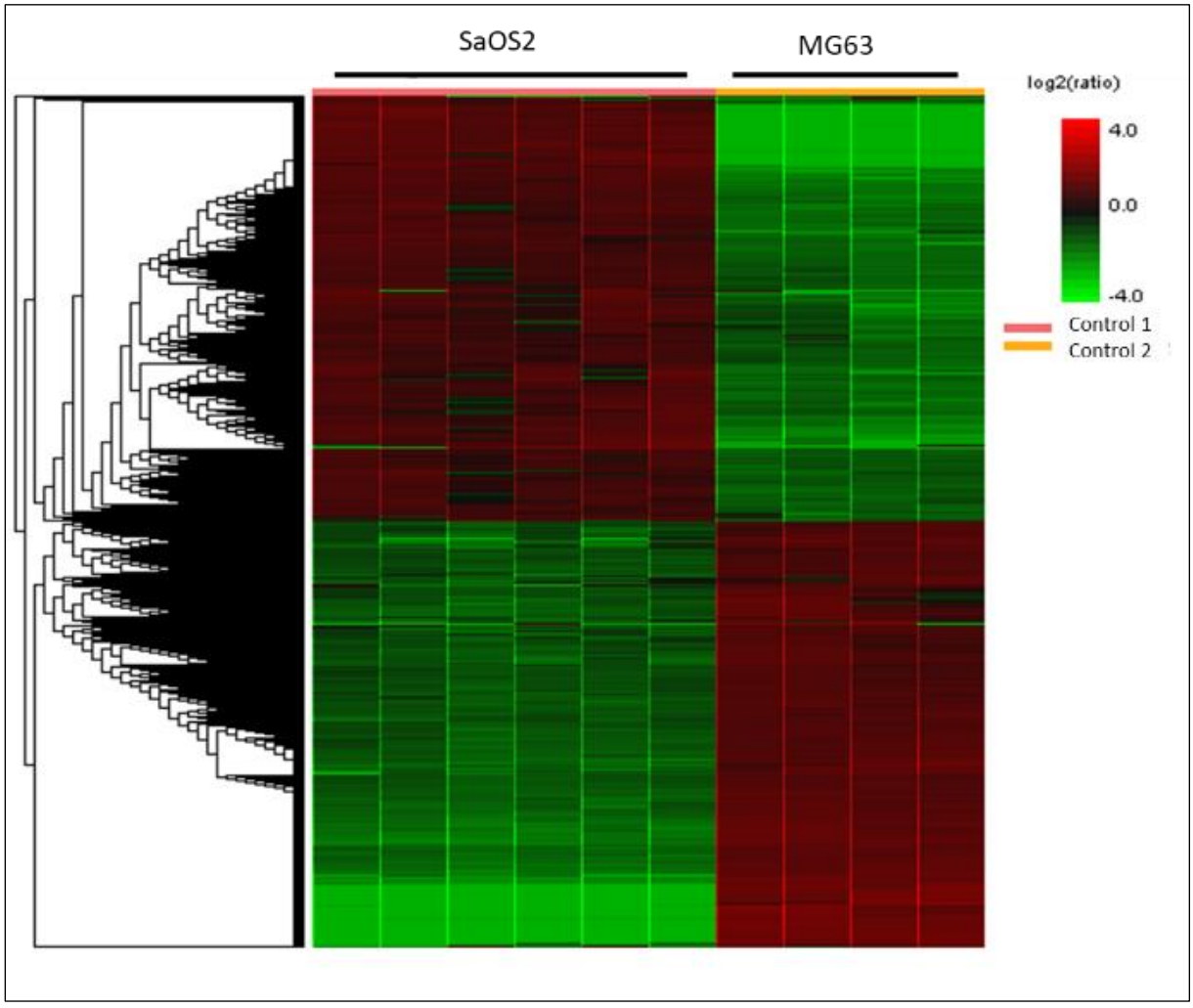

Figure 26. Protein profile heatmap: Comparison of the proteomes of SaOS2 and MG63. Cells were seeded in 75 cm^2 cell culture flasks and cultured to confluence in DMEM supplemented with 10% FCS and 1% Penicillin/Streptomycin before protein isolation.

Among all differentially regulated autophagy proteins between the two controls, such as Microtubule-associated proteins 1A/1B light chain, Lysosome-associated membrane glycoprotein 2, etc., the amount of them was at least 2 times higher in SaOS2 than in MG63. This could be attributed to a possible impairment of autophagy in SaOS2 cells. In detail, the proteins are listed in the Table 8.

Table 8. Identification of highly expressed proteins in SaOS2 with respect to autophagy.

Accession	SIG	CVGE (%)	Peptides	Unique	PTM	Avg. Mass	Sample Profile	Group Profile	Description
Q9GZQ8|ML P3B_HUMAN A6NCE7|MP 3B2_HUMAN	50.80	11	1	1	Y	14688			Microtubule-associated proteins 1A/1B light chain 3B OS=Homo sapiens OX=9606 GN=MAP1LC3B PE=1 SV=3
P13473|LAM P2_HUMAN	14.22	4	2	2	N	44961			Lysosome-associated membrane glycoprotein 2 OS=Homo sapiens OX=9606 GN=LAMP2 PE=1 SV=2
O00161|SNP 23_HUMAN	94.29	7	1	1	N	23354			Synaptosomal-associated protein 23 OS=Homo sapiens OX=9606 GN=SNAP23 PE=1 SV=1
O00116|ADA S_HUMAN	77.13	7	4	4	Y	72912	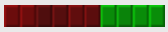		Alkyldihydroxyacetonephosphate synthase, peroxisomal OS=Homo sapiens OX=9606 GN=AGPS PE=1 SV=1
P04792|HSP B1_HUMAN	75.38	86	13	13	Y	22783			Heat shock protein beta-1 OS=Homo sapiens OX=9606 GN=HSPB1 PE=1 SV=2
P10909|CLUS _HUMAN	72.36	12	3	3	N	52495			Clusterin OS=Homo sapiens OX=9606 GN=CLU PE=1 SV=1
Q9UNF1|MA GD2_HUMA N	70.17	10	3	3	N	64954			Melanoma-associated antigen D2 OS=Homo sapiens OX=9606 GN=MAGED2 PE=1 SV=2
Q14315|FLN C_HUMAN	60.11	27	55	51	Y	291020			Filamin-C OS=Homo sapiens OX=9606 GN=FLNC PE=1 SV=3
P17174|AAT C_HUMAN	59.87	34	8	8	Y	46248			Aspartate aminotransferase, cytoplasmic OS=Homo sapiens OX=9606 GN=GOT1 PE=1 SV=3
P0DMV8|HS 71A_HUMAN	57.27	40	21	14	Y	70052			Heat shock 70 kDa protein 1A OS=Homo sapiens OX=9606 GN=HSPA1A PE=1 SV=1
Q15181|IPYR _HUMAN	53.01	50	10	9	Y	32660			Inorganic pyrophosphatase OS=Homo sapiens OX=9606 GN=PPA1 PE=1 SV=2
P43490|NAM PT_HUMAN	52.59	23	6	6	Y	55521			Nicotinamide phosphoribosyltransferase OS=Homo sapiens OX=9606 GN=NAMPT PE=1 SV=1
P31947|1433 S_HUMAN	51.98	34	7	3	Y	27774			14-3-3 protein sigma OS=Homo sapiens OX=9606 GN=SFN PE=1 SV=1

P31350|RIR2_HUMAN	51.90	22	5	5	Y	44878			Ribonucleoside-diphosphate reductase subunit M2 OS=Homo sapiens OX=9606 GN=RRM2 PE=1 SV=1
P09455|RET1_HUMAN	50.44	50	6	6	Y	15850			Retinol-binding protein 1 OS=Homo sapiens OX=9606 GN=RBP1 PE=1 SV=2

SIG: Significance; CVGE: Coverage; PTM: Post-Translational Modifications; Avg.: Average. The six squares on the left side of the colour bar represent SaOS2; The four squares on the right side of the colour bar represent MG63.

On the other hand, Fibronectin, Collagen alpha-1 (I/III/V/VI) chain, Collagen alpha-2 (VI) chain, and Insulin-like growth factor 2 mRNA-binding protein 3, were less expressed in SaOS2, whereas Collagen alpha-3 (VI) chain was overexpressed, as shown in Table 9. These proteins might be correlated with the adhesion.

Table 9. Identification of proteins in SaOS2 with respect to bacterial infection.

Accession	SIG	CVGE (%)	Peptides	Unique	PTM	Avg. Mass	Sample Profile	Group Profile	Description
P02751|FINC_HUMAN	37.87	2	4	4	N	272318			Fibronectin OS=Homo sapiens OX=9606 GN=FN1 PE=1 SV=5
P02452|CO1A1_HUMAN	63.28	3	3	3	Y	138942			Collagen alpha-1(I) chain OS=Homo sapiens OX=9606 GN=COL1A1 PE=1 SV=5
P02461|CO3A1_HUMAN	12.67	2	2	2	Y	138564	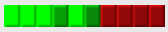		Collagen alpha-1(III) chain OS=Homo sapiens OX=9606 GN=COL3A1 PE=1 SV=4
P20908|CO5A1_HUMAN	49.66	1	1	1	N	183559			Collagen alpha-1(V) chain OS=Homo sapiens OX=9606 GN=COL5A1 PE=1 SV=3
P12109|CO6A1_HUMAN	55.45	14	7	7	Y	108529			Collagen alpha-1(VI) chain OS=Homo sapiens OX=9606 GN=COL6A1 PE=1 SV=3
P12110|CO6A2_HUMAN	47.50	6	3	3	N	108579			Collagen alpha-2(VI) chain OS=Homo sapiens OX=9606 GN=COL6A2 PE=1 SV=4
P12111|CO6A3_HUMAN	28.64	26	50	50	Y	343668			Collagen alpha-3(VI) chain OS=Homo sapiens OX=9606 GN=COL6A3 PE=1 SV=5
O00425|IF2B3_HUMAN	66.03	11	5	3	N	63705			Insulin-like growth factor 2 mRNA-binding protein 3 OS=Homo sapiens OX=9606 GN=IGF2BP3 PE=1 SV=2

SIG: Significance; CVGE: Coverage; PTM: Post-Translational Modifications; Avg.: Average; The six squares on the left side of the colour bar represent SaOS2; The four squares on the right side of the colour bar represent MG63.

Quantitative proteomics of two different osteoblast cell lines with and without isolate Pat 36 infection were carried out. As shown in Figure 27, hierarchical clustering shows an overview of these peptides' expression variations and patterns between the two groups.

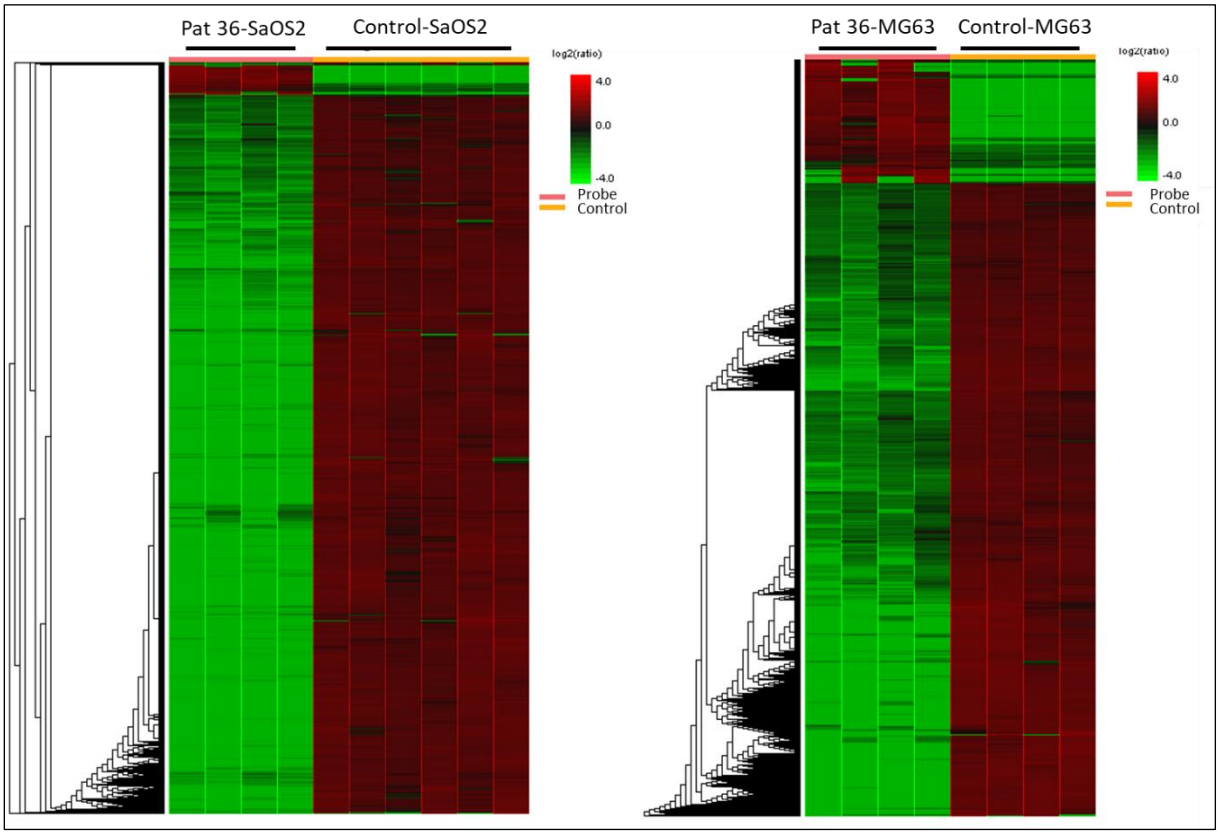

Figure 27. Protein profile heatmap: Comparison of the proteomes of SaOS2 and MG63 with and without infection with isolate Pat 36. Cells were seeded in 75 cm^2 cell culture flasks and cultured to confluence in DMEM supplemented with 10% FCS and 1% Penicillin/Streptomycin. Then antibiotics were removed and cells were infected with isolate Pat 36. After 30 min gentamycin was added in order to kill extracellular bacteria and cell were cultured for one day before protein isolation.

Focusing on marker proteins referred to autophagy flux, several of them, such as Microtubule-associated proteins 1A/1B light chain 3B, Lysosome-associated membrane glycoprotein 1 and 2, Ras-related protein Rab-7a, Histone deacetylase 2, Cathepsin B/D/Z, Annexin A1/2/4/5/6/7/11, etc. (Table 10) were lowered in SaOS2 after infection with isolate Pat 36.

Table 10. Selected proteins related to autophagy in cell line SaOS2 differentially expressed after infection with isolate Pat 36.

Accession	SIG	CVGE (%)	Peptides	Unique	PTM	Avg. Mass	Sample Profile	Group Profile	Description
P11279|LAMP1_HUMAN	55.75	5	2	2	N	44882			Lysosome-associated membrane glycoprotein 1 OS=Homo sapiens OX=9606 GN=LAMP1 PE=1 SV=3

P13473|LAMP2_HUMAN	57.12	4	2	2	N	44961			Lysosome-associated membrane glycoprotein 2 OS=Homo sapiens OX=9606 GN=LAMP2 PE=1 SV=2
P51149|RAB7A_HUMAN	30.82	42	6	6	N	23490			Ras-related protein Rab-7a OS=Homo sapiens OX=9606 GN=RAB7A PE=1 SV=1
Q92769|HDAC2_HUMAN	24.72	14	4	2	Y	55364			Histone deacetylase 2 OS=Homo sapiens OX=9606 GN=HDAC2 PE=1 SV=2
P07858|CATB_HUMAN	20.49	13	3	3	Y	37822			Cathepsin B OS=Homo sapiens OX=9606 GN=CTSB PE=1 SV=3
P07339|CATD_HUMAN	19.17	10	3	3	Y	44552			Cathepsin D OS=Homo sapiens OX=9606 GN=CTSD PE=1 SV=1
Q9UBR2|CATZ_HUMAN	24.94	4	1	1	N	33868			Cathepsin Z OS=Homo sapiens OX=9606 GN=CTSZ PE=1 SV=1
P51784|UBP11_HUMAN	72.35	4	2	2	Y	109817			Ubiquitin carboxyl-terminal hydrolase 11 OS=Homo sapiens OX=9606 GN=USP11 PE=1 SV=3
Q93009|UBP7_HUMAN	17.11	5	3	3	N	128302			Ubiquitin carboxyl-terminal hydrolase 7 OS=Homo sapiens OX=9606 GN=USP7 PE=1 SV=2
Q15019|SEPT2_HUMAN	25.01	36	10	10	Y	41487			Septin-2 OS=Homo sapiens OX=9606 GN=SEPTIN2 PE=1 SV=1
Q9Y4P1|ATG4B_HUMAN	49.31	5	1	1	N	44294			Cysteine protease ATG4B OS=Homo sapiens OX=9606 GN=ATG4B PE=1 SV=2
Q9NT62|ATG3_HUMAN	29.18	9	2	2	N	35864			Ubiquitin-like-conjugating enzyme ATG3 OS=Homo sapiens OX=9606 GN=ATG3 PE=1 SV=1
P04083|ANXA1_HUMAN	22.80	67	25	25	Y	38714			Annexin A1 OS=Homo sapiens OX=9606 GN=ANXA1 PE=1 SV=2
P07355|ANXA2_HUMAN	38.26	80	50	50	Y	38604			Annexin A2 OS=Homo sapiens OX=9606 GN=ANXA2 PE=1 SV=2
P09525|ANXA4_HUMAN	53.88	10	2	2	N	35883			Annexin A4 OS=Homo sapiens OX=9606 GN=ANXA4 PE=1 SV=4
P08758|ANXA5_HUMAN	18.74	89	36	36	Y	35937			Annexin A5 OS=Homo sapiens OX=9606 GN=ANXA5 PE=1 SV=2
P08133|ANXA6_HUMAN	13.20	35	19	19	Y	75873			Annexin A6 OS=Homo sapiens OX=9606 GN=ANXA6 PE=1 SV=3
P20073|ANXA7_HUMAN	12.57	5	2	2	N	52739			Annexin A7 OS=Homo sapiens OX=9606 GN=ANXA7 PE=1 SV=3
P50995|ANXA11_HUMAN	15.08	15	5	5	Y	54390			Annexin A11 OS=Homo sapiens OX=9606 GN=ANXA11 PE=1 SV=1

SIG: Significance; CVGE: Coverage; PTM: Post-Translational Modifications; Avg.: Average. The four squares on the left side of the colour bar represent Pat 36-SaOS2; The six squares on the right side of the colour bar represent Control-SaOS2.

However, among differently expressed proteins in MG63 infected with isolate Pat 36, only Ras-related protein Rab-7a and Annexin A1/2/5/6/11 were found to be modulated in a comparable way to SaOS2 (Table 11). Rabankyrin-5, COP9 signalosome complex subunit 1, Clathrin light chain A, Dynamin-1-like protein, Dynamin-1-like protein, and GRIP1-associated protein 1 were also found to be possibly related to autophagy.

Table 11. Selected proteins related to autophagy in cell line MG63 differentially expressed after infection with isolate Pat 36.

Accession	SIG	CVGE (%)	Peptides	Unique	PTM	Avg. Mass	Sample Profile	Group Profile	Description
P51149|RAB7A_HUMAN	17.28	47	7	7	Y	23490			Ras-related protein Rab-7a OS=Homo sapiens OX=9606 GN=RAB7A PE=1 SV=1
P04083|ANXA1_HUMAN	25.14	60	22	22	Y	38714			Annexin A1 OS=Homo sapiens OX=9606 GN=ANXA1 PE=1 SV=2
P07355|ANXA2_HUMAN	29.07	71	39	39	Y	38604			Annexin A2 OS=Homo sapiens OX=9606 GN=ANXA2 PE=1 SV=2
P08758|ANXA5_HUMAN	32.99	88	37	37	Y	35937			Annexin A5 OS=Homo sapiens OX=9606 GN=ANXA5 PE=1 SV=2
P08133|ANXA6_HUMAN	23.93	53	29	29	Y	75873			Annexin A6 OS=Homo sapiens OX=9606 GN=ANXA6 PE=1 SV=3
P50995|ANX11_HUMAN	18.19	18	7	7	Y	54390			Annexin A11 OS=Homo sapiens OX=9606 GN=ANXA11 PE=1 SV=1
Q9P2R3|ANFY1_HUMAN	22.03	2	1	1	N	128399			Rabankyrin-5 OS=Homo sapiens OX=9606 GN=ANKFY1 PE=1 SV=2
Q13098|CSN1_HUMAN	75.51	2	1	1	Y	55537			COP9 signalosome complex subunit 1 OS=Homo sapiens OX=9606 GN=GPS1 PE=1 SV=4
P09496|CLCA_HUMAN	72.32	7	2	2	N	27077			Clathrin light chain A OS=Homo sapiens OX=9606 GN=CLTA PE=1 SV=1
O00429|DNM1L_HUMAN	17.76	5	2	2	N	81877			Dynamin-1-like protein OS=Homo sapiens OX=9606 GN=DNM1L PE=1 SV=2
Q4V328|GRAP1_HUMAN	73.22	2	1	1	Y	96005			GRIP1-associated protein 1 OS=Homo sapiens OX=9606 GN=GRIPAP1 PE=1 SV=2

SIG: Significance; CVGE: Coverage; PTM: Post-Translational Modifications; Avg.: Average. The four squares on the left side of the colour bar represent Pat 36-MG63; The four squares on the right side of the colour bar represent Control-MG63.

Quantitative proteomics were performed to analyse the protein profile of two different osteoblast cell lines with and without isolate Pat 9 infection. As shown in Figure 28, hierarchical clustering shows an overview of these peptides' expression variations and patterns between the two groups.

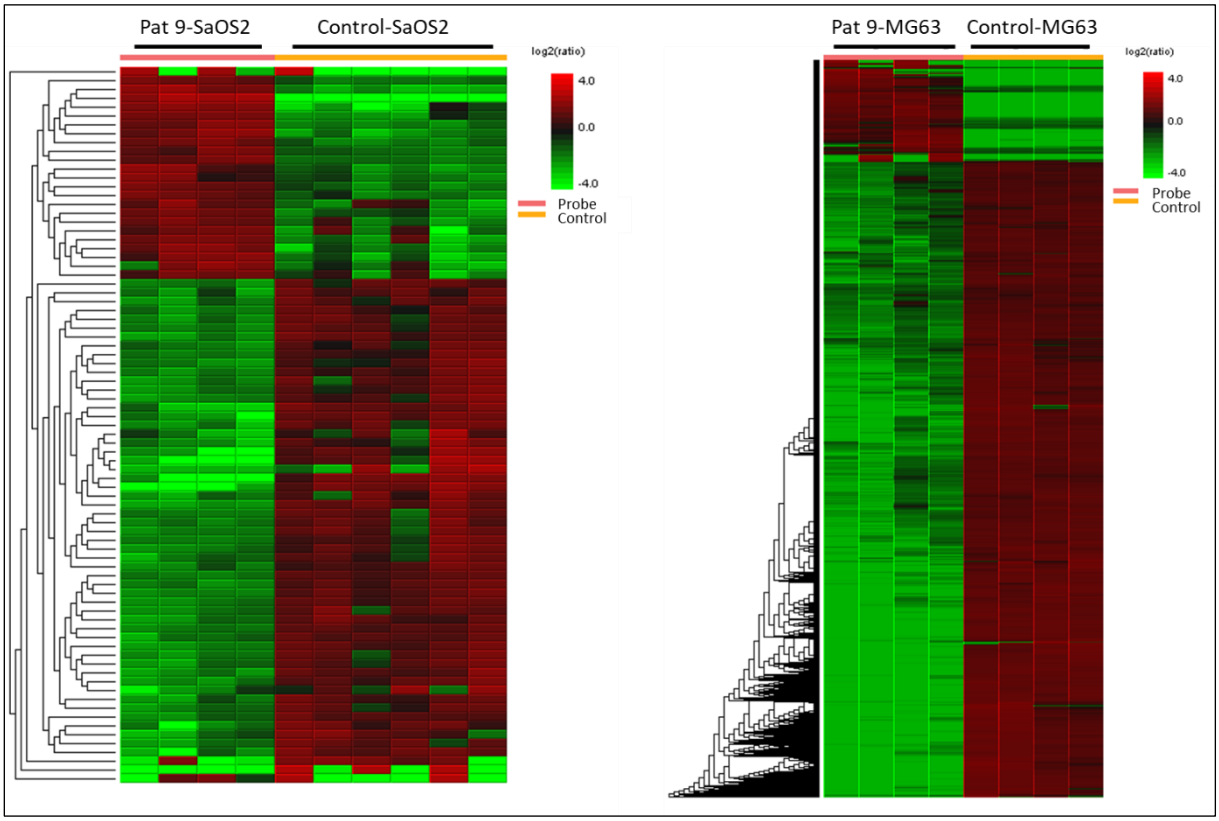

Figure 28. Protein profile heatmap: Comparison of the proteomes of SaOS2 and MG63 with and without infection with isolate Pat 9. Cells were seeded in 75 cm^2 cell culture flasks and cultured to confluence in DMEM supplemented with 10% FCS and 1% Penicillin/Streptomycin. Then Antibiotics were removed and cell were infected with isolate Pat 9. After 30 min gentamycin was added in order to kill extracellular bacteria and cells were cultured for one day before protein isolation.

The infection with isolate Pat 9 although resulted in a down regulation of several proteins. However, within SaOS2 these proteins were not related to autophagy flux. In case of MG63, the reduced presence of Cathepsin B/D, Lysosome-associated membrane glycoprotein 1/2, Ras-related protein Rab-1A/2A/7a (Table 12) in the proteome indicated an activated autophagy.

Table 12. Selected proteins related to autophagy in cell line MG63 differentially expressed after infection with isolate Pat 9.

Accession	SIG	CVGE (%)	Peptides	Unique	PTM	Avg. Mass	Sample Profile	Group Profile	Description
P07858|CATB_HUMAN	11.37	13	3	3	Y	37822			Cathepsin B OS=Homo sapiens OX=9606 GN=CTSB PE=1 SV=3
P07339|CATD_HUMAN	17.93	19	4	4	Y	44552			Cathepsin D OS=Homo sapiens OX=9606 GN=CTSD PE=1 SV=1

P11279|LAMP1_HUMAN	68.17	7	3	3	N	44882			Lysosome-associated membrane glycoprotein 1 OS=Homo sapiens OX=9606 GN=LAMP1 PE=1 SV=3
P13473|LAMP2_HUMAN	62.47	2	1	1	N	44961			Lysosome-associated membrane glycoprotein 2 OS=Homo sapiens OX=9606 GN=LAMP2 PE=1 SV=2
P62820|RAB1A_HUMAN	11.21	63	10	4	Y	22678			Ras-related protein Rab-1A OS=Homo sapiens OX=9606 GN=RAB1A PE=1 SV=3
P51149|RAB7A_HUMAN	15.13	64	10	10	Y	23490			Ras-related protein Rab-7a OS=Homo sapiens OX=9606 GN=RAB7A PE=1 SV=1
P61019|RAB2A_HUMAN	10.65	36	7	4	Y	23546			Ras-related protein Rab-2A OS=Homo sapiens OX=9606 GN=RAB2A PE=1 SV=1

SIG: Significance; CVGE: Coverage; PTM: Post-Translational Modifications; Avg.: Average. The four squares on the left side of the colour bar represent Pat 9-MG63; The four squares on the right side of the colour bar represent Control-MG63.

Likewise, quantitative proteomics of two different osteoblast cell lines with and without isolate *S. aureus* ATCC 29213 infection were carried out. As shown in Figure 29, hierarchical clustering shows an overview of these peptides' expression variations and patterns between the two groups. Focusing on the osteoblasts infected with *S. aureus* ATCC 29213 compared to the other tests, only a few proteins were regulated at a level of 2-fold, and proteins related to autophagy were not observed in both SaOS2 and MG63 cell lines.

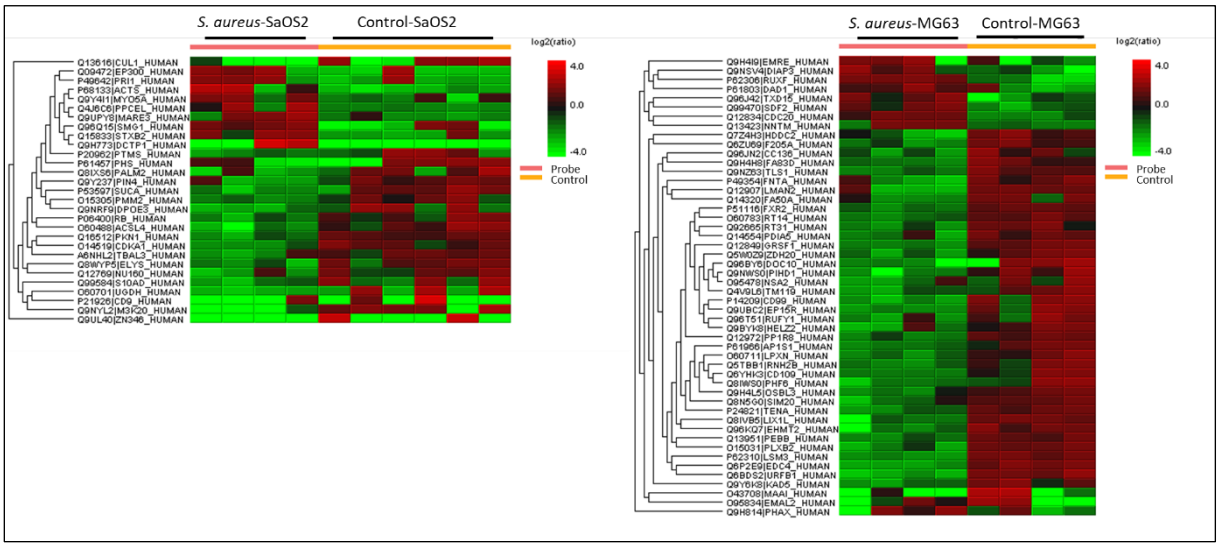

Figure 29. Protein profile heatmap: Comparison of the proteomes of SaOS2 and MG63 with and without infection with *S. aureus* ATCC 29213. Cells were seeded in 75 cm^2 cell culture flasks and cultured to confluence in DMEM supplemented with 10% FCS and 1% Penicillin/Streptomycin. Then antibiotics were removed and cell were infected with *S. aureus* ATCC 29213. After 30 min, gentamycin was added in order to kill extracellular bacteria and cell were cultured for one day before protein isolation.

4 DISCUSSION

This study comparatively analysed the interaction of different clinical isolates of *S. aureus*, the most frequently isolated pathogen in implant-associated bone infection (Barth et al., 2011), with osteoblasts. Substantial differences were identified concerning cell adhesion as well as invasion and bacterial persistence in the cytosol of osteoblasts. Furthermore, changes within the proteome of the host cells, depending on the *S. aureus* isolate, as well as the osteoblast cell lines, indicating a more complex interaction. Within this study, clinical isolates obtained from implant-associated infections were used due to the finding that healthcare-associated *S. aureus* posed a higher pathogenicity, compared to the others (Rasigade et al., 2013; Li et al., 2021; Chalmers and Wylam, 2020; Arciola et al., 2005a; Montanaro et al., 2011; Aggarwal et al., 2014).

The first step of this study was to classify the clinical isolates according to their characterization. Based on methods, such as clear zone formation, growth curve analyzation, collagenase test, oxidase test, API® Staph. test, and 16S rRNA sequencing, isolates were classified as *S. aureus* (Pat 2, 4, 6, 9, 28, 36, 42, 45) or *S. epidermidis* (Pat 29, 32, 37, 47). *S. aureus* is usually beta haemolytic on blood agar, whereas *S. epidermidis* are usually non-haemolytic. Much to our surprise, clear zone was not formed by Pat 36, which was also confirmed as a strong adhesive *S. aureus* as with Pat 42, 45. With respect to growth curve, *S. aureus* were found to proliferate faster than *S. epidermidis*. Pat 42, 45, 36 and *S. aureus* ATCC 29213 were the fastest growing isolates. It is therefore likely that such connections exist between bacteria growth condition and their adhesive ability because Pat 42, 45, 36 and *S. aureus* ATCC 29213 were also identified to be the most adhesive ones in the later adhesion assay. With better understanding of the molecular mechanisms as well as the new strategies to target the coagulases, the importance of coagulases in *S. aureus* virulence has been highlighted (Peetermans et al., 2015). Up to now, the *S. aureus* coagulase is the only enzyme being responsible for bacteria-mediated disease in humans. Thus, this enzyme can be a good indicator of the pathogenic potential of *S. aureus*. The observation of collagenase test was in line with expectations, which showed that *S. aureus* isolates (Pat 2, 4, 6, 9, 28, 36, 42, 45) were coagulase-positive and *S. epidermidis* isolates (Pat 29, 32, 37, 47) coagulase-negative. Additionally, it is well known that both *S. aureus* and *S. epidermidis* are oxidase-negative. The results of oxidase test performed in this study indicated that all isolates were oxidase-negative. API® Staph test was a further proof of the classification of all isolates, and the result was consistent with the above conclusions. The final confirmation was carried out by 16S rRNA sequencing. After comparing the sequencing results with NCBI reference sequence database, clinical isolates were confirmed to be classified into two different homologies: *S. aureus* (Pat 2, 4, 6, 9, 28, 36, 42, 45) and *S. epidermidis* (Pat 29, 32, 37, 47). Various tests were used in the first characterization step to build the foundation of the whole study frame and make sure the follow-up research reliable.

Further characterization with respect to biofilm and antibiotic resistance gave evidence that *S. aureus* isolates (except Pat 2) induced biofilm when cultured under appropriate conditions (Michel et al., 2016). This was accompanied by increased antibiotic resistance in most of the isolates in this study, indicating that the proposed function of biofilm was present in these isolates (Stewart, 2002). Adhesion and biofilm formation have been clarified as pivotal roles in the pathogenesis of implant infections (Arciola et al., 2012). On metal plates, increased biofilm formation was only found with isolate Pat 36, 42 and 45 as well as the *S. aureus* ATCC 29213 and interestingly correlated with the ability of the isolates to adhere to osteoblasts to some extent, indicating that the initial step, namely adhesion, might play a critical role under these circumstances. Previous research has showed that changes in the surface of biomaterials are necessary to prevent biofilm formation (Kuehl et al., 2016). This was coincidentally identified by the fluorescent microscopy assay, which showed that PE surface were easier for biofilm formation when compared with metal surface, thus suggesting that biomaterial itself can be a major contributor to prevent the implant-associated infection.

Infection assay was established to demonstrate the *S. aureus* infection and intracellular growth in osteoblasts by using *S. aureus* ATCC 29213 and the osteoblast cell lines SaOS2 and MG63, which are suitable models for osteoblasts and represent immature (MG63) and mature (SaOS2) osteoblasts (Czekanska et al., 2012). The first finding was that *S. aureus* needed 30 min to make an effective adhesion to osteoblasts. This is consistent with the incubation described in a previous study (Mohamed et al., 2014), indicating that *S. aureus* can be seen as a facultative intracellular pathogen or pathogenic principle in bone infections (Wright and Nair, 2010).

Besides, *S. aureus* ATCC 29213 was found to be significantly more adhesive to SaOS2 than to MG63. *S. aureus* harvested in the stationary growth phase showed a stronger adherence towards osteoblasts as compared to that harvested in the logarithmic growth phase. However, in another study it was found that *S. aureus* taken from the exponential phase of growth, when compared to *S. aureus* taken from the stationary phase, had a noticeable higher ability to adhere or invade host cells (Ji et al., 2020). Moreover, it was described that different human MRSA isolates possessed different abilities to adhere to and invade the epithelial cells (Yang and Ji, 2014).

Based on these findings, invasion model assay was performed with *S. aureus* harvested in the stationary growth phase infecting SaOS2 and MG63 for 30 min, and then 30 µg/mL gentamicin was added to kill only the remaining extracellular bacteria without affecting the intracellular bacteria. This concentration was showed to be high enough to inhibit extracellular *S. aureus* isolates, and it was consistent with the finding of a previous study (Schafer et al., 2006), at least under growth conditions, and was low enough to allow intracellular survival (Mohamed et al., 2014).

Focusing on the intracellular survival of *S. aureus*, only a small percentage of the adhesive isolates was found to be able to invade osteoblasts. In accordance with the present results, previous studies have demonstrated that osteoblasts exhibit a much smaller number of internalized bacteria when compared with other type of cells (Niemann et al., 2021). This observation prompted us to inquire into the mechanisms underlying this significant difference in more detail.

Focusing on the long-term survival of *S. aureus* in osteoblasts over a period of 3 days, it was demonstrated that intracellular *S. aureus* ATCC 29213 remained nearly constant in MG63 but decreased significantly in SaOS2. Moreover, MTT assay was used to compare the metabolic activity between infected osteoblasts and non-infected ones. Results indicated that the metabolic activity was not influenced by the infection with *S. aureus*, suggesting that decreasing survival of *S. aureus* in SaOS2 was probably not caused by the death of infected SaOS2. This finding is contrary to a previous study which has showed that *S. aureus* could significantly induce apoptosis in SAOS2 cells already after 24 h of post-infection (Mohamed et al., 2014).

The adhesion of *S. aureus* isolates clearly showed a strain dependency of *S. aureus* towards osteoblasts. *S. aureus* isolates Pat 36 and Pat 45 as well as ATCC 29213 showed significant increase of adhesion on the osteoblasts as compared to the other isolates. Although this is a small collective, it seems that this ability is not widespread with regard to osteoblasts (Ménard et al., 2020). Furthermore, this increased adhesion is not correlated with invasion of the cells. Independent of the isolates used, only a small number of bacteria adhering to osteoblasts were able to invade the cells (approximately 33.33%).

In fact, an increasing number of different *S. aureus* adhesion molecules have been identified (Rooijakkers et al., 2005). The fnbA and fnbB genes contribute to bacterial invasion and adhesion (Ahmed et al., 2001; Fowler et al., 2000). In this study, a low incidence of the fnbB gene (11.11%) was observed. Whereas, the fnbA gene was detected in 100% of the isolates, similar to that observed by Ikawaty et al. (Ikawaty et al.). Researchers reported that all MRSA isolated from hospital outbreaks in Japan lacked of the fnbB gene (Taneike et al., 2006). However, a high incidence of fnbB gene (99.5%) was reported by Arciola et al. (Arciola et al., 2005b). This difference may be partly attributed to the different genetic testing techniques used, and the different regions of the locus analysed by the pair of primers. Both the clfA and clfB genes had a prevalence of 100% in the present study, which was consistent with previous report that these genes play a decisive role in bacterial virulence (Moreillon et al., 1995). Fibrinogen binding protein is an important virulence factor in infections caused by *S. aureus* because it not only binds to fibrinogen but also interferes with platelet aggregation and complement cascade reactions within the host (Kumar et al., 2011). With respect to the gene fib, 66.67% of our isolates were detected to express it. The cna gene has been shown to be a significant virulence

factor in staphylococcal infections (Montanaro et al., 1999), but it was not identified in the present study. In all *S. aureus* isolates, the incidence of cna was only 33.33% (Pat 4, 6, 9). A higher incidence of cna gene was reported by Nashev et al. (46.7%) (Nashev et al., 2004) and Arciola et al. (46%) (Arciola et al., 2005b), respectively. Cna was reported to exert an important role in the process of *S. aureus* infection in bone tissue (Kang et al., 2013). However, it was not related to the increased invasion in our study because cna gene was not detectable in the invasive isolates (Pat 36, 42, 45 and *S. aureus* ATCC 29213), indicating that cna gene may play a less important role in osteoblasts infection. In this study, the bbp gene related to human osteomyelitis and arthritis (Tung et al., 2000) was absent in nearly all strains except Pat 2. This result was in line with Vancraeynest et al. (Vancraeynest et al., 2006), where the bbp gene was not detected in all their isolates. Moreover, we identified the presence of ebpS gene in 100% of our isolates. This gene encodes for eastin-binding protein, promoting binding of soluble elastin peptides and tropoelastin to *S.aureus*. Notably, previous studies were performed using isolates of methicillin-resistant *S. aureus* of high clinical significance, revealing that PSMs of all *S. aureus* are involved in biofilm structuring processes (Periasamy et al., 2012). Consistent with this finding, the presence of both psmA and psmB genes were confirmed in 100% of our isolates. Eap was found to be able to curb acute inflammatory responses and enhance internalization of the microorganism into eukaryotic cells (Athanasopoulos et al., 2006; Haggar et al., 2003). The result of the present study highlighted that the eap gene was detectable in all *S. aureus* isolates, thus sustaining the previous finding. Previously, it has been demonstrated that the presence of sdrD promotes adhesion of *S. aureus* in HaCaT cells (Askarian et al., 2016). This study evidenced the expression of sdrD gene was detected in all isolates. The inactivation of the fmtB gene, a gene encoding for a cell-wall-associated protein, has been shown to drastically reduce the resistance of *S. aureus* to β-lactam antibiotics such as methicillin, cefoxitin and imipenem (Komatsuzawa et al., 2000; Sung et al., 2008). FmtB gene was found expressed in all the isolates in this study. Walker et al. found that the ebh gene, encoding the Giant *Staphylococcal* Surface Protein (GSSP), was closely correlated with bacterial agglutination (Walker et al., 2013). And correspondingly, we found ebh gene in all *S. aureus* isolates.

To further clarify if the corresponding adhesion genes are expressed in our isolates and *S. aureus* ATCC 29213, the proteome of the *S. aureus* isolates were analysed, using mass spectrometry. Comparing with PCR results, the eno, fnbA, ebpS, psmB, and ebh genes were found expressed consistently in all isolated *S. aureus*. However, clfA, psmA, sdrD, clfB, fmtB genes were only partially found expressed. One unanticipated finding was that eap gene was detected in all isolates, but the encoded extracellular adherence protein Eap was not identified in any isolates. Eap was found expressed in 5 out of 140 clinical *S. aureus* isolates in a previous study (Hussain et al., 2001). Probably, the absence of Eap in our *S. aureus* isolates, especially not in the most adhesive ones, could be compensated by the presence of

other adhesins with overlapping functions that may be more important than Eap for adhesion, or that adherence is the result of the additive effects of several different adhesins (Harraghy et al., 2003). Since *S. aureus* ATCC 29213 has a stronger adherence to SaOS2 cell line as compared to MG63, the proteomes of the two different osteoblast cell lines were compared. The proteins involved in adhesion were mostly not expressed in osteoblasts. Only fibronectin and collagen were identified by mass spectrometry. Taken together, it can be seen that neither the presence of the respective genes nor the gene products can be regarded as a sufficient predictive marker for adhesion.

Furthermore, the gene eno, fnbA, clfB, ebpS, sdrD were found to be overexpressed not only in the adhesive *S. aureus* isolates (Pat 36, 42, 45 and *S. aureus* ATCC 29213), but also in non-adhesive isolates. Thus, clfA gene may be a candidate gene because it was overexpressed only in the adhesive *S. aureus* isolates (Pat 36, 42, 45 and *S. aureus* ATCC 29213). Regarding to adhesion of *S. aureus* isolates cultured in biofilm conditions on osteoblasts, it was found that selected *S. aureus* isolates (Pat 9, 36 and *S. aureus* ATCC 29213) cultured in LB-medium supplemented with 0.5% glucose and/or 3% NaCl significantly reduced their ability to adhere to osteoblasts. The expression levels of adhesin genes of selected *S. aureus* isolates (Pat 9, 36 and *S. aureus* ATCC 29213) cultured in different media had considerable discrepancies, suggesting that there are uncertain effects of culture media related to composition of the growth media.

Above all, it indicates that there may not be a uniform mechanism behind the adhesion of the examined *S. aureus* isolates, but the different adhesion proteins could be involved.

Focusing on the invasion and intracellular survival, the results here indicated that the increased adhesion was not necessarily linked to the invasion or intracellular survival. Isolates Pat 42, which possessed a strong adherence, invaded MG63 cell line similarly to the weak adhesion isolates Pat 2, 4, 9, and 28. Furthermore, intracellular survival was independent of adhesion, which could favour the bacterial invasion. In this study, isolates Pat 6, 28 and 42 were killed in both SaOS2 and MG63; whereas isolates Pat 36 and, to some extent, *S. aureus* ATCC 29213 could survive in both cell lines. This strain dependent killing of *S. aureus* was observed earlier in dendritic cells, macrophages, and epithelial cells (O'Keeffe et al., 2015; Watkins and Unnikrishnan, 2020; Parker et al., 2014). *S. aureus* has been reported to persist inside phagocytes or endothelial cells for prolonged periods as reviewed in previous study (Sendi and Proctor, 2009). Focusing on the colonialization and survival of *S. aureus* within osteoblast-like cells, the results showed that the survival was dependent on both the bacterial isolates and the osteoblast cells, which was consistent with previous research, studying the interaction between *S. aureus* (strains 6850, USA300, LS1, SH1000, Cowan1) and epithelial cells, endothelial cells, keratinocytes, fibroblasts, osteoblasts (Strobel et al., 2016).

However, the host cell also had an influence on the survival of the bacteria. Here in the present study, isolates Pat 4 and Pat 9 survived in MG63 cell line representing immature osteoblast phenotype, while isolates Pat 2 and Pat 45 survived in SaOS2, which represents a mature osteoblast (Czekanska et al., 2012). The effect that different cell types respond differently to an infection with *S. aureus* has been described earlier (Moldovan and Fraunholz, 2019). Rasigade et al. had described such a strain dependency, divining strains in community-acquired and healthcare-associated *S. aureus*, differing in cell toxicity (Rasigade et al., 2013), which was only found to a very limited extent in this study using MTT assay. However, these were different cell types and not different cells of one type. To our knowledge, this effect was not described in connection with early or late osteoblasts. The reason might be seen in xenophagy, a special form of autophagy, a mechanism by which intracellular bacteria can be eliminated (Knodler and Celli, 2011).

Autophagy is an orchestrated homeostatic process to recycle proteins and damaged organelles, which can be also useful to remove intracellular microbial pathogens (Levine and Kroemer, 2008; Mizushima et al., 2008). Several signalling pathways sense different types of cell stress, ranging from nutrient deprivation to microbial invasion, and converge to regulate autophagy at multiple stages of the process (Netea-Maier et al., 2016). The dynamic membrane processes of autophagy follow sequential steps: autophagy initiation; phagophore formation; double-membrane nucleation and phagophore elongation; cytoplasmic microorganism engulfment; autophagosome fusion with lysosome; and cargo degradation (Kuo et al., 2018). Several discoveries have shown that autophagy exerts an important role in host cell defense against *S. aureus* (Lv et al., 2019; Gibson et al., 2021).

And in-deed, the western blot of Beclin1, p62 and LC3B showed that the autophagy in the host cells is turned on after infection with the *S. aureus* isolates tested here, indicating an onset of autophagy (Klionsky et al., 2021). This suggests that the isolates of this study trigger autophagy in the infected osteoblast cell lines, regardless of the outcome. Previous studies have identified the autophagy pathway as a mechanism of intracellular survival for *S. aureus* during infection in several cell types like NIH/3T3 fibroblasts, HeLa cells and Chinese hamster ovary (CHO) cells in vitro (Neumann et al., 2016; Schnaith et al., 2007; Mestre et al., 2010). Therefore, in this study we can conclude that in case of osteoblasts, autophagy is necessary but not sufficient for infection.

Study results dealing with *S. aureus* within phagosomes of professional phagocytes were summarized by Moldovan and Fraunholz (Moldovan and Fraunholz, 2019). Here maturation quickly acquires the late phagosomal marker lysosome-associated membrane protein-1 (LAMP-1) and Rab7. LAMP-1 positivity and acidification of *S. aureus* containing phagosome seem to be independent of host species and cell type, indicating that *S. aureus* does not interfere with initial phagosomal maturation.

Interestingly, a low phagosomal pH level is required for survival and replication of the community-acquired *S. aureus* type USA300 inside macrophages (Moldovan and Fraunholz, 2019).

The results of the proteome analysis, at least for isolates Pat 36 and Pat 9, indicate that a similar mechanism was present in non-professional phagocytes, in this case osteoblasts. However, that is not the whole story. Things are very different when cells with starvation-induced autophagy were infected. In this case, bacteria tested here were killed in all cells, which might suggest that starvation-induced and bacteria-induced autophagy differ. Furthermore, the bacteria induced down regulation of p62 and (in some cases) Beclin1 was abolished, indicating that the bacteria further activated an established autophagy. Nevertheless, they were eliminated from the cells. This indicates that a bacteria-induced autophagy differs from a starvation-induced one and could have far-reaching clinical relevance. If the effect, i.e., the dying of the bacteria in the osteoblasts, also occurs with other inducers of autophagy, this would represent a possibility of treating the implant-associated infection.

The speculation that external (bacteria) and internal (starvation) induced autophagy had different effect on the survival on bacteria might be supported by the experiments using Bafilomycin A1, an inhibitor of auto-phagosome lysosome fusion (Mauvezin and Neufeld, 2015). When Bafilomycin A1 pre-treated cells were infected with *S. aureus* isolates the bacteria survived in larger numbers and seemed to be protected from elimination.

The alteration of normal autophagy flux was although observed within Polymorphonuclear neutrophils, however with completely different outcome. Here the autophagy inhibitor Bafilomycin A1 significantly reduced intracellular survival of *S. aureus*. Furthermore, accumulation of the autophagic flux markers were associated with survival, also something that is different in the case of osteoblast infection (Mulcahy et al., 2020). However, the authors note that previous studies have described divergent mechanisms for *S. aureus* intracellular survival and replication using the autophagic pathway in non-professional phagocytes. *S. aureus* was reported to survive and replicate in LC3-decorated autophagosomes in HeLa cells, followed by eventual escape into the cytoplasm (Schnaith et al., 2007). In murine fibroblasts, ubiquitinated *S. aureus* was trafficked to autophagosomes by selective autophagic chaperone proteins such as p62 but prevented autophagosome-lysosome fusion (Neumann et al., 2016).

To conclude, it can be seen that neither the presence of the respective genes nor the gene products can be regarded as a sufficient predictive marker for adhesion. Gene expression analysis suggests that there may not be a uniform mechanism behind the adhesion of the examined *S. aureus* isolates, but that different adhesion proteins are involved. The increased adhesion is not correlated with increased invasion, which makes adhesion uninteresting as a possible therapeutic target. With respect to

intracellular survival, autophagy in the host cells was turned on after infection with the *S. aureus* isolates tested here, indicating an onset of autophagy, which was regardless of the outcome. This study highlights a controversial role of the autophagy pathways with respect to clearance of *S. aureus* indicating that autophagy is necessary but not sufficient for infection. Furthermore, bacteria-induced autophagy differs from a starvation-induced one, making autophagy an interesting treatment option for the implant-associated infection.

5 SUMMARY/ZUSAMMENFASSUNG

5.1 SUMMARY

Implant-associated infections are severe complications in orthopaedic surgery. Beneath *S. epidermidis*, *S. aureus* is the most prevalent pathogen responsible for orthopaedic infection. Treatments using antibiotics are often unsuccessful due to biofilm formation or the intracellular persistence of *S. aureus*. In the literature, few reports have taken *S. aureus* as a facultative intracellular pathogen. This study focuses on adhesion, invasion and intracellular survival of clinical isolates of *S. aureus* on/in osteoblasts.

Isolates obtained from implant-associated infection were determined by API® Staph. test and 16S rRNA sequencing. Further characterization was carried out using clear zone formation, collagenase and oxidase test, growth analysis, antibiotic resistance and biofilm formation analysis. For bacteria-osteoblasts interaction studies, *S. aureus* ATCC 29213 and eight *S. aureus* isolates (Pat 2, 4, 6, 9, 28, 36, 42, 45), as well as confluent layers of osteoblast like cell lines SaOS2 and MG63 were used.

Standard infection model was established using *S. aureus* ATCC 29213 to infect SaOS2 and MG63. Based on this model, adhesion and invasion assay with *S. aureus* isolates were processed. MTT and respiration assay were performed to get the metabolic activity results of the infected osteoblasts. PCR and qPCR were applied to identify genes involved in adhesion and the corresponding expression level. Mass spectrometry was used for quantitative protein analysis. Induced and inhibited autophagy, Western blot were carried out to analyse the role of autophagy in bacteria-osteoblasts interactions.

Based on the characterization and sequence analysis from the perspective of homology, isolates Pat 2, 4, 6, 9, 28, 36, 42, 45 were classified as *S. aureus*. In the infection model, a significant stronger adherence of *S. aureus* ATCC 29213 to SaOS2, rather than MG63, was observed. Bacteria harvested in stationary growth phase showed a stronger adherence to osteoblasts as compared to bacteria harvested in the logarithmic growth phase. Three *S. aureus* isolates (Pat 36, 42, 45) were found to adhere to and invade in osteoblasts strongly. PCR showed that eno, fnbA, clfA, clfB, ebpS, psmA, psmB, eap, sdrD, fmtB and ebh genes were expressed in all *S. aureus* isolates. Furtherly, qPCR showed that clfA might be a candidate gene related to bacterial adherence, because it was overexpressed only in in the adhesive *S. aureus* (Pat36, Pat42, Pat45) and *S. aureus* ATCC 29213. MTT assay showed that metabolic activity was independent of the infection with *S. aureus*. Respiration assay indicated that metabolic activity of both SaOS2 and MG63 cell lines were stimulated after being infected with selected *S. aureus* isolates (Pat 9, 36 and *S. aureus* ATCC 29213). The relation of cell adhesion and the gene expression under biofilm condition was not closely correlated. Proteome analysis of two different

osteoblast cell lines with or without infection with *S. aureus showed* that genes involved in adhesion were mostly not expressed in osteoblasts. Only fibronectin and collagen were detectable by mass spectrometry.

To conclude, it can be seen that neither the presence of the respective genes nor the gene products can be regarded as a sufficient predictive marker for adhesion. Gene expression analysis suggests that there may not be a uniform mechanism behind the adhesion of the examined *S. aureus* isolates, but that different adhesion proteins are involved. The increased adhesion is not correlated with increased invasion, which makes adhesion uninteresting as a possible therapeutic target. With respect to intracellular survival, autophagy in the host cells was turned on after infection with the *S. aureus* isolates tested here, indicating an onset of autophagy, which was regardless of the outcome. This study highlights a controversial role of the autophagy pathways with respect to clearance of *S. aureus* indicating that autophagy is necessary but not sufficient for infection. Furthermore, bacteria-induced autophagy differs from a starvation-induced one, making autophagy an interesting treatment option for the implant-associated infection.

5.2 ZUSAMMENFASSUNG

Implantatassoziierte Infektionen sind schwerwiegende Komplikationen in der orthopädischen Chirurgie. Neben *S. epidermidis* ist *S. aureus* der am weitesten verbreitete Erreger, der für orthopädische Infektionen verantwortlich ist. Behandlungen mit Antibiotika sind aufgrund der Biofilmbildung oder der intrazellulären Persistenz von *S. aureus* oft erfolglos. In der Literatur haben wenige Berichte *S. aureus* als fakultatives intrazelluläres Pathogen genommen. Diese Studie konzentriert sich auf Adhäsion, Invasion und intrazelluläres Überleben klinischer Isolate von *S. aureus* auf/in Osteoblasten.

Von Implantat-assoziierten Infektionen erhaltene Isolate wurden mit API® Staph Test und 16S-rRNA-Sequenzierung bestimmt. Die weitere Charakterisierung erfolgte mittels clear-zone-formation, Collagenase- und Oxidasetest, Wachstumsanalyse, Antibiotikaresistenz- und Biofilmbildungsanalyse. Für Bakterien-Osteoblasten-Interaktionsstudien wurden *S. aureus* ATCC 29213 und acht *S. aureus*-Isolate (Pat 2, 4, 6, 9, 28, 36, 42, 45) sowie konfluente Schichten von Osteoblasten wie die Zelllinien SaOS2 und MG63 verwendet.

Es wurde ein Standardinfektionsmodell mit *S. aureus* ATCC 29213 erstellt, um SaOS2 und MG63 zu infizieren. Auf der Grundlage dieses Modells wurden Adhäsions- und Invasionstests mit *S. aureus*-Isolaten durchgeführt. MTT- und Respirationstests wurden durchgeführt, um die Ergebnisse der metabolischen Aktivität der infizierten Osteoblasten zu erhalten. PCR und qPCR wurden eingesetzt, um Gene zu identifizieren, die an der Adhäsion beteiligt sind, und um das entsprechende Expressionsniveau zu bestimmen. Massenspektrometrie wurde für die quantitative Proteinanalyse eingesetzt. Induzierte und gehemmte Autophagie wurden mit Western Blot-Analysen durchgeführt, um die Rolle der Autophagie bei der Interaktion zwischen Bakterien und Osteoblasten zu analysieren.

Basierend auf der Charakterisierung und Sequenzanalyse aus Sicht der Homologie wurden die Isolate Pat 2, 4, 6, 9, 28, 36, 42, 45 als *S. aureus* klassifiziert. Im Infektionsmodell wurde eine signifikant stärkere Adhärenz von *S. aureus* ATCC 29213 an SaOS2 statt an MG63 beobachtet. Bakterien, die in der stationären Wachstumsphase geerntet wurden, zeigten eine stärkere Adhärenz an Osteoblasten im Vergleich zu Bakterien, die in der logarithmischen Wachstumsphase geerntet wurden. Es wurde festgestellt, dass drei *S. aureus*-Isolate (Pat 36, 42, 45) stark an Osteoblasten anhaften und in diese eindringen. Die PCR zeigte, dass eno-, fnbA-, clfA-, clfB-, ebpS-, psmA-, psmB-, eap-, sdrD-, fmtB- und ebh-Gene in allen *S. aureus*-Isolaten exprimiert wurden. Darüber hinaus zeigte qPCR, dass clfA ein Kandidatengen im Zusammenhang mit der bakteriellen Adhärenz sein könnte, da es nur in adhäsiven *S. aureus* (Pat36, Pat42, Pat45) und *S. aureus* ATCC 29213 überexprimiert wurde. Der MTT-Assay zeigte, dass die metabolische Aktivität unabhängig von einer Infektion mit *S. aureus* war. Der

Respirationsassay zeigte, dass die metabolische Aktivität sowohl der SaOS2- als auch der MG63-Zelllinien stimuliert wurde, nachdem sie mit ausgewählten *S. aureus*-Isolaten (Pat 9, 36 und *S. aureus* ATCC 29213) infiziert worden waren. Das Verhältnis von Zelladhäsion und Genexpression unter Biofilmbedingungen war nicht eng korreliert. Proteomanalysen zweier verschiedener Osteoblastenzelllinien mit oder ohne Infektion mit *S. aureu*s zeigten, dass an der Adhäsion beteiligte Gene in Osteoblasten meist nicht exprimiert wurden. Mittels Massenspektrometrie waren nur Fibronektin und Kollagen nachweisbar.

Zusammengenommen ist ersichtlich, dass weder das Vorhandensein der jeweiligen Gene noch der Genprodukte als ausreichender prädiktiver Marker für die Adhäsion angesehen werden kann. Genexpressionsanalysen deuten darauf hin, dass möglicherweise kein einheitlicher Mechanismus hinter der Adhäsion der untersuchten *S. aureus*-Isolate steht, sondern dass unterschiedliche Adhäsionsproteine beteiligt sind. Die erhöhte Adhäsion korreliert nicht mit einer erhöhten Invasion, was die Adhäsion als mögliches therapeutisches Ziel uninteressant macht. In Bezug auf das intrazelluläre Überleben wurde die Autophagie in den Wirtszellen nach der Infektion mit den hier getesteten *S. aureus*-Isolaten eingeschaltet, was auf einen Beginn der Autophagie hinweist, der unabhängig vom Ausgang war. Diese Studie zeigt eine ambivalente Rolle der Autophagiewege in Bezug auf die Clearance von *S. aureus*, was darauf hindeutet, dass Autophagie für eine Infektion notwendig, aber nicht ausreichend ist. Darüber hinaus unterscheidet sich die bakterieninduzierte Autophagie von einer hungerinduzierten Autophagie, was die Autophagie zu einer interessanten Behandlungsoption für die Implantat-assoziierte Infektion macht.

6 REFERENCES

Aggarwal VK, Bakhshi H, Ecker NU, et al. (2014) Organism profile in periprosthetic joint infection: pathogens differ at two arthroplasty infection referral centers in Europe and in the United States. *J Knee Surg* 27: 399-406.

Ahmed S, Meghji S, Williams RJ, et al. (2001) Staphylococcus aureus fibronectin binding proteins are essential for internalization by osteoblasts but do not account for differences in intracellular levels of bacteria. *Infect Immun* 69: 2872-2877.

Alexander EH and Hudson MC. (2001) Factors influencing the internalization of Staphylococcus aureus and impacts on the course of infections in humans. *Appl Microbiol Biotechnol* 56: 361-366.

Apostu D, Lucaciu O, Berce C, et al. (2018) Current methods of preventing aseptic loosening and improving osseointegration of titanium implants in cementless total hip arthroplasty: a review. *J Int Med Res* 46: 2104-2119.

Arciola CR, An YH, Campoccia D, et al. (2005a) Etiology of implant orthopedic infections: a survey on 1027 clinical isolates. *Int J Artif Organs* 28: 1091-1100.

Arciola CR, Campoccia D, Gamberini S, et al. (2005b) Prevalence of cna, fnbA and fnbB adhesin genes among Staphylococcus aureus isolates from orthopedic infections associated to different types of implant. *FEMS Microbiol Lett* 246: 81-86.

Arciola CR, Campoccia D and Montanaro L. (2018) Implant infections: adhesion, biofilm formation and immune evasion. *Nat Rev Microbiol* 16: 397-409.

Arciola CR, Campoccia D, Ravaioli S, et al. (2015) Polysaccharide intercellular adhesin in biofilm: structural and regulatory aspects. *Front Cell Infect Microbiol* 5: 7.

Arciola CR, Campoccia D, Speziale P, et al. (2012) Biofilm formation in Staphylococcus implant infections. A review of molecular mechanisms and implications for biofilm-resistant materials. *Biomaterials* 33: 5967-5982.

Askarian F, Ajayi C, Hanssen AM, et al. (2016) The interaction between Staphylococcus aureus SdrD and desmoglein 1 is important for adhesion to host cells. *Sci Rep* 6: 22134.

Athanasopoulos AN, Economopoulou M, Orlova VV, et al. (2006) The extracellular adherence protein (Eap) of Staphylococcus aureus inhibits wound healing by interfering with host defense and repair mechanisms. *Blood* 107: 2720-2727.

Baba T, Takeuchi F, Kuroda M, et al. (2002) Genome and virulence determinants of high virulence community-acquired MRSA. *Lancet* 359: 1819-1827.

Barth RE, Vogely HC, Hoepelman AI, et al. (2011) 'To bead or not to bead?' Treatment of osteomyelitis and prosthetic joint-associated infections with gentamicin bead chains. *Int J Antimicrob Agents* 38: 371-375.

Becker S, Frankel MB, Schneewind O, et al. (2014) Release of protein A from the cell wall of Staphylococcus aureus. *Proc Natl Acad Sci U S A* 111: 1574-1579.

Beenken KE, Blevins JS and Smeltzer MS. (2003) Mutation of sarA in Staphylococcus aureus limits biofilm formation. *Infect Immun* 71: 4206-4211.

Belikova D, Jochim A, Power J, et al. (2020) "Gene accordions" cause genotypic and phenotypic heterogeneity in clonal populations of Staphylococcus aureus. *Nat Commun* 11: 3526.

Boles BR and Horswill AR. (2008) Agr-mediated dispersal of Staphylococcus aureus biofilms. *PLoS Pathog* 4: e1000052.

Bowden MG, Chen W, Singvall J, et al. (2005) Identification and preliminary characterization of cell-wall-anchored proteins of Staphylococcus epidermidis. *Microbiology (Reading)* 151: 1453-1464.

Brady RA, O'May GA, Leid JG, et al. (2011) Resolution of Staphylococcus aureus biofilm infection using vaccination and antibiotic treatment. *Infect Immun* 79: 1797-1803.

Campoccia D, Baldassarri L, Pirini V, et al. (2008) Molecular epidemiology of Staphylococcus aureus from implant orthopaedic infections: ribotypes, agr polymorphism, leukocidal toxins and antibiotic resistance. *Biomaterials* 29: 4108-4116.
Campoccia D, Montanaro L and Arciola CR. (2006) The significance of infection related to orthopedic devices and issues of antibiotic resistance. *Biomaterials* 27: 2331-2339.
Campoccia D, Montanaro L, von Eiff C, et al. (2009a) Cluster analysis of ribotyping profiles of Staphylococcus epidermidis isolates recovered from foreign body-associated orthopedic infections. *J Biomed Mater Res A* 88: 664-672.
Campoccia D, Speziale P, Ravaioli S, et al. (2009b) The presence of both bone sialoprotein-binding protein gene and collagen adhesin gene as a typical virulence trait of the major epidemic cluster in isolates from orthopedic implant infections. *Biomaterials* 30: 6621-6628.
Chalmers SJ and Wylam ME. (2020) Methicillin-Resistant Staphylococcus aureus Infection and Treatment Options. *Methods Mol Biol* 2069: 229-251.
Czekanska EM, Stoddart MJ, Richards RG, et al. (2012) In search of an osteoblast cell model for in vitro research. *Eur Cell Mater* 24: 1-17.
Dale H, Fenstad AM, Hallan G, et al. (2012) Increasing risk of prosthetic joint infection after total hip arthroplasty. *Acta Orthop* 83: 449-458.
Dallas SL and Bonewald LF. (2010) Dynamics of the transition from osteoblast to osteocyte. *Ann N Y Acad Sci* 1192: 437-443.
de Mesy Bentley KL, Trombetta R, Nishitani K, et al. (2017) Evidence of Staphylococcus Aureus Deformation, Proliferation, and Migration in Canaliculi of Live Cortical Bone in Murine Models of Osteomyelitis. *J Bone Miner Res* 32: 985-990.
DeLong EF. (1992) Archaea in coastal marine environments. *Proc Natl Acad Sci U S A* 89: 5685-5689.
Drevets DA, Canono BP, Leenen PJ, et al. (1994) Gentamicin kills intracellular Listeria monocytogenes. *Infect Immun* 62: 2222-2228.
Dusane DH, Kyrouac D, Petersen I, et al. (2018) Targeting intracellular Staphylococcus aureus to lower recurrence of orthopaedic infection. *J Orthop Res* 36: 1086-1092.
Edwards JR and Mundy GR. (2011) Advances in osteoclast biology: old findings and new insights from mouse models. *Nat Rev Rheumatol* 7: 235-243.
El-Sayed D and Nouvong A. (2019) Infection Protocols for Implants. *Clin Podiatr Med Surg* 36: 627-649.
Ellington JK, Harris M, Hudson MC, et al. (2006) Intracellular Staphylococcus aureus and antibiotic resistance: implications for treatment of staphylococcal osteomyelitis. *J Orthop Res* 24: 87-93.
Ellington JK, Reilly SS, Ramp WK, et al. (1999) Mechanisms of Staphylococcus aureus invasion of cultured osteoblasts. *Microb Pathog* 26: 317-323.
Etkin CD and Springer BD. (2017) The American Joint Replacement Registry-the first 5 years. *Arthroplast Today* 3: 67-69.
Fisher RA, Gollan B and Helaine S. (2017) Persistent bacterial infections and persister cells. *Nat Rev Microbiol* 15: 453-464.
Flemming HC, Wingender J, Szewzyk U, et al. (2016) Biofilms: an emergent form of bacterial life. *Nat Rev Microbiol* 14: 563-575.
Foster TJ, Geoghegan JA, Ganesh VK, et al. (2014a) Adhesion, invasion and evasion: the many functions of the surface proteins of Staphylococcus aureus. *Nat Rev Microbiol* 12: 49-62.
Foster TJ, Geoghegan JA, Ganesh VK, et al. (2014b) Adhesion, invasion and evasion: the many functions of the surface proteins of Staphylococcus aureus. *Nat Rev Microbiol* 12: 49-62.
Fowler T, Wann ER, Joh D, et al. (2000) Cellular invasion by Staphylococcus aureus involves a fibronectin bridge between the bacterial fibronectin-binding MSCRAMMs and host cell beta1 integrins. *Eur J Cell Biol* 79: 672-679.
Gay CV, Gilman VR and Sugiyama T. (2000) Perspectives on osteoblast and osteoclast function. *Poult Sci* 79: 1005-1008.

Gibson JF, Prajsnar TK, Hill CJ, et al. (2021) Neutrophils use selective autophagy receptor Sqstm1/p62 to target Staphylococcus aureus for degradation in vivo in zebrafish. *Autophagy* 17: 1448-1457.
Gordon O, Miller RJ, Thompson JM, et al. (2020) Rabbit model of Staphylococcus aureus implant-associated spinal infection. *Dis Model Mech* 13.
Götz F. (2002) Staphylococcus and biofilms. *Mol Microbiol* 43: 1367-1378.
Gristina AG. (1987) Biomaterial-centered infection: microbial adhesion versus tissue integration. *Science* 237: 1588-1595.
Gristina AG and Costerton JW. (1985) Bacterial adherence to biomaterials and tissue. The significance of its role in clinical sepsis. *J Bone Joint Surg Am* 67: 264-273.
Griswold A, Chen YY, Snyder JA, et al. (2004) Characterization of the arginine deiminase operon of Streptococcus rattus FA-1. *Appl Environ Microbiol* 70: 1321-1327.
Grzesik WJ and Robey PG. (1994) Bone matrix RGD glycoproteins: immunolocalization and interaction with human primary osteoblastic bone cells in vitro. *J Bone Miner Res* 9: 487-496.
Gunn NJ, Zelmer AR, Kidd SP, et al. (2021) A Human Osteocyte Cell Line Model for Studying Staphylococcus aureus Persistence in Osteomyelitis. *Front Cell Infect Microbiol* 11: 781022.
Guo G, Wang J, You Y, et al. (2017) Distribution characteristics of Staphylococcus spp. in different phases of periprosthetic joint infection: A review. *Exp Ther Med* 13: 2599-2608.
Guo H, Tong Y, Cheng J, et al. (2022) Biofilm and Small Colony Variants-An Update on Staphylococcus aureus Strategies toward Drug Resistance. *Int J Mol Sci* 23.
Haggar A, Hussain M, Lönnies H, et al. (2003) Extracellular adherence protein from Staphylococcus aureus enhances internalization into eukaryotic cells. *Infect Immun* 71: 2310-2317.
Harraghy N, Hussain M, Haggar A, et al. (2003) The adhesive and immunomodulating properties of the multifunctional Staphylococcus aureus protein Eap. *Microbiology (Reading)* 149: 2701-2707.
Harris SR, Cartwright EJ, Torok ME, et al. (2013) Whole-genome sequencing for analysis of an outbreak of meticillin-resistant Staphylococcus aureus: a descriptive study. *Lancet Infect Dis* 13: 130-136.
Heilbronner S, Holden MT, van Tonder A, et al. (2011) Genome sequence of Staphylococcus lugdunensis N920143 allows identification of putative colonization and virulence factors. *FEMS Microbiol Lett* 322: 60-67.
Heilmann C. (2011) Adhesion mechanisms of staphylococci. *Adv Exp Med Biol* 715: 105-123.
Hirschhausen N, Schlesier T, Schmidt MA, et al. (2010) A novel staphylococcal internalization mechanism involves the major autolysin Atl and heat shock cognate protein Hsc70 as host cell receptor. *Cell Microbiol* 12: 1746-1764.
Hudson MC, Ramp WK, Nicholson NC, et al. (1995) Internalization of Staphylococcus aureus by cultured osteoblasts. *Microb Pathog* 19: 409-419.
Hussain M, Becker K, von Eiff C, et al. (2001) Analogs of Eap protein are conserved and prevalent in clinical Staphylococcus aureus isolates. *Clin Diagn Lab Immunol* 8: 1271-1276.
Hussain M, von Eiff C, Sinha B, et al. (2008) eap Gene as novel target for specific identification of Staphylococcus aureus. *J Clin Microbiol* 46: 470-476.
Ibrahim I. (2016) 16S rRNA Gene Sequencing For Identification of Some Enterobacteriaceae Species Isolated from Tigris River. *Al-Mustansiriyah Journal of Science* 27: 13-16.
Ikawaty R, Brouwer E, Van Duijkeren E, et al. Virulence factors of genotyped bovine mastitis Staphylococcus aureus isolates in the Netherlands. *New insights into molecular typing methods for Staphylococcus aureus*: 103.
Jamsen E, Huhtala H, Puolakka T, et al. (2009) Risk factors for infection after knee arthroplasty. A register-based analysis of 43,149 cases. *J Bone Joint Surg Am* 91: 38-47.
Jauregui CE, Mansell JP, Jepson MA, et al. (2013) Differential interactions of Streptococcus gordonii and Staphylococcus aureus with cultured osteoblasts. *Mol Oral Microbiol* 28: 250-266.

Ji N, Yang J and Ji Y. (2020) Determining Impact of Growth Phases on Capacity of Staphylococcus aureus to Adhere to and Invade Host Cells. *Methods Mol Biol* 2069: 187-195.
Josse J, Velard F and Gangloff SC. (2015) Staphylococcus aureus vs. Osteoblast: Relationship and Consequences in Osteomyelitis. *Front Cell Infect Microbiol* 5: 85.
Kang M, Ko YP, Liang X, et al. (2013) Collagen-binding microbial surface components recognizing adhesive matrix molecule (MSCRAMM) of Gram-positive bacteria inhibit complement activation via the classical pathway. *J Biol Chem* 288: 20520-20531.
Khalil H, Williams RJ, Stenbeck G, et al. (2007) Invasion of bone cells by Staphylococcus epidermidis. *Microbes Infect* 9: 460-465.
Klionsky DJ, Abdel-Aziz AK, Abdelfatah S, et al. (2021) Guidelines for the use and interpretation of assays for monitoring autophagy (4th edition)(1). *Autophagy* 17: 1-382.
Knodler LA and Celli J. (2011) Eating the strangers within: host control of intracellular bacteria via xenophagy. *Cell Microbiol* 13: 1319-1327.
Komatsuzawa H, Ohta K, Sugai M, et al. (2000) Tn551-mediated insertional inactivation of the fmtB gene encoding a cell wall-associated protein abolishes methicillin resistance in Staphylococcus aureus. *J Antimicrob Chemother* 45: 421-431.
Krauss JL, Roper PM, Ballard A, et al. (2019) Staphylococcus aureus Infects Osteoclasts and Replicates Intracellularly. *mBio* 10.
Krut O, Utermohlen O, Schlossherr X, et al. (2003) Strain-specific association of cytotoxic activity and virulence of clinical Staphylococcus aureus isolates. *Infect Immun* 71: 2716-2723.
Kuehl R, Brunetto PS, Woischnig AK, et al. (2016) Preventing Implant-Associated Infections by Silver Coating. *Antimicrob Agents Chemother* 60: 2467-2475.
Kumar R, Yadav BR, Anand SK, et al. (2011) Prevalence of adhesin and toxin genes among isolates of Staphylococcus aureus obtained from mastitic cattle. *World Journal of Microbiology and Biotechnology* 27: 513-521.
Kuo CJ, Hansen M and Troemel E. (2018) Autophagy and innate immunity: Insights from invertebrate model organisms. *Autophagy* 14: 233-242.
Kuroda M, Ohta T, Uchiyama I, et al. (2001) Whole genome sequencing of meticillin-resistant Staphylococcus aureus. *Lancet* 357: 1225-1240.
Kurtz S, Ong K, Lau E, et al. (2007) Projections of primary and revision hip and knee arthroplasty in the United States from 2005 to 2030. *J Bone Joint Surg Am* 89: 780-785.
Le KY, Dastgheyb S, Ho TV, et al. (2014) Molecular determinants of staphylococcal biofilm dispersal and structuring. *Front Cell Infect Microbiol* 4: 167.
Levine B and Kroemer G. (2008) Autophagy in the pathogenesis of disease. *Cell* 132: 27-42.
Lew DP and Waldvogel FA. (2004) Osteomyelitis. *Lancet* 364: 369-379.
Li B and Webster TJ. (2018) Bacteria antibiotic resistance: New challenges and opportunities for implant-associated orthopedic infections. *J Orthop Res* 36: 22-32.
Li J, Chen J, Yang G, et al. (2021) Sublancin protects against methicillin-resistant Staphylococcus aureus infection by the combined modulation of innate immune response and microbiota. *Peptides* 141: 170533.
Limoli DH, Jones CJ and Wozniak DJ. (2015) Bacterial Extracellular Polysaccharides in Biofilm Formation and Function. *Microbiol Spectr* 3.
Löffler B, Tuchscherr L, Niemann S, et al. (2014) Staphylococcus aureus persistence in non-professional phagocytes. *Int J Med Microbiol* 304: 170-176.
Lv Y, Fang L, Ding P, et al. (2019) PI3K/Akt-Beclin1 signaling pathway positively regulates phagocytosis and negatively mediates NF-κB-dependent inflammation in Staphylococcus aureus-infected macrophages. *Biochem Biophys Res Commun* 510: 284-289.
Mauvezin C and Neufeld TP. (2015) Bafilomycin A1 disrupts autophagic flux by inhibiting both V-ATPase-dependent acidification and Ca-P60A/SERCA-dependent autophagosome-lysosome fusion. *Autophagy* 11: 1437-1438.

McCarthy AJ and Lindsay JA. (2010) Genetic variation in Staphylococcus aureus surface and immune evasion genes is lineage associated: implications for vaccine design and host-pathogen interactions. *BMC Microbiol* 10: 173.
Ménard G, Bonnaure-Mallet M and Donnio PY. (2020) Adhesion of Staphylococcus aureus to epithelial cells: an in vitro approach to study interactions within the nasal microbiota. *J Med Microbiol* 69: 1253-1261.
Mestre MB, Fader CM, Sola C, et al. (2010) Alpha-hemolysin is required for the activation of the autophagic pathway in Staphylococcus aureus-infected cells. *Autophagy* 6: 110-125.
Metsemakers WJ, Kuehl R, Moriarty TF, et al. (2018) Infection after fracture fixation: Current surgical and microbiological concepts. *Injury* 49: 511-522.
Michel NS, Paletta JR, Kerwart M, et al. (2016) Role of Electrochemically Activated Solution in Asepsis in Osteoblasts and Chondrocytes in vitro. *J Invest Surg* 29: 157-166.
Mizushima N, Levine B, Cuervo AM, et al. (2008) Autophagy fights disease through cellular self-digestion. *Nature* 451: 1069-1075.
Mohamed W, Sommer U, Sethi S, et al. (2014) Intracellular proliferation of S. aureus in osteoblasts and effects of rifampicin and gentamicin on S. aureus intracellular proliferation and survival. *Eur Cell Mater* 28: 258-268.
Moldovan A and Fraunholz MJ. (2019) In or out: Phagosomal escape of Staphylococcus aureus. *Cell Microbiol* 21: e12997.
Montanaro L, Arciola CR, Baldassarri L, et al. (1999) Presence and expression of collagen adhesin gene (cna) and slime production in Staphylococcus aureus strains from orthopaedic prosthesis infections. *Biomaterials* 20: 1945-1949.
Montanaro L, Speziale P, Campoccia D, et al. (2011) Scenery of Staphylococcus implant infections in orthopedics. *Future Microbiol* 6: 1329-1349.
Moormeier DE and Bayles KW. (2017) Staphylococcus aureus biofilm: a complex developmental organism. *Mol Microbiol* 104: 365-376.
Moreillon P, Entenza JM, Francioli P, et al. (1995) Role of Staphylococcus aureus coagulase and clumping factor in pathogenesis of experimental endocarditis. *Infect Immun* 63: 4738-4743.
Mulcahy ME, O'Brien EC, O'Keeffe KM, et al. (2020) Manipulation of Autophagy and Apoptosis Facilitates Intracellular Survival of Staphylococcus aureus in Human Neutrophils. *Front Immunol* 11: 565545.
Nair SP, Bischoff M, Senn MM, et al. (2003) The sigma B regulon influences internalization of Staphylococcus aureus by osteoblasts. *Infect Immun* 71: 4167-4170.
Naparstek L, Carmeli Y, Navon-Venezia S, et al. (2014) Biofilm formation and susceptibility to gentamicin and colistin of extremely drug-resistant KPC-producing Klebsiella pneumoniae. *J Antimicrob Chemother* 69: 1027-1034.
Nashev D, Toshkova K, Salasia SI, et al. (2004) Distribution of virulence genes of Staphylococcus aureus isolated from stable nasal carriers. *FEMS Microbiol Lett* 233: 45-52.
Netea-Maier RT, Plantinga TS, van de Veerdonk FL, et al. (2016) Modulation of inflammation by autophagy: Consequences for human disease. *Autophagy* 12: 245-260.
Neumann Y, Bruns SA, Rohde M, et al. (2016) Intracellular Staphylococcus aureus eludes selective autophagy by activating a host cell kinase. *Autophagy* 12: 2069-2084.
Niemann S, Nguyen MT, Eble JA, et al. (2021) More Is Not Always Better-the Double-Headed Role of Fibronectin in Staphylococcus aureus Host Cell Invasion. *mBio* 12: e0106221.
Noone JC, Helmersen K, Leegaard TM, et al. (2021) Rapid Diagnostics of Orthopaedic-Implant-Associated Infections Using Nanopore Shotgun Metagenomic Sequencing on Tissue Biopsies. *Microorganisms* 9.
O'Keeffe KM, Wilk MM, Leech JM, et al. (2015) Manipulation of Autophagy in Phagocytes Facilitates Staphylococcus aureus Bloodstream Infection. *Infect Immun* 83: 3445-3457.
Ogston A. (1881) Report upon Micro-Organisms in Surgical Diseases. *Br Med J* 1: 369.b362-375.

Oliveira WF, Silva PMS, Silva RCS, et al. (2018) Staphylococcus aureus and Staphylococcus epidermidis infections on implants. *J Hosp Infect* 98: 111-117.
Paharik AE and Horswill AR. (2016) The Staphylococcal Biofilm: Adhesins, Regulation, and Host Response. *Microbiol Spectr* 4.
Parker D, Planet PJ, Soong G, et al. (2014) Induction of type I interferon signaling determines the relative pathogenicity of Staphylococcus aureus strains. *PLoS Pathog* 10: e1003951.
Peetermans M, Verhamme P and Vanassche T. (2015) Coagulase Activity by Staphylococcus aureus: A Potential Target for Therapy? *Semin Thromb Hemost* 41: 433-444.
Pérez-Tanoira R, Aarnisalo AA, Eklund KK, et al. (2017) Prevention of Biomaterial Infection by Pre-Operative Incubation with Human Cells. *Surg Infect (Larchmt)* 18: 336-344.
Periasamy S, Chatterjee SS, Cheung GY, et al. (2012) Phenol-soluble modulins in staphylococci: What are they originally for? *Commun Integr Biol* 5: 275-277.
Phillips G and Ker J. (2006) Champion students! Experience with a standardized infection control training package in medical students. *J Hosp Infect* 62: 518-519.
Ramzan R, Staniek K, Kadenbach B, et al. (2010) Mitochondrial respiration and membrane potential are regulated by the allosteric ATP-inhibition of cytochrome c oxidase. *Biochim Biophys Acta* 1797: 1672-1680.
Rand JA, Trousdale RT, Ilstrup DM, et al. (2003) Factors affecting the durability of primary total knee prostheses. *J Bone Joint Surg Am* 85: 259-265.
Rasigade JP, Trouillet-Assant S, Ferry T, et al. (2013) PSMs of hypervirulent Staphylococcus aureus act as intracellular toxins that kill infected osteoblasts. *PLoS One* 8: e63176.
Reilly SS, Hudson MC, Kellam JF, et al. (2000) In vivo internalization of Staphylococcus aureus by embryonic chick osteoblasts. *Bone* 26: 63-70.
Rooijakkers SH, van Kessel KP and van Strijp JA. (2005) Staphylococcal innate immune evasion. *Trends Microbiol* 13: 596-601.
Saks V, Monge C and Guzun R. (2009) Philosophical basis and some historical aspects of systems biology: from Hegel to Noble - applications for bioenergetic research. *Int J Mol Sci* 10: 1161-1192.
Schafer JA, Hovde LB and Rotschafer JC. (2006) Consistent rates of kill of Staphylococcus aureus by gentamicin over a 6-fold clinical concentration range in an in vitro pharmacodynamic model (IVPDM). *Journal of Antimicrobial Chemotherapy* 58: 108-111.
Schierholz JM and Beuth J. (2001) Implant infections: a haven for opportunistic bacteria. *J Hosp Infect* 49: 87-93.
Schnaith A, Kashkar H, Leggio SA, et al. (2007) Staphylococcus aureus subvert autophagy for induction of caspase-independent host cell death. *J Biol Chem* 282: 2695-2706.
Seghrouchni K, van Delden C, Dominguez D, et al. (2012) Remission after treatment of osteoarticular infections due to Pseudomonas aeruginosa versus Staphylococcus aureus: a case-controlled study. *Int Orthop* 36: 1065-1071.
Selan L, Papa R, Ermocida A, et al. (2017) Serratiopeptidase reduces the invasion of osteoblasts by Staphylococcus aureus. *Int J Immunopathol Pharmacol* 30: 423-428.
Sendi P and Proctor RA. (2009) Staphylococcus aureus as an intracellular pathogen: the role of small colony variants. *Trends Microbiol* 17: 54-58.
Serray B, Oufrid S, Hannaoui I, et al. (2016) Genes encoding adhesion factors and biofilm formation in methicillin-resistant Staphylococcus aureus in Morocco. *J Infect Dev Ctries* 10: 863-869.
Shi S and Zhang X. (2012) Interaction of Staphylococcus aureus with osteoblasts (Review). *Exp Ther Med* 3: 367-370.
Shuaib A, Motan D, Bhattacharya P, et al. (2019) Heterogeneity in The Mechanical Properties of Integrins Determines Mechanotransduction Dynamics in Bone Osteoblasts. *Sci Rep* 9: 13113.
Siebers MC, ter Brugge PJ, Walboomers XF, et al. (2005) Integrins as linker proteins between osteoblasts and bone replacing materials. A critical review. *Biomaterials* 26: 137-146.

Singh SK. (2017) Staphylococcus aureus intracellular survival: A closer look in the process. *Virulence* 8: 1506-1507.
Speziale P, Pietrocola G, Foster TJ, et al. (2014) Protein-based biofilm matrices in Staphylococci. *Front Cell Infect Microbiol* 4: 171.
Stewart PS. (2002) Mechanisms of antibiotic resistance in bacterial biofilms. *Int J Med Microbiol* 292: 107-113.
Strobel M, Pfortner H, Tuchscherr L, et al. (2016) Post-invasion events after infection with Staphylococcus aureus are strongly dependent on both the host cell type and the infecting S. aureus strain. *Clin Microbiol Infect* 22: 799-809.
Sung JM, Lloyd DH and Lindsay JA. (2008) Staphylococcus aureus host specificity: comparative genomics of human versus animal isolates by multi-strain microarray. *Microbiology (Reading)* 154: 1949-1959.
Taneike I, Otsuka T, Dohmae S, et al. (2006) Molecular nature of methicillin-resistant Staphylococcus aureus derived from explosive nosocomial outbreaks of the 1980s in Japan. *FEBS Lett* 580: 2323-2334.
Testoni F, Montanaro L, Poggi A, et al. (2011) Internalization by osteoblasts of two Staphylococcus aureus clinical isolates differing in their adhesin gene pattern. *Int J Artif Organs* 34: 789-798.
Thomer L, Schneewind O and Missiakas D. (2016) Pathogenesis of Staphylococcus aureus Bloodstream Infections. *Annu Rev Pathol* 11: 343-364.
Tristan A, Ying L, Bes M, et al. (2003) Use of multiplex PCR to identify Staphylococcus aureus adhesins involved in human hematogenous infections. *J Clin Microbiol* 41: 4465-4467.
Tuchscherr L, Kreis CA, Hoerr V, et al. (2016) Staphylococcus aureus develops increased resistance to antibiotics by forming dynamic small colony variants during chronic osteomyelitis. *J Antimicrob Chemother* 71: 438-448.
Tung H, Guss B, Hellman U, et al. (2000) A bone sialoprotein-binding protein from Staphylococcus aureus: a member of the staphylococcal Sdr family. *Biochem J* 345 Pt 3: 611-619.
Valour F, Trouillet-Assant S, Riffard N, et al. (2015) Antimicrobial activity against intraosteoblastic Staphylococcus aureus. *Antimicrob Agents Chemother* 59: 2029-2036.
Vancraeynest D, Hermans K and Haesebrouck F. (2004) Genotypic and phenotypic screening of high and low virulence Staphylococcus aureus isolates from rabbits for biofilm formation and MSCRAMMs. *Vet Microbiol* 103: 241-247.
Vancraeynest D, Hermans K and Haesebrouck F. (2006) Prevalence of genes encoding exfoliative toxins, leucotoxins and superantigens among high and low virulence rabbit Staphylococcus aureus strains. *Vet Microbiol* 117: 211-218.
Walker JN, Crosby HA, Spaulding AR, et al. (2013) The Staphylococcus aureus ArlRS two-component system is a novel regulator of agglutination and pathogenesis. *PLoS Pathog* 9: e1003819.
Watkins KE and Unnikrishnan M. (2020) Evasion of host defenses by intracellular Staphylococcus aureus. *Adv Appl Microbiol* 112: 105-141.
Webb LX, Wagner W, Carroll D, et al. (2007) Osteomyelitis and intraosteoblastic Staphylococcus aureus. *J Surg Orthop Adv* 16: 73-78.
Weiss JN, Yang L and Qu Z. (2006) Systems biology approaches to metabolic and cardiovascular disorders: network perspectives of cardiovascular metabolism. *J Lipid Res* 47: 2355-2366.
Wright JA and Nair SP. (2010) Interaction of staphylococci with bone. *Int J Med Microbiol* 300: 193-204.
Xu T, Wang XY, Cui P, et al. (2017) The Agr Quorum Sensing System Represses Persister Formation through Regulation of Phenol Soluble Modulins in Staphylococcus aureus. *Front Microbiol* 8: 2189.
Yang D, Wijenayaka AR, Solomon LB, et al. (2018) Novel Insights into Staphylococcus aureus Deep Bone Infections: the Involvement of Osteocytes. *mBio* 9.
Yang J and Ji Y. (2014) Investigation of Staphylococcus aureus adhesion and invasion of host cells. *Methods Mol Biol* 1085: 187-194.

Zapotoczna M, Jevnikar Z, Miajlovic H, et al. (2013) Iron-regulated surface determinant B (IsdB) promotes Staphylococcus aureus adherence to and internalization by non-phagocytic human cells. *Cell Microbiol* 15: 1026-1041.

Zimmerli W, Trampuz A and Ochsner PE. (2004) Prosthetic-joint infections. *N Engl J Med* 351: 1645-1654.

Zong Y, Xu Y, Liang X, et al. (2005) A 'Collagen Hug' model for Staphylococcus aureus CNA binding to collagen. *EMBO J* 24: 4224-4236.

7 APPENDIX

a. Curriculum vitae

b. Directory of academic teachers

My academic teachers at Tianjin Medical University were: Cao Haiyan, Cao Jingwen, Ji Qiang, Jian Tianming, Jiang Lin, Li Guohui, Li Jia, Li Jinru, Li Kun, Li Liangang, Li Liyu, Li Mei, Li Yi, Luo Zheng, Miao Xuhong, Qi Wei, Shao Heng, Shi Fang, Song Junqiu, Sun Baocun, Wang Lin, Wang Qiming, Wang Xinchao, Wang Yingjuan, Xing Youkun, Yang Wenying, Zhang Jiuliang, Zhang Lijun, Zhao Yudong.

My academic teachers at Jinzhou Medical University were: Wang Wenliang, Zhao Dong.

My academic teachers at Philipps-University Marburg were: Pietro Di Fazio, Jürgen Paletta, Steffen Ruchholtz.

c. Ackowledgements

First of all, I sincerely thank my mentor Univ.-Prof. Dr. med. Steffen Ruchholtz for his meticulous care and guidance over the past three years. Simultaneously, I would like to express my gratitude to PD Dr. rer. nat. Jürgen Paletta for his practical direction, intensive supervision and immense support in all phases of this work. Furthermore, I greatly appreciate the help of my fellow, doctoral candidate Lea-Sophie Schwinn, Mr. Gisbert Seelbach, and the entire laboratory team of Orthopedics and Trauma Surgery Department for the good cooperation and instruction, making it possible for me to get access to their extensive knowledge and experience in a pleasant working atmosphere.

Then, I especially wish to thank Dr. rer. nat. Pietro Di Fazio in the laboratory of Visceral, Thoracic and Vascular Surgery for inspiring me to link this exciting topic to his specialty, autophagy. The scientific experience and knowledge he shared with me are really appreciated. At the same time, I would like to thank Dr. Fazio to review my dissertation.

I also thank Prof. Dr. Sebastian Vogt and Petra Weber in the laboratory of Cardiac and Thoracic Vascular Surgery for giving me the possibility to apply their mature technology to my project. Through close cooperation with them, I could examine my project from a new point of view.

l would also like to thank PD Dr. rer. nat. Volker Ruppert and Dr. rer. nat. Muhidien Soufi in the laboratory of Cardiology for prvoding necessary insturctions and materials. Simultaneously, I want to thank Dr. Ruppert to review my dissertaion. Likewise, I appreciate Dr. Uwe Linne from Department of Mass Spectrometry and Element Analysis, with his help I obtained some important data. Moreover, I am grateful for Mr. Bernhard Watzer from the laboratory of Core Facility Medical Mass Spectrometry, with his kindness I got access to the ultrasound device.

Finally, I would like to appreciate all members of the laboratory of Orthopedics and Trauma Surgery and the laboratory of Visceral, Thoracic and Vascular Surgery of the University Hospital of Philipps-University Marburg for the time they invested in instructing me to apply the necessary methods and to discuss results and interpretations with me.